I hereby certify that this correspondence is being delivered by Hand Delivery to:

Commissioner for Patents
P.O. Box 1450
Alexandria, VA 22313-1450

On 7/21/03

on behalf of TOWNSEND and TOWNSEND and CREW LLP

By: MAIHANH VO

PATENT
Atty. Docket No.: 014210-000730US
Client Ref. No.: OHSU Ref. No.: 386

IN THE UNITED STATES PATENT AND TRADEMARK OFFICE

In re application of:

ADELMAN et al.

Application No.: 09/254,590

Filed: May 24, 1999

For: SMALL AND INTERMEDIATE-CONDUCTANCE, CALCIUM-ACTIVATED POTASSIUM CHANNELS AND USES THEREOF

Examiner: Michael D. Pak

Technology Center/Art Unit: 1646

SUPPLEMENTAL COMMUNICATION

Commissioner for Patents
P.O. Box 1450
Alexandria, VA 22313-1450

Sir:

This is a Supplemental Communication. The purpose of this Communication is to address issues surrounding the outstanding utility rejection raised by the Examiner in his October 1, 2002 Office Action. The bases for the rejection were clarified during an interview on March 4, 2003. Applicants acknowledge with appreciation the Examiner's time in speaking with applicants' representatives and clarifying the remaining issues.

This invention is the discovery of a family of genes encoding small-conductance calcium activated potassium channels (SK). As noted in the specification, these genes are useful for making screening assays to identify modulators of these ion channels.

During the interview, the Examiner acknowledged these facts and did not dispute their correctness. However, he maintained his position on the utility rejection clarifying two issues of concern. First, the Examiner alleged that there was no known therapeutic utility associated with the SK channels and second, there was concern that not all the members of the gene family would have the same utility.

In response, applicants urge that the small-conductance calcium-activated potassium channels are known to play a role in memory and learning and that the family members are so homologous in structure that they can be used interchangeably in the screening assays described in the specification.

The Small-Conductance Calcium-Activated Potassium Channels are Known To Play A Role in Memory and Learning

On page 5, lines 9-11 of the specification, applicants generally state that there is a need to develop assays which modulate the SK and IK channels for a variety of uses. Among the stated uses are "memory and learning." A specific teaching is found on page 12, lines 15-18 where applicants teach,

> Since SK channels underlie the slow component of the afterhyperpolarization (sAHP) of neurons, alteration of neuronal sAHP provides a means to inhibit epileptic seizures or modulate learning or memory disorders.

The academic literature has been reporting on electrophysiology studies of SK channels for many years prior to the applicants' discovery of the genes encoding the subunits. As early as 1981, it was reported that apamin was a selective blocker of these channels and the channels

were studied using voltage clamps and biochemical methodologies. **Exhibit 1**, Hugues, et al., 1981, Apamin as a selective blocker of the calcium-dependent potassium channel in neuroblastoma cells: Voltage-clamp and biochemical characterization of the toxin receptor, *PNAS USA* 79:1308-1312.

When applicants disclosed that the SK channels play a role in memory and learning, they were not merely speculating as to possible uses. The understanding that these channels play a role in memory and learning was widely reported in the literature from studies involving both electrophysiological experiments and *in vivo* animal experiments. The following articles are representative of this body of literature. Behnisch and Reymann, 1998, Inhibition of apamin-sensitive calcium-dependent potassium channels facilitates the induction of long-term potentiation in the CA1 region of rat hippocampus, *Neuroscience Letters* 253:91-94 (**Exhibit 2**). Induction of long-term potentiation (LTP) is known to play a key role in the physiology of learning.

In addition to the electrophysiology experiments of Behnisch and Reymann, the following three articles describe *in vivo* work in animals leading to the conclusion that the SK channels play a role in learning and memory: **Exhibit 3**, Deschaux *et al.*, 1997, Apamin improves learning in an object recognition task in rats, *Neuroscience Letters*, 222:159-162; **Exhibit 4,** Ikonen *et al.*,1998, Apamin improves spatial navigation in medial septal-lesioned mice, *European J. Pharmacology*, 347:13-21; and **Exhibit 5**, Stackman, *et al.*, 2002, Small Conductance CA^{2+} -Activated K^{+} Channels Modulate Synaptic Plasticity and Memory Encoding, *Journal of Neuroscience*, 22(23) 10163-10171 Collectively, these exhibits show that inhibition of SK channels with apamin improves learning and memory in animals.

Based upon these exhibits, applicants submit that the record fully evidences that the SK family of channels has a known and recognized physiological utility and that this utility is both

specific to that family of genes and is of immediate and practical use. Nothing more is required under the law.

All the members of the SK gene family would have utility in screening assays.

During the interview, the Examiner also raised the possibility that the pending claim scope could embody a gene for which there is no known utility. Presumably, the Examiner is concerned that another SK channel might be found outside the central nervous system. To date applicants are not aware of any SK channels found outside the central nervous system. (**Exhibit 6**, Kohler et al.,1996, Small-conductance, calcium-activated potassium channels from mammalian brain, Science, 273:1709-1714). However, even if an SK channel were found outside the CNS, applicants urge that the claims are sufficiently limited by structure that only evolutionarily related channels are included. And all these channel proteins would be of such similarity in structure that all members of the genus would have utility in the screening assays.

Of course, if one were intent on identifying modulators of memory and learning, one would not optimally choose a gene expressed outside the CNS. But that does not mean that the gene would have no use in the assays described in the specification because its similar structure imputes to similar function in an assay.

The specification teaches that the rat and human genomes each have three variants each of the SK channels. They are designated SK1, SK2, and SK3. They are highly conserved at 80-90% over a core sequence of some 300 amino acids. At page 1710 of **Exhibit 6**, the authors wrote: "The sequences are highly conserved across their transmembrane cores (80 to 90% identity) but diverge in sequence and length within their NH2- and COOH-terminal domains." Thus they all have a similar primary structure.

This structural similarity leads to similar pharmacological function as defined by their common sensitivity to apamin. Apamin is an 18 amino acid protein isolated from bee venom and was described in 1981 (**Exhibit 1**) as a drug that specifically blocks SK channels. Apamin's ability to bind and interact with all the known subtypes of the SK channels is described in **Exhibit 7**, Grunnet et al., 2001, Apamin interacts with all subtypes of cloned small-conductance Ca2+ -activated K+ channels, Pflugers Arch-Eur. J Physiology 441:544-550.

Because apamin inhibits all three SK subtypes, it is submitted that any SK channel that falls within the structural limitations of claim 1 would also be inhibited by apamin. Thus one can easily envision any of the claimed genes being used in screening assays for identifying novel analogs of apamin with improved pharmacological properties. Furthermore, if one wanted to alter target selectivity in either direction, screening assays using different subtypes would be essential.

Applicants submit that **Exhibits 3, 6** and **7**, and these remarks, fully address the Examiner's concerns regarding the possibility that not all members of the SK family would have the same utility. Based on the available information, one of skill would clearly recognize that any of the subtypes could be used in a screening assay for the modulators of the other subtypes.

CONCLUSION

Should the Examiner maintain the utility rejection in spite of the above remarks, he is reminded that the law requires that the PTO shoulder the initial burden of coming forward with evidence as to why an invention lacks utility. Procedurally, it is not the applicants' evidentiary burden until the Examiner has provided scientific and objective reasoning explaining why those of skill would properly question a utility as lacking practical use and lacking specificity.

In the October 1, 2002 Examiner's Action, the basis for rejection under Section 101 has improperly reversed that procedural burden. The Examiner's statements on page 3 and 4, while lengthy, do not provide the requisite objective reasons that might lead one to conclude that the claimed SK channels *would not* have a role in developing assays for drugs that would improve memory and learning. In conflict with the law, the Examiner has impermissibly required the applicants provide evidence in support of their utility statements.

Nonetheless, Applicants were willing to submit evidence and remarks to address the Examiner's concerns in hope that prosecution will be expedited. It is expected that these remarks and exhibits provide that evidence. Should this Supplemental Communication be deemed insufficient in any way, applicants request a detailed explanation supported by sound scientific reasoning as to why the Examiner finds the evidence deficient as well as evidence in support of the Examiner's initial reasoning and conclusion that the SK channels are not involved in memory and learning and therefore would not have any practical and substantial use in screening assays for drugs to modulate memory and learning.

Applicants respectfully submit that all of the outstanding concerns raised by the Examiner in the latest action have been fully addressed and that the claims are in condition for allowance. Should the Examiner believe that a telephonic interview would expedite prosecution he is invited to call the undersigned attorney at the address provided below.

Respectfully submitted,

Dated July 18, 2003

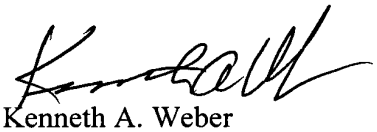

Kenneth A. Weber
Reg. No. 31,677

TOWNSEND and TOWNSEND and CREW LLP
Two Embarcadero Center, 8th Floor
San Francisco, California 94111-3834
Tel: (415) 576-0200
Fax: (415) 576-0300
KAW/dk/jhd

SF 1474570 v1

Proc. Natl. Acad. Sci. USA
Vol. 79, pp. 1308–1312, February 1982
Neurobiology

Apamin as a selective blocker of the calcium-dependent potassium channel in neuroblastoma cells: Voltage-clamp and biochemical characterization of the toxin receptor

(receptor binding/neuroblastoma cell differentiation)

M. HUGUES, G. ROMEY, D. DUVAL, J. P. VINCENT, AND M. LAZDUNSKI

Centre de Biochimie du Centre National de la Recherche Scientifique, Faculté des Sciences, Parc Valrose, 06034 Nice Cedex, France

Communicated by Jean-Marie P. Lehn, October 13, 1981

ABSTRACT This paper describes the interaction of apamin, a bee venom neurotoxin, with the mouse neuroblastoma cell membrane. Voltage-clamp analyses have shown that apamin at low concentrations specifically blocks the Ca^{2+}-dependent K^+ channel in differentiated neuroblastoma cells. Binding experiments with highly radiolabeled toxin indicate that the dissociation constant of the apamin–receptor complex in differentiated neuroblastoma cells is 15–22 pM and the maximal binding capacity is 12 fmol/mg of protein. The receptor is destroyed by proteases, suggesting that it is a protein. The binding capacity of neuroblastoma cells for radiolabeled apamin dramatically increases during the transition from the nondifferentiated to the differentiated state. The number of Ca^{2+}-dependent K^+ channels appears to be at most 1/5th the number of fast Na^+ channels in differentiated neuroblastoma. The binding of radiolabeled apamin to its receptor is antagonized by monovalent and divalent cations. Na^+ inhibition of the binding of ^{125}I-labeled apamin is of the competitive type ($K_{d(Na^+)} = 44$ mM). Guanidinium and guanidinated compounds such as amiloride or neurotensin prevent binding of ^{125}I-labeled apamin, the best antagonist being neurotensin.

In recent years neurotoxins have become essential tools in neurobiological studies (1, 2). Apamin is a bee venom polypeptide of 18 amino acids with two disulfide bridges (3). It is the only polypeptide neurotoxin, as far as we know, that passes the blood–brain barrier. Arg-13 and Arg-14 are in the active site of the toxin (4). Apamin does not seem to interact with receptors of the most classical neurotransmitters (5). Recent K^+ flux studies have suggested that it blocks a Ca^{2+}-dependent K^+ channel (6, 7, 8).

Moolenaar and Spector (8, 9) have reported that the action potential of N1E 115 mouse neuroblastoma cells in solutions containing a high Ca^{2+} concentration was followed by a long-lasting after-hyperpolarization (a.h.p.). This a.h.p. was inferred to be mediated by the activation of a Ca^{2+}-dependent K^+ conductance that is voltage dependent and tetraethylammonium (Et_4N^+) insensitive. The existence of a Ca^{2+}-dependent K^+ conductance has also been demonstrated in a variety of excitable cells such as vertebrate motoneurons, cardiac Purkinje fibers, smooth muscles (10), skeletal myotube cultures (11), etc. It is likely that the Ca^{2+}-dependent K^+ conductance plays a major role in the regulation of the repetitive firing frequency (11).

Two approaches have been used in this paper to study the mode of action of apamin on neuroblastoma cells: first, an electrophysiological approach to determine the specificity of action of apamin on the Ca^{2+}-dependent K^+ conductance; second, a biochemical approach to investigate the properties of the specific binding of apamin to the cell membranes.

The publication costs of this article were defrayed in part by page charge payment. This article must therefore be hereby marked "*advertisement*" in accordance with 18 U. S. C. §1734 solely to indicate this fact.

MATERIALS AND METHODS

Cultures of Neuroblastoma Cells. Neuroblastoma cells (clone N1E 115) were grown as described (12); they were induced to differentiate in the presence of 1% fetal calf serum and 1.5% dimethyl sulfoxide.

Iodination of Apamin. Apamin was purified as described (13). There is no tyrosine residue in the sequence, but there is histidine residue that is not essential for activity (4) and that can be iodinated. It has been found that the procedure previously described to prepare ^{125}I-labeled apamin (^{125}I-apamin) (14) could not be used for the characterization of the ^{125}I-apamin receptor on neuroblastoma cells. The labeled apamin obtained by this technique has a specific radioactivity of only 200–500 Ci/mmol (1 Ci = 3.7×10^{10} becquerels). Apamin (100 μg) was incubated with 2 mCi of $Na^{125}I$ (IMS.30, Amersham) in a 10 mM Tris·HCl buffer at pH 8.6 in a final volume of 200 μl. Four 3-μl portions of 10 mM chloramine-T (Merck) were added at 30-sec intervals. After the last addition of chloramine-T, the mixture was acidified to pH 6 with 0.1 M HCl and the monoiodo derivative was purified on a SP-Sephadex C-25 (Pharmacia) column (0.6 × 21 cm) equilibrated with a 100 mM NaCl/50 mM NaH_2PO_4 buffer at pH 6. The column was eluted first with the equilibration buffer (10 ml) then with a 50 mM NaH_2PO_4 buffer at pH 6 containing 300 mM NaCl. Fractions were 1 ml. The monoiodo derivative was eluted in fraction 32. The specific radioactivity of the monoiodo derivative was 2000 Ci/mmol.

Binding Assays under Various Standard Conditions. Neuroblastoma cells were scraped from culture dishes in an ice-cold medium consisting of 20 mM Tris·HCl, 0.25 M sucrose, and 1 mM EDTA at pH 7.5, centrifuged for 5 min at 1000 × g, resuspended in the same buffer (11–18 mg of protein per ml), divided into aliquots, and stored in liquid nitrogen. The concentration of protein was measured by Hartree's method (15), using bovine serum albumin as a standard. Frozen N1E 115 cells kept their apamin receptor in a stable form. Homogenates from the neuroblastoma cells were obtained with a Potter homogenizer (900 rpm, five strokes). The standard incubation medium for binding experiments consisted of a 20 mM Tris·HCl buffer at pH 7.5 containing bovine serum albumin at 0.5 mg/ml and 5.4 mM KCl.

Cellulose acetate filters (Sartorius, SM 11107, 0.2 μm pore size) used in binding experiments were incubated in 10 mM Tris·HCl (pH 7.5) and 0.1% serum albumin for 1 hr and then washed once with 5 ml of the same buffer at 0°C just before use.

(i) *Kinetics of association and dissociation of ^{125}I-apamin to neuroblastoma cells.* N1E 115 homogenates (0.3 mg of protein per ml) were incubated in the standard medium at 0°C. The

Abbreviations: a.h.p., long-lasting after-hyperpolarization; Et_4N^+, tetraethylammonium.

onset of binding was studied by adding ^{125}I-apamin at 40 pM. Aliquots (0.8 ml) were taken at different times and filtered under reduced pressure. Filters were rapidly washed twice with 5 ml of the washing buffer containing 10 mM Tris·HCl (pH 7.5) and 0.1% bovine serum albumin. Radioactivity bound to filters was measured with an Intertechnique CG 4000 gamma counter.

After 75 min of association the amount of specifically bound ^{125}I-apamin reached a plateau value. At that time, a large excess of unlabeled apamin (1 μM) was added to the incubation medium, thereby displacing the ^{125}I-apamin associated with the receptor. Dissociation kinetics were followed by measuring the decrease in bound ^{125}I-apamin with the filtration technique described above.

A series of experiments has also been carried out in the physiological buffer for neuroblastoma cells: 5.4 mM KCl, 2.8 mM $CaCl_2$, 1.3 mM $MgSO_4$, 140 mM NaCl buffered by 20 mM Tris·HCl at pH 7.5.

(ii) *Equilibrium binding experiments.* N1E 115 homogenate (0.3 mg/ml) was incubated with ^{125}I-apamin at increasing concentrations for 60 min at 0°C. Duplicate aliquots (0.8 ml) were then filtered and the bound radioactivity was measured as described above. Nonspecific binding was determined in parallel experiments in the presence of an excess of unlabeled toxin (1 μM).

(iii) *Competition experiments between labeled and unlabeled apamin.* N1E 115 homogenates (0.3 mg/ml) were incubated for 60 min at 0°C with a fixed concentration of labeled iodotoxin (3.3 pM) and various concentrations of unlabeled toxin in 2 ml of the standard or of the physiological incubation medium. The amount of labeled iodotoxin that remained bound to neuroblastoma cells in the presence of the unlabeled toxin was estimated as described in *ii*.

(iv) *Competition experiments between labeled apamin and monovalent cations, divalent cations, and other drugs.* Experiments were carried out as described in *iii*.

(v) *Protease digestion of the apamin receptor.* N1E 115 homogenates (18 mg/m^1) were incubated for 1 hr at 25°C in the presence of the different proteases in 20 mM Tris·HCl (pH 7.5) containing 1 mM EDTA and 0.25 M sucrose. For papain the digestion was carried out in 6.6 mM dithiothreitol and 1.6 mM cysteine.

Electrophysiological Experiments. Culture dishes containing N1E 115 neuroblastoma cells were used directly for electrophysiological analysis after replacing the culture medium with a modified Earle's medium (90 mM NaCl/5.4 mM KCl/25 mM $CaCl_2$/0.8 mM $MgSO_4$/25 mM Hepes–Tris/25 mM Et_4N^+/5 mM glucose) buffered at pH 7.4. Choline cations were used as a substitute for Na^+ in Na^+-free solution. The culture dish was placed on the warm stage of an inverted microscope (Leitz Diavert) and the temperature was maintained at about 30°C. Experiments were performed by using a suction pipette method which combines internal perfusion with voltage clamp of isolated cells (16–19). The suction pipette had a tip diameter of about 10 μm. The measured tip resistance ranged between 200 and 300 kΩ; the ionic composition of the solution used for internal perfusion was 10 mM NaH_2PO_4, 1 mM $MgCl_2$, 115 mM glutamic acid adjusted to pH 7.1 with KOH and to the osmotic pressure of the external solution (305 milliosmolar) with sucrose.

RESULTS

Voltage-clamp analyses of differentiated N1E 115 neuroblastoma cells have revealed the existence of four voltage-dependent membrane currents: a fast inward Na^+ current blocked by tetrodotoxin, a delayed outward Et_4N^+-sensitive K^+ current, a slow inward Ca^{2+} current, and a slow outward Ca^{2+}-dependent Et_4N^+-insensitive K^+ current (9, 19). In our experiments, only a fraction (about 20%) of the cells bathed in a solution containing 25 mM Ca^{2+} and 20 mM Et_4N^+ displayed an a.h.p. following the spike. Fig. 1 *A* and *B* (*Left*) presents typical a.h.p. obtained by anodal break stimulation when the cells were bathed either in a 90 mM Na^+/25 mM Ca^{2+}/20 mM Et_4N^+ solution or in a 25 mM Ca^{2+}/20 mM Et_4N^+ Na^+-free solution.

In a Na^+-free external solution containing 20 mM Et_4N^+ and 25 mM Ca^{2+}, the only measurable currents in voltage-clamp experiments upon prolonged step depolarizations were the inward Ca^{2+} current and the slow Ca^{2+}-dependent outward K^+ current (Fig. 1*C*, *Left*). The slow outward current was inhibited by Ca^{2+} channel blockers such as La^{3+} (2 mM) (Fig. 2*A*) and Co^{2+} (10 mM) (Fig. 2*B*). For a fixed level of depolarization (+20 mV in the experiment shown in Fig. 2*C*), the maximal intensity of the slow outward current was dependent on the degree of inactivation of the Ca^{2+} channel (Fig. 2*C*). Furthermore, the slow outward current was greatly reduced by internal perfusion with the Ca^{2+}-chelating agent EGTA (1 mM) (Fig. 2*D*). These results are additional indications supporting the view (9) that the slow outward current is due to an internal free Ca^{2+}-mediated K^+ channel activation in neuroblastoma cells.

The only effect of apamin (0.1 μM) was to suppress the a.h.p.

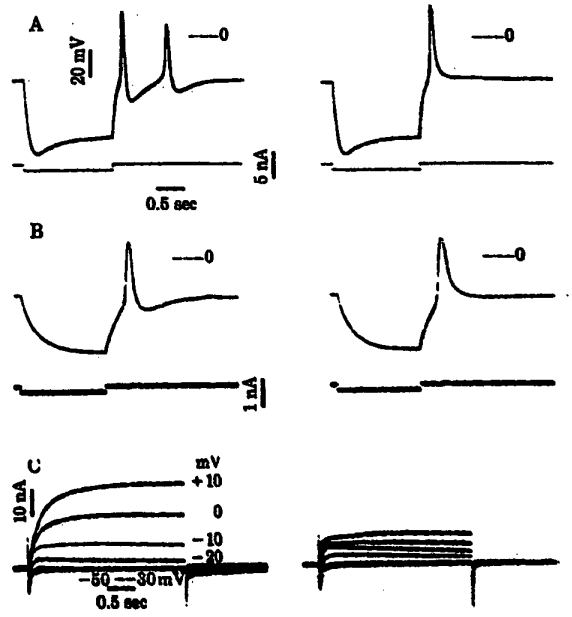

FIG. 1. Selective block by apamin of the a.h.p. following the action potentials of N1E 115 neuroblastoma cells bathed in solutions containing a high concentration of Ca^{2+} (25 mM); voltage-clamp analysis. (*A*) (*Left*) Multiple spike response evoked by anodal break stimulation in a 25 mM Ca^{2+}/90 mM Na^+ solution containing 25 mM Et_4N^+. The a.h.p. following the first spike has partially reactivated the Na^+ conductance, allowing the initiation of a second spike. (*Right*) Same cell, 2 min after the application of 0.1 μM apamin. Note the absence of a.h.p.. (*B*) (*Left*) Ca^{2+} action potential and a.h.p. evoked by anodal break stimulation in a 25 mM Ca^{2+}, Na^+-free solution containing 25 mM Et_4N^+. (*Right*) Suppression of the a.h.p. after a 2-min application of 0.1 μM apamin. In *A* and *B*, the zero voltage line is indicated. (*C*) Voltage-clamp analysis of the effect of apamin on neuroblastoma cells bathed in a 25 mM Ca^{2+}, Na^+-free solution containing 25 mM Et_4N^+. Families of membrane currents associated with different step depolarizations from a holding potential (V_H) of −90 mV. (*Left*) Control currents. (*Right*) Currents 5 min after the addition of 0.1 μM apamin. The Ca^{2+} current was not affected; the Ca^{2+}-dependent slow outward current was strongly depressed.

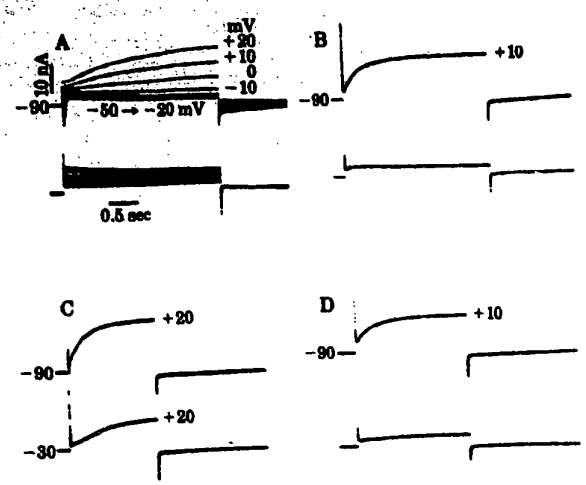

FIG. 2. Evidence for a Ca^{2+}-dependent slow outward current in N1E 115 neuroblastoma cells; voltage-clamp analysis. Inhibition of the slow outward current by Ca^{2+} blockers such as La^{3+} (*A*) or Co^{2+} (*B*), by inactivation of the Ca^{2+} current (*C*) and by internal perfusion with EGTA (*D*). (*A*) Families of membrane currents associated with different step depolarizations from $V_H = -90$ mV. Upper traces, control currents. Lower traces, 2 min after the addition of 2 mM La^{3+}. Note that both the Ca^{2+} inward current and the slow outward current were blocked. (*B*) Upper trace, control current associated with a step depolarization from $V_H = -90$ mV to +10 mV. Lower trace, 5 min after the addition of 10 mM Co^{2+}, the slow outward current was blocked. (*C*) Upper trace, control current associated with a step depolarization from $V_H = -90$ mV to +20 mV. Lower trace, membrane current associated with a step depolarization from $V_H = -30$ mV to +20 mV, 1.5-sec duration followed by a step repolarization to −90 mV. Note the significant reduction of the slow outward current. (*D*) Upper trace, control current associated with a step depolarization from $V_H = -90$ mV to +10 mV. Lower trace, 10 min after the normal internal perfusion solution has been switched to a solution containing 1 mM EGTA. Note the large reduction of the slow outward current.

(Fig. 1 *A* and *B*, *Right*). Voltage-clamp analyses showed that apamin (0.1 μM) is a specific blocker of the slow outward current. The remaining current after 0.1 μM apamin treatment (Fig. 1*C*, *Right*) or after treatment with Ca^{2+} blockers (Fig. 2 *A* and *B*) can be attributed to a nonlinear leakage current; i.e., the leakage conductance is higher in depolarization than around the holding potential (9). The concentration of apamin that blocked 50% of the slow outward current was around 10 nM.

Independent voltage-clamp analyses of the tetrodotoxin-sensitive fast Na^+ current and of the Et_4N^+-sensitive K^+ current showed that the corresponding ionic conductances were unaltered by apamin.

Association and Dissociation Kinetics of the Interaction Between ^{125}I-Apamin and Neuroblastoma Cell Membranes. Typical kinetics of association between ^{125}I-apamin and neuroblastoma cell homogenates are represented in Fig. 3*A*. These experiments were carried out with an ^{125}I-apamin concentration of 40 pM. The concentration of specifically bound ^{125}I-apamin that corresponds to 100% in Fig. 3*A* was 2.28 pM. The free ^{125}I-apamin concentration varied less than 6% during the course of the association kinetics. Fig. 3*A Inset* shows that a semilogarithmic plot of the data is linear, which is expected for a pseudo-first-order reaction. The rate constant of the association is then $k = k_a[^{125}\text{I-apamin}] + k_d$, in which k_a and k_d represent the rate constants of association and dissociation, respectively, of the ^{125}I-apamin–receptor complex. The value of k under conditions used in Fig. 3*A* is 1.3×10^{-3} sec^{-1}.

Fig. 3*B* demonstrates that ^{125}I-apamin bound to neuroblastoma cells can be displaced by unlabeled apamin. Because the presence of a large excess of unlabeled apamin (1 μM) prevents the reassociation of ^{125}I-apamin with neuroblastoma cells, the dissociation process should be first-order with k_d as rate constant. As expected, the semilogarithmic representation of the dissociation data is linear (Fig. 3*B Inset*). The calculated value of k_d from data in Fig. 3*B Inset* is 2×10^{-4} sec^{-1}. The value of k_a calculated from k, k_d, and the ^{125}I-apamin concentration is 2.7×10^7 M^{-1} sec^{-1}. These kinetic data enable us to calculate the dissociation constant of the ^{125}I-apamin–receptor complex: $K_d^* = k_d/k_a = 7.3$ pM.

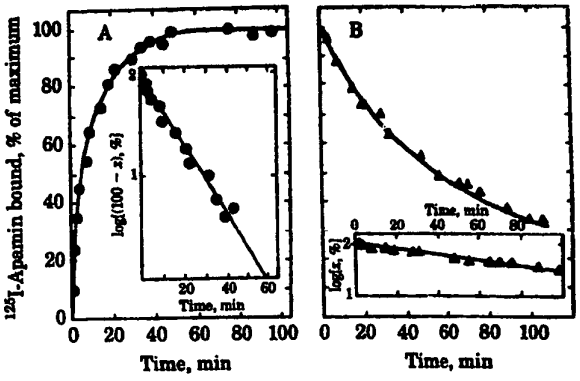

FIG. 3. Association and dissociation kinetics for the binding of ^{125}I-apamin to N1E 115 homogenate. (*A*) Association kinetics of ^{125}I-apamin (40 pM) binding at 0°C to N1E 115 homogenate (0.3 mg/ml). (*Inset*) Semilogarithmic representation of the data; x represents the percentage of maximal ^{125}I-apamin bound. The plateau value (100%) corresponds to 7.6 fmol of ^{125}I-apamin bound per mg of protein. (*B*) Dissociation kinetics of ^{125}I-apamin initiated by addition of 1 μM unlabeled apamin. (*Inset*) Semilogarithmic representation of the data.

Equilibrium Binding of ^{125}I-Apamin to its Receptor in Neuroblastoma Cells. Fig. 4*A* shows typical results of binding experiments in which increasing concentrations of ^{125}I-apamin are added to a fixed concentration of a homogenate of differentiated N1E 115 cells. The specific binding is represented by the difference between total and nonspecific binding. Linearity of the Scatchard plot (Fig. 4*B*) demonstrates that ^{125}I-apamin binds to a single class of noninteracting sites. The dissociation constant, K_d^*, of the complex formed between ^{125}I-apamin and neuroblastoma cells is 22 pM and the maximal binding capacity is 12 fmol/mg of protein.

The Scatchard plot obtained with nondifferentiated neuroblastoma (Fig. 4*B*) indicates a dissociation constant of 32 pM and a maximal binding capacity of 3.2 fmol/mg of protein.

Apamin Receptor Is Degraded by Proteases. Fig. 5 shows drastically decreased levels of ^{125}I-apamin binding to its receptor after treatment of the neuroblastoma cell homogenate with trypsin, chymotrypsin, Pronase, or papain.

Competition Between Unlabeled Apamin and ^{125}I-Apamin. Fig. 6*A* shows that increasing concentrations of unlabeled apamin gradually inhibit ^{125}I-apamin binding to the specific toxin receptor. Half-maximal inhibition of ^{125}I-apamin binding to neuroblastoma cells is at $K_{0.5}$ = 18 pM. The equation for $K_{0.5}$ is: $K_{0.5} = K_d[1 + ([^{125}\text{I-apamin}]_{0.5}/K_d^*)]$, in which $[^{125}\text{I-apamin}]_{0.5}$ is the concentration of free labeled ligand at half-displacement. K_d^* and K_d are the dissociation constants of complexes formed between neuroblastoma and ^{125}I-apamin or unlabeled apamin, respectively. K_d^* is 22 pM (see above) and $[^{125}\text{I-apamin}]_{0.5}$ is 3 pM under the experimental conditions of Fig. 6*A*. K_d is then 16 pM.

Fig. 6*A* also presents a competition experiment under conditions in which the physiological buffer is used instead of the

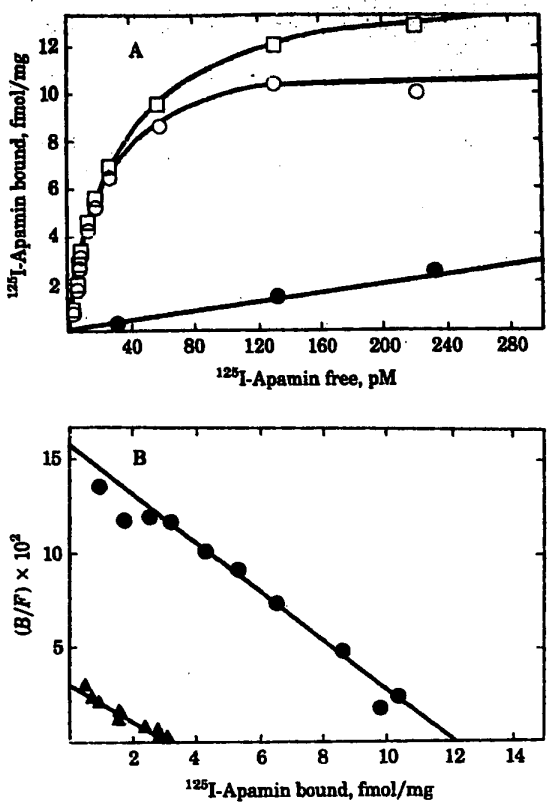

FIG. 4. Binding of ^{125}I-apamin to N1E 115 homogenate under standard conditions. (*A*) N1E 115 homogenate (0.3 mg/ml) was incubated with increasing concentrations of ^{125}I-apamin. □, Total binding. Nonspecific binding (●) was determined in the presence of a large excess of unlabeled toxin (1 μM). Specific binding (○) is the difference between total binding and nonspecific binding. (*B*) Scatchard plot of the data. *B*, bound; *F*, free. Data from differentiated (●) and nondifferentiated (▲) N1E 115 neuroblastoma cells.

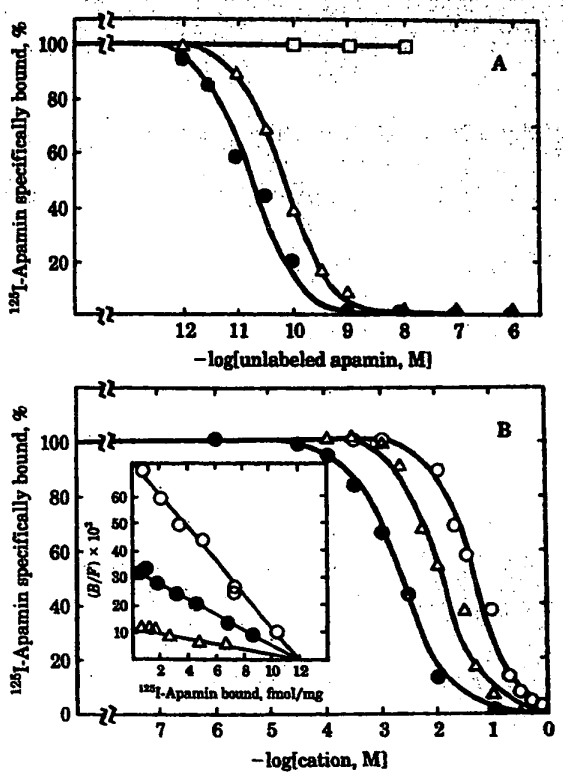

FIG. 6. (*A*) Competition between ^{125}I-apamin and unlabeled apamin in standard conditions (●) and in physiological buffer (△). Competition between ^{125}I-apamin and apamin modified on Arg-13 and Arg-14 by 1,2-cyclohexanedione (□). The concentrations of ^{125}I-apamin were 3.3 pM (●, □) and 26 pM (△). (*B*) Competition in standard conditions between ^{125}I-apamin (3.3 pM) and Ca^{2+} (●), Na^+ (○), and guanidinium (△). (*Inset*) Scatchard plots of the data obtained from binding of ^{125}I-apamin to N1E 115 homogenate (0.15 mg/ml) in the presence of 0 Na^+ (○), 50 mM Na^+ (●), or 100 mM Na^+ (△).

standard buffer. In this case, $K_{0.5}$ = 75 pM and K_d = 49 pM. The nontoxic apamin derivative in which Arg-13 and Arg-14 have been modified by 1,2-cyclohexanedione (4) was unable to prevent ^{125}I-apamin binding to its receptor at concentration up to 0.1 μM (Fig. 6*A*).

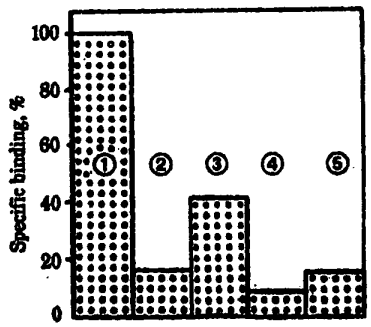

FIG. 5. Protease degradation of the apamin receptor. The homogenate (18 mg/ml) was incubated in 20 mM Tris·HCl/1 mM EDTA/0.25 M sucrose (pH 7.5) for 1 hr at 25°C in the absence of protease (bar 1) or in the presence of trypsin at 0.1 mg/ml (bar 2), chymotrypsin at 0.5 mg/ml (bar 3), Pronase at 0.1 mg/ml (bar 4), or papain at 0.1 mg/ml (bar 5). Proteolysis was stopped by washing the homogenate with ice-cold buffer (20 vol) three times, then specific binding of ^{125}I-apamin (3.3 pM) to each homogenate was measured.

Effect of Monovalent and Divalent Cations on ^{125}I-Apamin Binding to its Receptor. In all these experiments N1E 115 homogenates were incubated under standard conditions (20 mM Tris·HCl/5.4 mM KCl, pH 7.5) in the presence of ^{125}I-apamin (3.3 pM) and at different concentrations of mono- and divalent cations. Na^+, guanidinium, and Ca^{2+} inhibit ^{125}I-apamin binding (Fig. 6*B*). Fifty percent inhibition ($K_{0.5}$) is observed at 2 mM Ca^{2+}, 44 mM Na^+, and 12 mM guanidinium. Choline inhibits ^{125}I-apamin binding like Na^+ or guanidinium, with a $K_{0.5}$ value of 25 mM. Et_4N^+ inhibits ^{125}I-apamin binding with a $K_{0.5}$ value of 6 mM.

The large differences in affinity of apamin for its receptor measured by electrophysiology on one hand and by binding experiments with ^{125}I-apamin on the other hand are explained by the experimental conditions required in the voltage-clamp approach—i.e., high Ca^{2+} (25 mM), choline (90 mM), and Et_4N^+ (20 mM) concentrations.

Scatchard plots of ^{125}I-apamin binding (Fig. 6*B*, *Inset*) show that increasing Na^+ concentrations do not change the maximal binding capacity of neuroblastoma membranes, they only change the apparent dissociation constant, which increases from 25 pM at 0 mM Na^+ to 150 pM at 100 mM Na^+. This is the typical indication that Na^+ is a competitive inhibitor of ^{125}I-apamin binding to its receptor.

Effects on ^{125}I-Apamin Binding of Neurotransmitters, Neuropeptides, and Drugs Acting on Transmitter Receptors or Ionic Channels. Histamine (10 μM), γ-aminobutyric acid (10 μM), glutamic acid (10 μM), epinephrine (1 μM), norepinephrine (1 μM), acetylcholine (1 μM), glycine (1 μM), serotonin (1 μM), and dopamine (1 μM) are without effect on ^{125}I-apamin binding. Diazepam (1 μM), lysergic acid diethyl amide (1 μM), strychnine (100 μM), and isoproterenol (1 μM) are also without effect. Toxins specific for the fast Na^+ channel (1, 2), such as tetrodotoxin, veratridine, sea anemone toxin II, or pure scorpion toxins from *Androctonus*, *Tityus*, or *Centruroides* venom are also without effect at concentrations as high as 1 μM.

Amiloride, a specific blocker of epithelial Na^+ channels (20), inhibits ^{125}I-apamin binding to its receptor with a $K_{0.5}$ of 0.25 mM. Verapamil, a blocker of the Ca^{2+} channel, also inhibits ^{125}I-apamin binding with a $K_{0.5}$ of 0.10 mM. The most active molecule in inhibiting ^{125}I-apamin binding is the polypeptide neurotensin. The $K_{0.5}$ value in that case is 0.4 μM.

DISCUSSION

This paper demonstrates by using voltage-clamp techniques that apamin blocks a Ca^{2+}-dependent K^+ conductance. This blockade is very selective, because apamin is without effect on other ionic channels such as the fast Na^+ channel, the Et_4N^+-sensitive K^+ channel, or the slow Ca^{2+} channel. Under the particular conditions used for the electrophysiological study of the Ca^{2+}-dependent K^+ conductance (25 mM Ca^{2+}), a complete block of the channel is observed at 100 nM apamin.

The use of a very highly radiolabeled derivative of apamin, ^{125}I-apamin, permitted a detailed study of the interaction of the toxin with its receptor in neuroblastoma cells. The binding is saturable and specific. Nontoxic derivatives modified on Arg-13 and Arg-14 (4) do not prevent ^{125}I-apamin binding to its receptor. The interaction of apamin with its receptor has the following properties: (*i*) the dissociation of the toxin from its receptor is slow, with a half-life that may be as low as 58 min at 0°C and pH 7.5; (*ii*) the K_d value of the apamin–receptor complex is 16–22 pM under standard conditions; (*iii*) the apamin receptor is destroyed by proteases (trypsin, chymotrypsin, Pronase, papain) and is therefore probably a protein.

The maximal number of binding sites found on differentiated neuroblastoma cells is 12 fmol/mg of protein; it is about 1/5th of that found for fast Na^+ channels in the same preparation using a radiolabeled tetrodotoxin derivative [58 fmol/mg of protein (21)].

One of the interesting properties of the Ca^{2+}-dependent K^+ channel is that it develops during differentiation in low serum concentrations and in the presence of dimethyl sulfoxide. Nondifferentiated neuroblastoma cells do not have Ca^{2+}-dependent K^+ conductances that can be detected electrophysiologically. Moreover, comparable titrations of the apamin receptor in undifferentiated and in differentiated cells show an increase in number of apamin sites by a factor of about 4, without modification of the receptor properties since the dissociation constant remains essentially unchanged. Because a small percentage of cells are already morphologically differentiated before treatment with dimethyl sulfoxide and because all of the cells are not differentiated after treatment with low serum concentration plus dimethyl sulfoxide, it is possible that Ca^{2+}-dependent K^+ conductances are completely absent in undifferentiated neuroblastoma cells, whereas they are fully developed after differentiation.

Ionic conditions are of particular importance for the binding of apamin to its receptor (14). Various monovalent and divalent cations prevent ^{125}I-apamin binding to its receptor (Na^+, guanidinium, choline, Ca^{2+}). Because of these inhibitory effects of cations, under physiological conditions (5.4 mM K^+/2.8 mM Ca^{2+}/1.3 mM Mg^{2+}/100 mM Na^+/20 mM Tris·HCl, pH 7.5), the K_d value of apamin for its receptor is shifted to 71 pM (Fig. 6A).

The competition of guanidinium ions for ^{125}I-apamin binding is probably the result of the fact that the active site of the toxin contains two guanidinium groups, on Arg-13 and Arg-14. Moreover, amiloride, which is also a guanidinated molecule, also prevents ^{125}I-apamin binding. However the most active compound in preventing ^{125}I-apamin association to its receptor is neurotensin. This neuropeptide of 13 amino acids has two contiguous arginines in its active site (22).† Other charged molecules like verapamil also interfere with ^{125}I-apamin binding to the neuroblastoma membrane.

Since Ca^{2+}-dependent K^+ channels are now found in a large number of excitable cells preparations, we feel that apamin will play a role for this channel analogous to that played by the different toxins specific for the fast Na^+ channel (1).

We thank Dr. C. Frelin and M. T. Ravier for providing neuroblastoma cells, Dr. H. Schweitz for purifying apamin, E. Van Obberghen-Schilling for a careful reading of the manuscript, and C. Bonifacino for skilful technical help. This work was supported by the Centre National de la Recherche Scientifique, the Commissariat à l'Energie Atomique, The Fondation pour la Recherche Médicale, and the Institut National de la Santé et de la Recherche Médicale (C.R.L. no. 80.60.15).

1. Narahashi, T. (1974) *Physiol. Rev.* 54, 813–889.
2. Howard, B. D. & Gunderson, C. B., Jr. (1980) *Annu. Rev. Pharmacol.* 20, 307–336.
3. Habermann, E. (1972) *Science* 177, 314–322.
4. Vincent, J. P., Schweitz, H. & Lazdunski, M. (1975) *Biochemistry* 14, 2521–2525.
5. Cavey, D., Vincent, J. P. & Lazdunski, M. (1979) *Toxicon* 17, 176–179.
6. Banks, B. E. C., Brown, C., Burgess, G. M., Burnstock, G., Claret, M., Cocks, T. M. & Jenkinson, D. H. (1979) *Nature (London)* 282, 415–417.
7. Burgess, G. M., Claret, M. & Jenkinson, D. H. (1981) *J. Physiol. (London)* 317, 67–90.
8. Moolenaar, W. H. & Spector, I. (1979) *J. Physiol. (London)* 292, 307–323.
9. Moolenaar, W. H. & Spector, I. (1979) *J. Physiol. (London)* 292, 297–306.
10. Meech, R. W. (1978) *Annu. Rev. Biophys. Bioeng.* 7, 1–18.
11. Barrett, J. N., Barrett, E. F. & Dribin, L. B. (1981) *Dev. Biol.* 82, 258–266.
12. Jacques, Y., Fosset, M. & Lazdunski, M. (1978) *J. Biol. Chem.* 253, 7383–7392.
13. Gauldie, J., Hanson, J. M., Rumjanek, F. D., Shipolini, R. A. & Vernon, C. A. (1976) *Eur. J. Biochem.* 61, 369–376.
14. Habermann, E. & Fischer, K. (1979) *Eur. J. Biochem.* 94, 355–364.
15. Hartree, E. F. (1972) *Anal. Biochem.* 48, 422–427.
16. Kostyuk, P. G. & Krishtal, O. A. (1977) *J. Physiol. (London)* 270, 545–568.
17. Lee, K. S., Akaike, N. & Brown, A. M. (1978) *J. Gen. Physiol.* 71, 489–508.
18. Reuter, H. & Stevens, C. F. (1980) *J. Membr. Biol.* 57, 103–118.
19. Moolenaar, W. H. & Spector, I. (1978) *J. Physiol. (London)* 278, 265–286.
20. Lindeman, B. (1980) *J. Membr. Biol.* 54, 1–11.
21. Frelin, C., Vigne, P. & Lazdunski, M. (1981) *Eur. J. Biochem.* 119, 437–442.
22. Kitabgi, P., Poustis, C., Granier, C., Van Rietschoten, J., Rivier, J., Morgat, J. L. & Freychet, P. (1980) *Mol. Pharmacol.* 18, 11–19.

† Whereas neurotensin prevents ^{125}I-apamin binding, apamin does not prevent [^{3}H]neurotensin binding to its receptor (P. Kitabgi, personal communication). This shows that the receptors for the two peptides are completely distinct.

ELSEVIER

Neuroscience Letters 253 (1998) 91–94

Neuroscience Letters

Inhibition of apamin-sensitive calcium dependent potassium channels facilitate the induction of long-term potentiation in the CA1 region of rat hippocampus in vitro

Thomas Behnisch[a,b,*], Klaus G. Reymann[a,b]

[a]Leibniz Institute for Neurobiology, Project Group Neuropharmacology, 39008 Magdeburg, Germany
[b]Institute of Applied Neurosciences gGmbH, P.O. Box 1860, 39008 Magdeburg, Germany

Received 15 June 1998; received in revised form 17 July 1998; accepted 22 July 1998

Abstract

Using field potential recording in the CA1-region of rat hippocampal slices we investigated the effect of apamin; a specific antagonist of small conductive calcium activated potassium channels on long-term potentiation (LTP). The experiments revealed that LTP of excitatory postsynaptic potentials induced by a single 100 Hz tetanization was intensified by extracellular application of apamin in a concentration range of 1–200 nM. No effects of apamin on LTP induced by triple 100 Hz tetanization were seen. We conclude that the positive modulation of LTP by apamin is effective in a nanomolar concentration range and dependent upon the employed tetanization. Because it has been shown that apamin-binding sites are affected by learning disorders including Alzheimer's disease, our finding suggests that changes in the sensitivity to apamin may result in memory disorders. © 1998 Elsevier Science Ireland Ltd. All rights reserved

Keywords: Hippocampus; Long-term potentiation; Apamin; Bee venom; Calcium dependent potassium channels

The stability of long-lasting synaptic efficacy enhancement is achieved by a diversity of signal cascades, which themselves have been affected by certain pre and/or postsynaptic activities during memory-specific consolidation processes [1,16]. The neuronal excitability and the properties of neuronal interactions can be partially influenced by changes of the efficiency of different classes of potassium channels. Inhibition of the calcium-dependent potassium channel, for example by apamin elicits in compact neurons of the substantia nigra, irregular firing or bursting by abolishing the slow after-hyperpolarization [15]. Apamin is a specific antagonist of small conductive calcium activated voltage-independent potassium channels, which can contribute to the regulation of firing rates of certain cell types [10]. Binding sites of the 18-amino acid toxin apamin [2], isolated from bee venom were found in various thalamic and hippocampal structures (review [5] and [6,13]). Whereas the involvement of calcium-dependent potassium channels in modulation of synaptic plasticity was described [14,17], the role of apamin sensitive channels in plasticity is not well studied. Apamin failed to induce a slow onset potentiation, which is in contrast to the described effects of the bee venom mast cell degranulating peptide [11]. However, investigations of the effects of apamin in vivo revealed its effectiveness to modify memory-specific consolidation processes [3,4,12]. Thus, application of apamin in vivo improved learning and memory retention of rats [4,7]. Moreover, apamin-binding sites are affected by learning disorder diseases of human, indicating those implications in learning and memory processes [8].

Thus, we were interested to investigate the relevancy of apamin-sensitive potassium channels for long-term potentiation (LTP) in hippocampus, a cellular model for synaptic plasticity thought to be required for memory formation. Here we describe the facilitatory effects of apamin on field potential potentiation induced in the hippocampal CA1 region.

Hippocampal slices were prepared from male rats (7–8 weeks old) of the Wistar outbred strain MOL: WIST

* Corresponding author. Tel.: +49 391 6263437; fax: +49 391 6263438; e-mail: behnisch@ifn-magdeburg. de

0304-3940/98/$19.00
PII S0304-3940(98)00612-0

(SHOE). After decapitation and dissection of the hippocampus 400 μm transverse slices were cut in ice-cold oxygenated artificial cerebrospinal fluid (ACSF in mM: NaCl 124, KCl 4.9, $MgSO_4$ 1.3, $CaCl_2$ 2.5, KH_2PO_4 1.2, $NaHCO_3$ 25.6, D-glucose 10, saturated with 95% O_2, 5% CO_2; pH 7.3). Hippocampal slices were transferred to a submerged slice chamber and perfused with 32°C ACSF (2.5 ml/min).

Synaptic responses were elicited by stimulation of the Schaffer collateral commissural fibres in the stratum radiatum of hippocampal Ca1-region using lacquer-coated stainless steel stimulating electrodes. Glass electrodes (filled with ACSF, 1–4 MΩ) were placed in the stratum radiatum of the CA1 region to record excitatory postsynaptic field potentials (fEPSPs). The slope of the negative fEPSF rise and the amplitude of population spikes (PSs) were used as parameters. fEPSF and PSs were recorded together in the most experiments with exception of the 200 nM apamin application experiments. In these experiments the fEPSPs were recorded without PS recording. After an analysis of a fEPSP input/output curve, the test stimulation strength was always adjusted to 35% of the fEPSP slope maximum. During the baseline recording four single stimuli (10 s intervals) were averaged every 5 min. After stabilization of the fEPSP and PSs values, LTP was induced either using a single 100 Hz frequency stimulation with a 400 ms duration (total biphasic pulse-width ~0.4 ms) or triple 100 Hz tetanization with a duration of 500 ms. FEPSP and PSs values were analyzed every 5 min within the whole experiment.

Apamin (Sigma) was applied by bath-application 10 min before and up to 5 min after the tetanization. The toxin was dissolved in ACSF and the solutions were adjusted to a pH of 7.3. For the interpretation of the statistical significance of differences between the control group and toxin-treated group the values within single time points were analysed with the Mann-Whitney *U*-test (independent samples $P \leq 0.05$).

To study the effect of apamin on hippocampal LTP induced with a single 100 Hz tetanization the toxin was applied 10 min before to 5 min after tetanization. The presence of 100-nM apamin led to an enhancement of the fEPSP potentiation (see Fig. 1A).

Both the initial and the late potentiation of the field potentials were affected and the difference between the toxin group and the control group was significant throughout immediately afterwards tetanization ($P < 0.05$). The described effect of apamin or LTP was dependent upon the toxin concentration used. As it is shown in Fig. 2A the fEPSP potentiation (60 min after tetanization) was enhanced significantly only by apamin concentrations of 10, 100 and 200 nM. No further increase of the fEPSF potentiation enhancement by 100 and 200 nM apamin was found, indicating the saturation of the mechanisms responsible for the apamin effect at low apamin concentration. In contrast to the described apamin actions on fEPSP potentiation, an effect on initial and late potentiation of population spikes was detected only at an apamin concentration of 100 nM (see Figs. 1B and 2B). Application of 100 nM apamin for 15 min did not alter the baseline values of fEPSPs or PSs within recording periods (before apamin application: fEPSP 99.6 ± 0.5% and PS 100 ± 0.9%; 10 min after apamin application: fEPSP 98.4 ± 0.6% and PS 103 ± 2.3%: see Fig. 1A,B). The control values for similar time periods in the baseline apamin experiments revealed: before, fEPSP

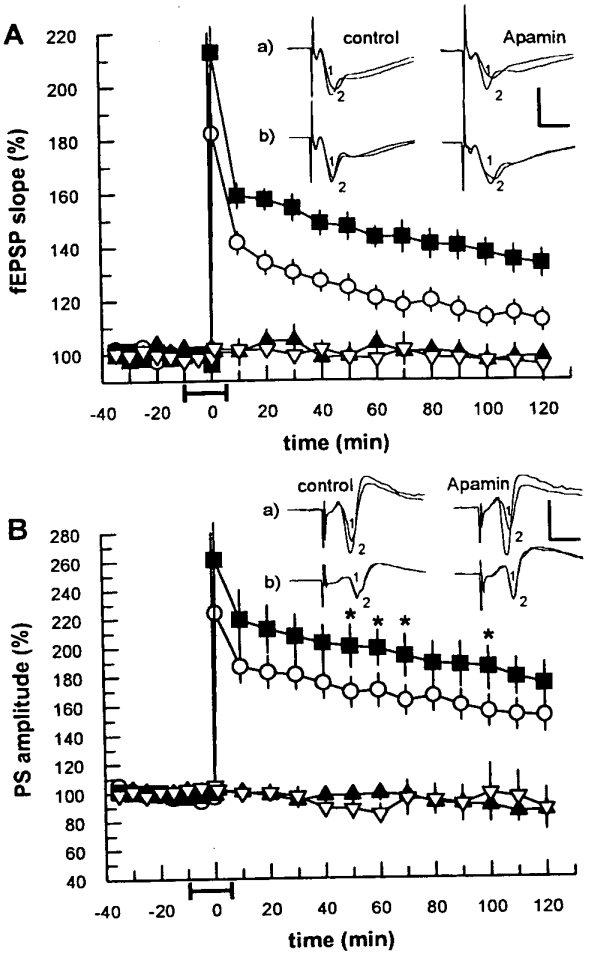

Fig. 1. Extracellular application of apamin (100 nM; black line) during single 400 ms 100 Hz tetanization enhanced fEPSP potentiation significantly throughout, after tetanization (A; control group: open circles ($n = 9$); toxin treated group: black squares ($n = 11$); black bracket: $P < 0.05$). No baseline effects of 100 nM apamin were observed (control: open triangle ($n = 6$); toxin: black triangle, ($n = 5$)). (B) A weak effect of apamin or the PS potentiation was observed (control group, $n = 9$; toxin treated group, $n = 11$). Asterisks mark the time points which were significantly different from the control group ($P < 0.05$). Baseline values of both control (open triangle, $n = 6$) and toxin-treated group (black triangle, $n = 5$) were similar. LTP was induced at the time zero with a 400 ms long single 100 Hz train. Analog traces on the right upper side of the diagrams (A) and (B) represent typical recordings of LTP (a) and baseline (b experiments taken 5 min before (1), and 60 min after tetanization (2). Calibration: vertical bar, 2mV; horizontal bar, 4 ms.

99.7 ± 0.6% and PS 100 ± 1%; after, fEPSP 99.7 ± 0.6% and PS 99 ± 1.7%.

Using another tetanization protocol (triple 100 Hz tetanization) LTP was inducer which was not affected by application of 100 nM apamin (initial potentiation: fEPSP 259 ± 17%, 274 ± 15% and PS: 223 ± 23%, 224 ± 24%; 4 h after tetanization: fEPSP 158 ± 16%, 143 ± 16% and PS 203 ± 18%, 186 ± 35% for control (n = 6) and toxin-treated group (n = 6); respectively).

To clarify, whether the apamin effect is mediated by changes in the excitability of CA1 neurons, half-maximum antidromic spikes were induced by a 50 Hz stimulation of the CA1 axon in the alveus without and with 100-nM apamin. Comparing the amplitudes of the antidromic spikes without and with apamin it was possible to show that apamin did not affect the antidromic spike burst (data not shown; toxin, n = 6; control, n = 61).

Experiments, reported in this paper show that apamin enhances LTP within a nanomolar concentration range. The effective concentration of apamin action on LTP was in the range of 1–200 nM. The effectiveness of apamin on fEPSP potentiation enhancement has been clearly shown only for LTP induced with a single tetanization and not for potentiation elicited with the triple tetanization protocol. A special feature of the used strong tetanization paradigm is that a triple tetanization induces a longer lasting more saturated potentiation, which probably impedes to recognize effects of apamin on such LTP.

The effect of apamin on PS potentiation was not similarly pronounced as in comparison to apamin effects on fEPSP potentiation. It is known, that the dependence of PS upon increasing fEPSPs is not linear and is determined by the experimental conditions and by the physiological state of the neuronal circuit elements [9]. Thus, we have analyzed the effect of 200-nM apamin on fEPSP potentiation alone, without PS recording. This experiment revealed that the apamin effect on fEPSP potentiation is already saturated by a 100-nM apamin concentration. Apamin antagonizes specific calcium-dependent potassium channels, which themselves have generally a high diversity and contribute differentially to the after-hyperpolarization occurring after spike generation. The afterhyperpolarization has several components: the fast one contributes to repolarization of the action potential and regulates interspike interval, whereas subsequent slow components are responsible for spike-frequency adaptation [10]. Calcium dependent potassium channels of excitatory CA1 neurons are not affected by apamin, and moreover, this compound is ineffective in inhibition of slow afterhyperpolarization and regulation of spike accommodation in CA1 neurons [18]. These observations are in agreement with our results, that apamin does not change the antidromic spike generation, used as an indicator for possible changes of CA1 neuron excitability. However calcium-dependent potassium channels of stratum oriens interneurons have a high sensitivity for apamin and their spike frequency is affected by this toxin [10,19]. Thus, we propose that the apamin-mediated facilitation of LTP is partially caused by changes of excitability of interneurons, regulating the strength of CA1 pyramidal cell excitation during orthodromic tetanization.

Despite the yet unidentified localisation of the apamin effect on LTP we could show that apamin-sensitive potassium channels could be involved in regulation of synaptic plasticity establishment. This positive modulatory effect of apamin on LTP might be responsible for the described observations that in vivo injections of apamin improved learning and memory retention [3,4,7,12]. On the other hand, apamin-binding, sites are affected by learning disor-

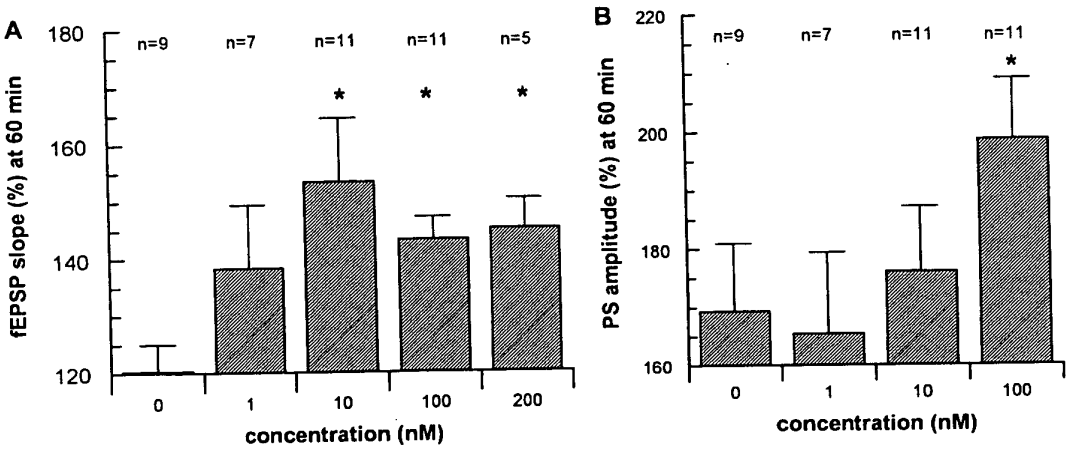

Fig. 2. (A) The effectiveness of apamin to enhance the fEPSP potentiation (values 60 min after tetanization) was investigated at a concentration range of 1–200 nM. The number of single experiments is indicated over the bars. Asterisks mark the experimental groups which were significant different from the control group ($P < 0.05$). (B) The apamin dependent facilitation of PS potentiation 60 min after tetanization is only significant at the concentration of 100 nM.

ders including Alzheimer's disease [8] that might indicate the relevancy of apamin binding sites for memory processes in human.

We are grateful to Katrin Böhm for expert technical assistance and Tariq Ahmed for critical comments.

[1] Bliss, T.V. and Collingridge, G.L., A synaptic model of memory: long-term potentiation in the hippocampus, Nature, 361 (1993) 31–39.
[2] Chau, M.H. and Nelson, J.W., Cooperative disulfide bond formation in apamin, Biochemistry, 31 (1992) 4445–4450.
[3] Deschaux, O. and Bizot, J.C., Effect of apamin, a selective blocker of Ca^{2+} activated K^+-channel on habituation and passive avoidance responses in rats, Neurosci. Lett., 227 (1997) 57–60.
[4] Deschaux, O., Bizot, J.C. and Goyffon, M., Apamin improves learning in an object recognition task in rats, Neurosci. Lett., 222 (1997) 159–162.
[5] Gehlert, D.R. and Gackenheimer, S.L., Comparison of the distribution of binding sites for the potassium channel ligands [^{125}I]apamin, [^{125}I]charybdotoxin and [^{125}I]iodoglyburide in the rat brain, Neuroscience, 52 (1993) 191–205.
[6] Habermann, E., Apamin, Pharmacol. Ther., 25 (1984) 255–265.
[7] Heurteaux, C., Messier, C., Destrade, C. and Lazdunski, M., Memory processing and apamin induce immediate early gene expression in mouse brain, Brain Res. Mol. Brain Res., 18 (1993) 17–22.
[8] Ikeda, M., Dewar, D. and McCulloch, J., Selective reduction of [^{125}I]apamin binding sites in Alzheimer hippocampus: a quantitative autoradiographic study, Brain Res., 567 (1991) 51–56.
[9] Izumi, Y. and Zorumski, C.F., Developmental changes in long-term potentiation in CA1 of rat hippocampal slices, Synapse, 20 (1995) 19–23.
[10] Kohler, M., Hirschberg, B., Bond, C.T., Kinzie, J.M., Marrion, N.V., Maylie, J. and Adelman, J.P., Small-conductance, calcium-activated potassium channels frog mammalian brain, Science, 273 (1996) 1709–1714.
[11] Kondo, T., Ikenaka, K., Fujimoto, I., Aimoto, S., Kato, H., Ito, K., Taguchi, T., Morita, T., Kasai, M. and Mikoshiba, K., K^+ channel involvement in induction of synaptic enhancement by mast cell degranulating (MCD) peptide, Neurosci. Res., 13 (1992) 207–216.
[12] Messier, C., Mourre, C., Bontempi, B., Sif, J., Lazdunski, M. and Destrade, C., Effect of apamin, a toxin that inhibits Ca^{2+}-dependent K channels, on learning and memory processes, Brain Res., 551 (1991) 322–326.
[13] Mourre, C., Fournier, C. and Soumireu-Mourat, B., Apamin, a blocker of the calcium-activated potassium channel, induces neurodegeneration of Purkinje cells exclusively, Brain Res., 778 (1997) 405–408.
[14] Murakami, N., Sakai, N., Nei, K., Matsuyama, S., Saito, N. and Tanaka, C., Potassium and calcium channel involvement in induction of long-lasting synaptic enhancement by calyculin A, a protein phosphatase inhibitor, in rat hippocampal CA1 region, Neurosci. Lett., 176 (1994) 181–184.
[15] Osmanovic, S.S., Shefner, S.A. and Brodie, M.S., Functional significance of thc apamin-sensitive conductance in rat locus coeruleus neurons, Brain Res., 530 (1993) 283–289.
[16] Reymann, K.G. and Staak, S., Molecular mechanism underlying long-term potentiation: postsynaptic glutamate receptors and protein kinase C. In P.L Canonico, U. Scapgnini, F. Pamparana and A. Routtenberg (Eds.), Protein Kinase C in the CNS: Focus on Neuronal Plasticity (Proceedings), Masson, Milan, 1994, pp. 31–38.
[17] Sah, P. and Bekkers, J.M., Apical dendritic location of slow afterhyperpolarization current in hippocampal pyramidal neurons: implications for the integration of long-term potentiation, J. Neurosci., 16 (1996) 4537–4542.
[18] Storm, J.F., An after-hyperpolarization of medium duration in rat hippocampal pyramidal cells, J. Physiol. (Lond.), 409 (1989) 171–190.
[19] Zhang, L. and McBain, C.J., Potassium conductances underlying repolarization and after-hyperpolarization in rat CA1 hippocampal interneurones, J. Physiol. (Lond.), 488 (1995) 661–672.

ELSEVIER

Neuroscience Letters 222 (1997) 159–162

NEUROSCIENCE LETTERS

Apamin improves learning in an object recognition task in rats

O. Deschaux[a,*], J.C. Bizot[a], M. Goyffon[b]

[a]*Service de Pharmacologie, Centre d'Etudes du Bouchet, ETCA- BP no. 3, 91710 Vert le Petit, France*
[b]*LERAI, Museum National d'Histoire Naturelle, 57 rue Cuvier, 75005 Paris, France*

Received 8 October 1996; revised version received 8 January 1997; accepted 8 January 1997

Abstract

Object recognition was investigated in rats in a two trial unrewarded task. In the first trial, two copies of the same object were presented. In the second trial, one of the familiar object and a new object were presented. Rats explored the new object longer than the familiar object when the intertrial time was 1 h, indicating that they remembered the familiar object, but not when the intertrial time was 24 h. Rats injected with apamin (a toxin which blocks specifically Ca^{2+}-activated K^+-channels) before the first trial spent more time in exploring the new object than the familiar object at the second trial, when it took place 24 h after the first trial. Injection of apamin just after the first trial or before the second trial did not modify the difference in exploration time between the new and the familiar object. These results suggest that the blockade of Ca^{2+}-activated K^+-channels could improve learning, but not consolidation nor restitution of the information, in an object recognition task. © 1997 Elsevier Science Ireland Ltd.

Keywords: Learning; Memory; Object recognition; Apamin; Toxin; Rat

Apamin, an active principle of the *Apis mellifera* honeybee venom, is an octadecapeptide with two disulphide bonds [7]. This toxin is a selective blocker of a particular class of Ca^{2+}-activated K^+-channel (K_{Ca} channel) which is characterized by its relatively high sensitivity to intracellular Ca^{2+} concentration, lack of voltage dependence, and small conductance. This channel is involved in the slow phase of the afterhyperpolarization that follows action potentials in many excitable cells [2,17]. In mice and rats, apamin produces signs of poisoning like tremors, ataxia and lethal respiratory insufficiency [11]. Auto radiographic binding studies with [^{125}I]apamin have shown that apamin binding sites are numerous in many regions of the central nervous system (CNS), with a highest density in the limbic forebrain [4,14] and there is evidence that apamin penetrates the blood–brain barrier [5].

It has been claimed that apamin could facilitate memory processes when injected at non-convulsant doses, either before or immediately after partial acquisition in an appetitively-motivated bar-pressing response in mice [13]. Moreover, apamin increases the expression of immediate early genes c-fos and c-jun by learning in the hippocampal formation. This immediate early gene can be related to the apamin induced facilitation of learning [8].

Therefore, apamin has been shown to increase the firing rate of cholinergic neurons of the medial septum diagonal band region [12], an area controlling both the cholinergic and glutamatergic innervations of the hippocampal formation (via the cholinergic septohippocampal pathway and the septal projection to the entorhinal cortex, respectively, which is the major source of hippocampal glutamatergic innervation) [10]. So apamin seems to act on the hippocampus, one of the principal areas controlling learning and memory.

In order to better delineate the implication of apamin sensitive K_{Ca} channel in memory processes, we investigated the effects of apamin on memory, as assessed in an object recognition task. This task measures innate exploratory behavior. It seems to be a useful tool to study memory in rats since it was likely to show either disruption or improvement of memory processes by drugs [1,9].

The animals used were male Wistar rats (Janvier, France) weighting 180–220 g. They were housed five per cage in a regulated environment with a 12-h light/dark cycle. They had free access to food and water. The

* Corresponding author. Tel.: +33 1 69908267; fax: +33 1 64935266

0304-3940/97/$17.00
PII S0304-3940(97)13367-5

animals were used for experimentation after adaptation to laboratory conditions for at least 5 days.

The apparatus of the object recognition task was an open box made of Plexiglas (60 cm length; 60 cm width; 30 cm height). The objects to be discriminated (pyramid or staircase, 5 cm height) were made of grey PVC and apparently, they had no natural significance for rats and they had never been associated with a reinforcer.

The day before testing the rats were allowed to explore the apparatus for 2 min. On the day of the test, at the first 2 min sample trial (T1), two identical objects (termed as sample objects) were presented in two corners of the box. In the second 2 min choice trial (T2), one of the objects presented in T1 was replaced by a new object. In a first experiment conducted in order to demonstrate that rats are able to recognize the object presented in T1, a short interval of 1 h separated T1 and T2. In the following experiments, since a promnesic effect of apamin was expected, a long interval of 24 h separated T1 and T2. In this way, control rats are unable to recognize the object presented at T1, as shown below. From rat to rat, the role (sample or new object) as well as the relative position of the two objects were counterbalanced and randomly permuted.

A new set of cleaned objects was always put into the box to rule out the possibility of scent traces left on the objects and therefore the dependency of the recognition capacity of rats on the olfactory cue.

The basic measure was the time (in seconds) taken by the rats in exploring objects in the two trials. Exploration was considered directing the nose to the object at a distance ≤2 cm and/or touching it with the nose; turning around or sitting on the object was not considered as exploratory behavior. The rats were observed on a closed-circuit TV screen and their exploration time was manually kept.

Apamin (Latoxan, France) was dissolved in saline, and administered intraperitoneally. All administrations were given in a volume of 1 ml/kg body weight. Control rats received saline (0.9% NaCl solution). In the first experiment, rats received saline 30 min before T1, and T2 was performed 1 h after T1. To study the effects of apamin on learning, consolidation and restitution of the information, the toxin was administered either 30 min before T1 (experiment 2), just after T1 (experiment 3) or 30 min before T2 (experiment 4), respectively.

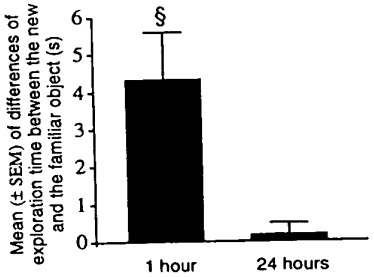

Fig. 1. Effect of the intertrial time on the exploration time between the new and the familiar object (± SEM) on T2. Saline was injected 30 min before T1, $^{\S}P < 0.01$.

Table 1

Experiment 2, mean (± SEM) of total exploration time on T1 and T2

Treatment (mg/kg)	*n*	Mean on T1 (s)	Mean on T2 (s)
Saline	47	13.86 ± 1.41	6.39 ± 0.95
0.1	15	15.57 ± 1.51	10.40 ± 1.32
0.2	16	11.31 ± 0.98	6.19 ± 0.93
0.4	16	12.47 ± 1.15	7.62 ± 1.00

Statistical analysis were carried out using the Statview 4.02 program. The exploration time on the familiar and on the new object in T2 was compared between experiments 1 and 2 for saline treated rats by two-way repeated measures analysis of variance (ANOVA) using intertrial time as a between-group variable and object (new versus familiar) as a repeated measure. Then, the exploration time in T2 was compared between the new object versus the familiar object independently for each group by the paired Student's *t*-test. In experiment 2, 3 and 4, for multiple comparisons between-groups an ANOVA and subsequent Bonferroni/Dunn test post-hoc analysis were applied for the total exploration time in T1 and in T2 and the difference of exploration time between the new object and the familiar object in T2. Results are expressed as mean ± SEM.

The intertrial time significantly affected the difference in exploration time between the new object versus familiar object in T2 (1 h versus 24 h $F(1,60) = 18.3$, $P < 0.001$; new versus familiar $F(1,60) = 6.2$, $P < 0.05$; interaction $F(1,60) = 23.0$, $P < 0.001$). Fig. 1 shows that rats spent significantly more time in exploring the new object than the familiar object when the intertrial time was 1 h, but not when it was 24 h.

In experiment 2, apamin did not significantly modify the total exploration time in T1 and T2 (see Table 1). Fig. 2A shows that apamin increased the difference of exploration time between the new object and the familiar object in T2 ($F(3,90) = 3.5$, $P < 0.05$). This effect was statistically significant for the dose of 0.4 mg/kg but not for the doses of 0.1 and 0.2 mg/kg.

In experiments 3 and 4, apamin administered either just after T1 or before T2 did not significantly modify the total exploration time on T2 (see Table 2). Fig. 2B,C shows that apamin did not modify the difference of exploration time between the new object and the familiar object in T2 (experiment 2: $F(2,60) = 0.7$, ns; experiment 3: $F(3,108) = 2.0$, ns).

Our results show that rats spend more time in exploring a new object than a familiar object when the interval

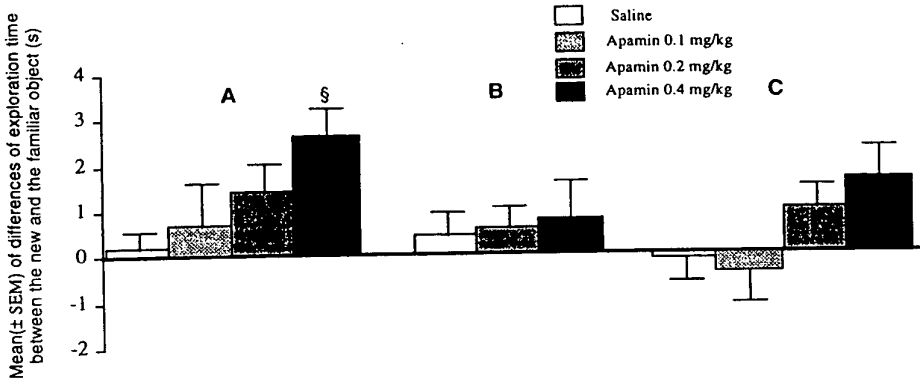

Fig. 2. Effect of apamin on object discrimination on T2. Injections were made 30 min before T1 (A), just after T1 (B) and 30 min before T2 (C). $^{§}P < 0.01$.

between the sample trial and the choice trial is 1 h, but not if the interval is 24 h. This finding, in agreement with results obtained by other authors [1,3] indicates that rats recognize the familiar object 1 h after its presentation, but not 24 h after.

Rats that received apamin before the sample trial were able to recognize the familiar object 24 h after. Since apamin was without effect when administered either just after the sample trial or before the choice trial, a possible explanation of our results is that apamin could improve acquisition of the information, but has no effects on memory processes that occur just after acquisition and does not influence the restitution of information. It has been shown that apamin induces hypermotility. Thus, it can be postulated that the promnesic effect of apamin could be secondary to an effect on motor and/or sensory behaviors. However, the hypermotility has been observed in mice after intralumbar or intraventricular microinjections of doses of apamin that induce severe signs of poisoning [6], or in rats after microinjections in A10 region [16]. Furthermore, in the present study, apamin did not induce any significant increase in the total exploration time, and we recently found that apamin induces a slight but significant decrease of rat's activity in an actimeter (Deschaux and Bizot, manuscript in preparation). Thus, these results are not in favor of the hypothesis that apamin induces an hyperactivity that could explain its promnesic effect.

Table 2

Experiments 3 and 4, mean (± SEM) of total exploration time on T2

Treatment (mg/kg)	*n*	Mean on T2 (s)
Experiment 3		
Saline	32	4.57 ± 1.32
0.2	15	4.13 ± 1.54
0.4	16	6.00 ± 0.51
Experiment 4		
Saline	56	6.46 ± 0.64
0.1	16	5.69 ± 0.43
0.2	20	5.15 ± 0.40
0.4	20	6.00 ± 0.88

This improvement of acquisition by pretraining injection of apamin is consistent with results obtained by other authors [13]. Messier et al. found that pretraining injection of apamin increased the number of response emitted by mice subjected to a bar-pressing task during both training session and retention test taking place 24 h later. Nevertheless, they also found that posttraining injection of apamin increased the number of responses emitted at the retention test. This finding suggests that apamin facilitates memory processes taking place just after training. The apparent discrepancy between this finding and our results could be due to a difference in the type of memory required in the two tasks. The bar-pressing task could be considered as a pure reference memory procedure, since, information is useful for many trials and for the entire experiment [15]. In contrast, the object recognition task has been claimed to measure non-spatial working memory in the rat, with the characteristics of the episodic memory assessed in non-human primates by visual recognition tests [3,15]. Thus, the effect of apamin could reflect two different phenomenons in the study of Messier et al. [13] and in our study. A facilitation of consolidation processes that takes place shortly after acquisition in a reference task could be relevant to explain the effect of apamin in the bar-pressing task, while our results could indicate that apamin improves only acquisition but has no effects on the other stages of memory, in a working memory task. The precise mechanisms underlying the effects of apamin still need to be analyzed more closely. It is hoped that further research will shed new light on the results we obtained.

During the course of this investigation O.D. was supported by a grant from the DRET/CNRS. The authors wish to thank Dr. O. Bergis for his helpful scientific and technical advice.

[1] Bartolini, L., Casamenti, F. and Pepeu, G., Aniracetam restores object recognition impaired by age, scopolamine, and nucleus basalis lesions, Pharmacol. Biochem. Behav., 53 (1996) 277–283.
[2] Bernard, P.J., Bazan, M. and Seagar, M., Effet de l'apamine sur le potentiel d'action et les courants de la cellule de neuroblastome N1E115, Rev. Med. Chir. Soc. Med. Nat. IASI, 90 (1986) 93–100.
[3] Ennaceur, A. and Delacour, J., A new one-trial test for neurobiological studies of memory in rats: behavioural data, Behav. Brain Res., 31 (1988) 47–59.
[4] Gehlert, D.R. and Gackenheimer, S.L., Comparison of the distribution of binding sites for the potassium channel ligands apamin, charybdotoxin and iodoglyburide in the rat brain, Neuroscience, 52 (1)(1993) 191–205.
[5] Habermann, E., Apamin, Pharmacol. Ther., 25(1984) 255–270.
[6] Habermann, E. and Cheng-Raude, D., Central neurotoxicity of apamin, crotamin, phospholipase A and alpha – amanitin, Toxicon, 13 (1975) 465–473.
[7] Habermann, E. and Horvath, E., Localization and effects of apamin after application to the central nervous system, Toxicon, 18 (1980) 549–560.
[8] Heurteaux, C., Messier, C., Destrade, C. and Lazdunski, M., Memory processing and apamin induce immediate early gene expression in mouse brain, Mol. Brain Res., 18 (1993) 17–22.
[9] Hlinak, Z. and Krejci, I., Kynurenic acid and 5,7-dichlorokynurenic acids improve social and object recognition in male rats, Psychopharmacology, 120 (1995) 463–469.
[10] Lallement, G., Denoyer, M., Collet, A., Pernot-Marino, I., Baubichon, D., Monmaur, P. and Blanchet, G., Changes in hippocampal acetylcholine and glutamate extracellular levels during soman-induced seizures: influence of septal cholinoceptive cells, Neurosci. Lett., 136 (1992) 1–4.
[11] Lallement, G., Fosbraey, P., Baille le Crom, V., Tatersall, J.E.H., Blanchet, G., Wetherell, J.R., Rice, P., Passingham, S.L. and Sentenac-Roumanou, H., Compared toxicity of potassium channel blockers, apamin and dendrotoxin, Toxicology, 104 (1995) 47–52.
[12] Matthews, R.T. and Lee, W.L., Effects of apamin on cholinergic and non-cholinergic medial septal/diagonal band (MS/DB) neurons of the guinea pig in vitro, Soc. Neurosci. Abstr., 16 (1990) 58.
[13] Messier, C., Mourre, C., Bontempi, B., Sif, J., Lazdunski, L. and Destrade, C., Effect of apamin, a toxin that inhibits Ca-dependent K channels, on learning and memory processes, Brain Res., 551 (1991) 322–326.
[14] Mourre, C., Cervera, P. and Ladzunski, M., Autoradiographic analysis in rat brain of the postnatal ontogeny of voltage-dependent sodium channels, calcium-dependent potassium channels and slow calcium channels identified as receptors for tetrodotoxin, apamin and (–)-desmethoxyverapamil, Brain Res., 417 (1987) 21–32.
[15] Olton, D.S., Becker, J.T. and Handelmann, G.E., Hippocampus, space and memory, Behav. Brain Sci., 2 (1979) 313–365.
[16] Steketee, J.D. and Kalivas, P.W., Effect of microinjections of apamin into the A10 dopamine region of rats: a behavioral and neurochemical analysis, J. Pharmacol. Exp. Ther., 254 (2)(1990) 711–719.
[17] Zhang, L. and McBain, C.J., Potassium conductances underlying repolarization and after-hyperpolarization in rat CA1 hippocampal interneurones, J. Physiol. (London), 488 (1995) 661–672.

ELSEVIER

European Journal of Pharmacology 347 (1998) 13–21

ejp

Apamin improves spatial navigation in medial septal-lesioned mice

Sami Ikonen [a,*], Bernard Schmidt [b], Paavo Riekkinen Jr. [a]

[a] *Department of Neuroscience and Neurology, University of Kuopio, Canthia-building, P.O.Box 1627, FIN-70211 Kuopio, Finland*
[b] *B.H.S.: CNS Research, Troponwerke, Neurather Ring 1, D-51063 Köln, Germany*

Received 9 October 1997; revised 22 December 1997; accepted 27 January 1998

Abstract

We investigated the effects of acute i.p. injections of the Ca^{2+}-dependent K^+ channel blocker, apamin, on water maze spatial navigation, Y-maze and passive avoidance behavior in intact and medial septal-lesioned mice. Apamin 0.02, 0.06 or 0.2 mg/kg (i.p.) administered 30 min before or immediately after the training did not affect the performance of intact mice. Apamin 0.02 or 0.06 mg/kg (i.p.) administered immediately after the daily training did not affect the performance of medial septal-lesioned mice. Apamin 0.02 and 0.06 mg/kg (i.p.) administered 30 min before daily training reversed the navigation failure present in medial septal-lesioned mice during the initial and reversal learning stages of the water maze task. Apamin had no effect on the cognitive performance in Y-maze or passive avoidance tests. The results indicate that blockade of Ca^{2+}-dependent K^+ channels may facilitate acquisition of spatial navigation performance, but has no effect on consolidation, inhibitory avoidance and spontaneous alternation behavior in mice. © 1998 Elsevier Science B.V.

Keywords: Septal lesion; Medial; Apamin; K^+ channel, Ca^{2+}-dependent; Spatial navigation; Reversal learning; Memory; (Mouse)

1. Introduction

Apamin is a neurotoxin extracted from bee venom, which specifically inhibits a particular class of Ca^{2+}-dependent K^+ channels. These channels are characterised by their relatively high sensitivity to intracellular Ca^{2+} concentration, lack of voltage dependence and small conductance (Dreyer, 1990; Habermann, 1984; Lazdunski et al., 1988; Strong, 1990), and they are involved in the generation of slow afterhyperpolarization that occurs subsequently to the action potential in many excitable cells (Kawai and Watanabe, 1986). In mice and rats, apamin at high doses produces signs of poisoning such as tremors, ataxia and lethal respiratory insufficiency (Lallement et al., 1995). There are many apamin binding sites in some of the brain areas implicated in learning and memory processing such as the septum, the hippocampal formation, cingulate cortex and the anteroventral thalamic nuclei (Mourre et al., 1986; Gehlert and Gackenheimer, 1993). Apamin has been shown to block the slow afterhyperpolarization and increase the firing of cholinergic neurons in a slice preparation of the medial septum-diagonal band region (Matthews and Lee, 1991), suggesting that drugs acting via Ca^{2+}-dependent K^+ channels may modulate cholinergic function.

Recent pharmacological studies have revealed that blockade of Ca^{2+}-dependent K^+ channels may stimulate some forms of memory and learning in rodents. Apamin administered before or after the training has been shown to facilitate memory processes in appetitively-motivated bar-pressing response in mice (Messier et al., 1991). Another study (Deschaux et al., 1997) showed that apamin can improve learning in an object recognition task in rats. Injections of apamin before the training were shown to be effective, but injections after the training were ineffective. Moreover, apamin increases the expression of immediate early genes c-*fos* and c-*jun* in the hippocampal formation induced by learning (Heurteaux et al., 1993). These immediate early genes are thought to be involved in the activation of neurons during the memory process, and some studies have reported the induction of c-*fos* gene in dentate gyrus following the induction of long term potentiation (Dragunow et al., 1989). This finding suggests that a blocker of Ca^{2+}-dependent K^+ channels could modulate memory via these immediate early genes.

* Corresponding author. Tel: +358-17-162222; fax: +358-17-162048; e-mail: ikonen@jalus.uku.fi

Medial septal-lesioning causes a cholinergic deficit, which removes most of the cholinergic input to the hippocampus. This defect can be used as a model for the degeneration of the cholinergic cells (Hagan and Morris, 1988; Riekkinen et al., 1997), thought to be associated with the development of cognitive disorders in Alzheimer's disease (Dunnett et al., 1991; Fibiger, 1991; Bowen et al., 1992; Dunnett and Fibiger, 1993). The most common approach to treat this cognitive defect has been to use cholinesterase inhibitors, such as tacrine and metrifonate. Tacrine is already being used for treatment for human patients with Alzheimer's disease, and metrifonate has been shown to be effective in reversing the cognitive defect present in medial septal-lesioned rats (Riekkinen et al., 1996) and mice (our unpublished results).

In order to study further the role of Ca^{2+}-dependent K^+ channels in memory processing, we investigated the effects of apamin on the performance of young mice in the Morris water maze, Y-maze and passive avoidance tasks. We also wanted to study the possible therapeutic role of potassium channel inhibitors in cognitive disorders associated with a cholinergic deficit, and therefore in addition to intact mice, we also studied the effects of apamin on memory failure induced by medial septal-lesion in mice. Medial septal-lesioning impairs spatial learning, which disrupts the performance in the Morris water maze (Hagan and Morris, 1988; Riekkinen et al., 1997). In order to characterise the different cognitive processes modulated by apamin, we studied the action of this drug on acquisition of spatial reference and reversal memory in the water maze, on spontaneous alternation behavior in a Y-maze, and on passive avoidance performance. Spontaneous alternation behavior is supposed to reflect a primitive form of spatial working memory.

2. Materials and methods

2.1. Animals

Young (3–4-month-old; $n = 151$) female C57BL/6J//Kuo mice were used in the present study. The mice were housed five per cage, except the sham- and medial septal-lesioned mice, which were housed one per cage. The environment conditions were controlled and constant (21 ± 1°C, humidity at 50 ± 10%, light period 0700–1900). Food and water were available ad libitum. The study plan was approved by the municipal government of Kuopio county.

2.2. Drugs

Apamin (Sigma) was dissolved in NaCl 0.9% and injected intraperitoneally (i.p.) at 0.02, 0.06 and 0.2 mg/kg (10 ml/kg). Controls received vehicle injections of equal volume. The groups received two injections: 30 min before and immediately after the daily water maze, Y-maze or passive avoidance training. No drug or vehicle injections were given during the passive avoidance testing day. Details of the treatment groups are presented in Table 1.

2.3. Surgery

Medial septal (A: 0.9 mm, M: 0.0 mm, D: −4.7 mm; relative to the bregma) lesions were made by passage of an anodal DC current (1 mA, 15 s) via tungsten electrodes (diameter 0.0625 mm, 0.5 mm tip uninsulated). Sham-lesioned mice were treated identically, but no current was applied. Mice were deeply anaesthetised with a 1:1 mixture of Dormicum (Roche) and Hypnorm (Janssen Pharmaceutica) (s.c.) during the operations and for analgesia the mice were given a 0.1 mg/kg injection of buprenorfin (Temgesic; Reckitt and Colman) (s.c.) after the surgery. The mice were allowed to recover from the surgery for 2 weeks before starting the first experiments.

2.4. Water maze

We used a black plastic circular pool, diameter 120 cm, and a black painted stainless steel square platform; 14 × 14 cm, 1.0 cm below the water line. The pool was divided into three annuli of equal surface area, and the submerged escape platform was always in the middle annulus. The starting locations, which were labelled North, South, East and West, were located arbitrarily on the pool rim (Riekkinen et al., 1990). The timing of the latency to find the

Table 1
The number of mice in each treatment group

		Vehicle	Apamin (mg/kg)		
			0.02	0.06	0.2
Before the daily training	intact (3.1.)	9	10	10	10
	sham (3.2.)	10	–	–	–
	ms-lesioned (3.2.)	9	–	8	8
	ms-lesioned (3.3.)	7	6	–	–
After the daily training	intact (3.1.)	10	10	10	10
	ms-lesioned (3.4.)	7	8	9	–

The mice that received the apamin or vehicle injections 30 min before the daily training received also a vehicle injection immediately after the daily training, and the mice that received the apamin or vehicle injections immediately after the daily training, received also a vehicle injection 30 min before the daily training.

submerged platform was started and ended by the experimenter. A computer connected to an image analyser (HVS Image, Hampton, UK) monitored the swim pattern. Mice were placed in the water with their nose pointing towards the wall at one of the starting points in a random manner. If the mouse failed to find the platform in the maximum time, it was placed there by the experimenter. Mice were allowed to stay on the platform for 5 s. A 30-s recovery period was allowed between the training trials. The temperature of the water was kept constant throughout the experiment (20.5 ± 0.5°C).

The training schedule consisted of 8 consecutive days of testing. Four platform trials of 60 s were assessed per day during the first 5 training days. The platform location was kept constant (the Southwest quadrant) during this period of training. On the sixth day the platform was removed from the pool and the mice were allowed to swim for 50 s. Immediately after this spatial bias test, the platform was placed in the Northeast quadrant and five 50 s platform trials were assessed. The schedule on the seventh day consisted also of five 50 s platform trials (platform in the Northeast quadrant). The water maze experiment was finished on the eighth day with a spatial bias test (a 50 s trial without the platform). During the platform training trial, the following parameters were measured: escape length, percentage of animals that found the platform and swimming speed. During the spatial bias test the number of counter crossings was measured. Counter crossing was defined as crossing a circular area, in which the platform had previously been located, and which was three times larger than the platform (radius = 12.1 cm).

2.5. Y-maze

The Y-maze experiment was started 24 h after the water maze testing sessions. The Y-maze used in this experiment had black plastic walls that were 10 cm high. Its arms consisted of three compartments (10 cm × 10 cm) connected with 4 cm × 5 cm passages. The mouse was placed in one of the arm compartments and was allowed to move freely for 6 min without reinforcers. An arm entry was defined as the body of a mouse except for its tail completely entering into an arm compartment. The sequence of arm entries was manually recorded. An alternation was defined as the entry into all three arms on consecutive choices. The number of maximum spontaneous alternations was then the total number of arms entered minus 2, and the percent alternation was calculated as (actual alternations/maximum alternations) × 100. The test was run on two consecutive days (days 9–10).

2.6. Passive avoidance

Passive avoidance training trial was performed immediately after the Y-maze trial on the tenth day. The passive avoidance box consisted of a lit and a dark compartment. During the training trial the mice were placed in the lit compartment and 30 s later the sliding guillotine door was opened. After the mice entered the dark compartment (the latency was measured), the door was closed and a foot shock of 0.1 mA (0.5 s) was given. Then the mice were returned to their home cage and 24 h later they were again placed in the lit compartment during the testing trial and the latency to enter the dark compartment was measured (900 s maximum latency). The final latency was defined as a difference between the latencies on the first and the second day.

2.7. Histology

After the passive avoidance testing trial, the lesioned mice were decapitated. The brains of the mice were removed and immersed for 1–2 days in 4% formaldehyde solution. Fifty-micrometer sections were cut with a vibratome and the sections were stained. The medial septum area was stained with cresyl fast violet to see the position of the lesion. The hippocampal sections were stained with acetylcholinesterase staining (Hedreen et al., 1985; butylcholinesterase inhibitor was included in the assay mixture)

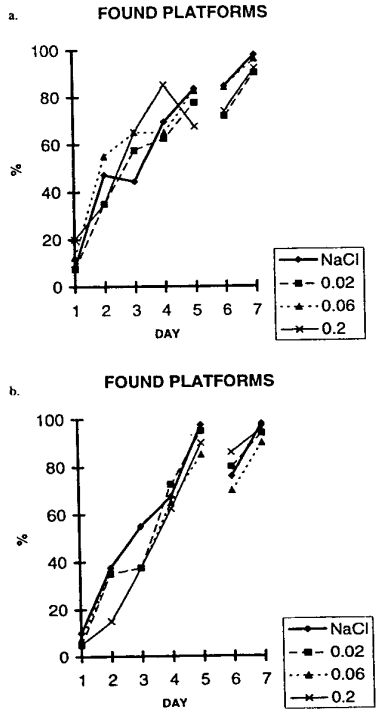

Fig. 1. Administration of apamin 0.02, 0.06 and 0.2 mg/kg 30 min before (a) or immediately after. (b) the daily training had no effect on reference memory or reversal learning, as there were no group differences in the number of found platforms. In both panels, the *X*-axis indicates the reference memory training days 1–5 (fixed platform location) and reversal learning days 6–7 (reversal of the platform location). The values are daily group means.

in order to confirm the decrease of acetylcholine-containing fibers in hippocampus.

2.8. Statistics

We evaluated the effect of the drugs on water maze escape distance and speed using analysis of variance for repeated measurements. We evaluated the effect of the drugs on the ability of the mice to find the water maze platform and the latencies in passive avoidance using Mann–Whitney test for two independent samples. The Bonferroni correction was used with analysis of variance and Mann–Whitney U-test. For analysis of the activity in Y-maze we used a one-way analysis of variance followed by Scheffe's post-hoc multiple group comparison.

3. Results

3.1. Intact mice; apamin administered before and after the daily training

3.1.1. Water maze

During the first 5 training days, apamin treatment administered before (0.02, 0.06 and 0.2 mg/kg) or after (0.02, 0.06 and 0.2 mg/kg) the daily training had no effect on the number of found platforms ($P > 0.05$) (Fig. 1), escape distance (Data not shown) or swimming speed (group: $F(3,35)/(3,36) < 1.09$, $P > 0.05$, for all comparisons) (speed, apamin administered before the daily training: vehicle: 16.8 ± 1.6; 0.02 mg/kg: 17.2 ± 4.0; 0.06 mg/kg: 17.6 ± 3.0; 0.2 mg/kg: 18.1 ± 2.5; speed, apamin administered after the daily training: vehicle: 18.3 ± 3.9; 0.02 mg/kg: 18.1 ± 3.4; 0.06 mg/kg: 16.8 ± 2.0; 0.2 mg/kg: 18.9 ± 2.9; group mean ± S.D.). There were no group differences in counter crossings during the first bias assessment ($F(3,35)/(3,36) < 3.018$, $P > 0.042$, Scheffe's test: $P > 0.05$) (counter crossings, apamin administered before the daily training: vehicle: 2.78 ± 1.39; 0.02 mg/kg: 2.1 ± 1.85; 0.06 mg/kg: 1.9 ± 1.6; 0.2 mg/kg: 1.6 ± 1.43; counter crossings, apamin administered after the daily training: vehicle: 2.30 ± 1.42; 0.02 mg/kg: 3.0 ± 2.11; 0.06 mg/kg: 1.40 ± 1.17; 0.2 mg/kg: 1.00 ± 1.70; group mean ± S.D.)

During the platform reversal stage on days 6 and 7, apamin treatment before or after the daily training had no effect on the number of mice that found the platform ($P > 0.05$) (Fig. 1), escape distance (Data not shown) or swimming speed (group: $F(3,35)/(3,36) < 1.73$, $P > 0.05$, for all comparisons) (speed, apamin administered before the daily training: vehicle: 16.0 ± 3.3; 0.02 mg/kg: 17.0 ± 4.1; 0.06 mg/kg: 18.8 ± 2.8; 0.2 mg/kg: 17.3 ± 3.2; speed, apamin administered after the daily training: vehicle: 13.7 ± 4.5; 0.02 mg/kg: 15.5 ± 4.9; 0.06 mg/kg: 12.9 ± 3.2; 0.2 mg/kg: 16.1 ± 3.7; group mean ± S.D. cm/s). During the second bias assessment measured on the eighth testing day, there were no differences in counter crossings ($F(3,35)/(3,36) < 1.175$, $P > 0.05$, for all com-

Table 2
The effects of apamin on Y-maze and passive avoidance tests of intact animals (apamin 0.02, 0.06 and 0.2 mg/kg administered before and after the daily training) and medial septal-lesioned animals (apamin 0.06 and 0.2 mg/kg administered before the daily training)

	Y-maze				PA		
	Day 1		Day 2		day 1 (s)	day 2 (s)	diff. (s)
	tot	%	tot	%			
Intact pre							
vehicle	16.4 ± 6.2	63.6 ± 13.8	9.5 ± 3.5	70.0 ± 16.2	26.7 ± 37.2	480.0 ± 243.1	422.0 ± 232.1
0.02	16.1 ± 6.8	66.5 ± 14.1	10.2 ± 6.1	52.9 ± 24.7	13.0 ± 5.9	752.5 ± 197.3	739.5 ± 194.7[b]
0.06	16.5 ± 5.3	55.4 ± 8.2	10.7 ± 4.0	54.1 ± 20.8	9.5 ± 2.8	470.5 ± 324.3	461.0 ± 325.9
0.2	18.3 ± 5.7	72.6 ± 15.3	12.5 ± 4.4	60.2 ± 15.0	55.5 ± 90.8	623.5 ± 245.6	568.0 ± 228.7
Intact post							
vehicle	19.5 ± 5.3	63.8 ± 7.7	10.0 ± 2.1	61.7 ± 15.3	18.0 ± 11.1	267.5 ± 218.0	249.5 ± 220.3
0.02	18.6 ± 5.9	64.2 ± 13.9	11.5 ± 4.7	60.1 ± 18.7	19.0 ± 17.3	419.0 ± 240.2	400.0 ± 233.1
0.06	16.6 ± 4.3	67.9 ± 14.4	11.2 ± 4.3	62.4 ± 21.4	36.0 ± 53.0	513.5 ± 309.3	477.5 ± 291.4
0.2	18.7 ± 4.2	64.8 ± 11.2	11.9 ± 5.1	70.4 ± 12.0	10.0 ± 2.3	153.5 ± 138.4	143.5 ± 137.4
MS-lesion pre							
sham	16.9 ± 9.5	45.0 ± 26.3	10.1 ± 6.6	42.5 ± 32.6	40.5 ± 32.7	587.5 ± 329.0	547.0 ± 323.8
vehicle	2.1 ± 1.1[a]	22.2 ± 44.1	5.3 ± 9.6	13.9 ± 27.7	300.0 ± 0.0[c]	708.9 ± 293.5	408.9 ± 293.5
0.06	7.6 ± 7.4[a]	47.8 ± 41.7	10.6 ± 8.2	50.6 ± 38.1	158.1 ± 123.1[d]	604.4 ± 366.0	446.3 ± 286.8
0.2	4.6 ± 3.9[a]	30.8 ± 38.3	11.3 ± 14.0	23.9 ± 33.2	285.0 ± 42.4[c]	540.0 ± 337.2	255.0 ± 316.3

These tests were not performed on other groups. Intact pre = Intact mice, apamin administered before the training; Intact post = Intact mice, apamin administered after the training; MS-lesion pre = medial septal-lesioned mice, apamin administered before the training, I; Y-maze: day 1 = first day of training; day 2 = second day of training; tot = number of total alternations; % = percent alternations. Passive avoidance: day 1 = entry latency of the training day; Day 2 = entry latency of the testing day; Diff. = the difference between the latencies of the testing day and the training day.
[a] $P = 0.000$ vs. sham-lesioned group, [b] $P = 0.017$ vs. vehicle group, [c] $P < 0.002$ vs. sham-lesioned group, [d] $P = 0.021$ vs. medial septal-lesioned-vehicle group. The values are expressed as mean ± S.D.

parisons) (counter crossings, apamin administered before the daily training: vehicle: 3.89 ± 2.76; 0.02 mg/kg: 4.00 ± 2.49; 0.06 mg/kg: 4.1 ± 2.85; 0.2 mg/kg: 3.6 ± 2.72; counter crossings, apamin administered after the daily training: vehicle: 4.50 ± 2.80; 0.02 mg/kg: 4.20 ± 2.20; 0.06 mg/kg: 2.80 ± 1.99; 0.2 mg/kg: 4.50 ± 2.42; group mean ± S.D.).

3.1.2. Y-maze and passive avoidance

Apamin administered before or after the daily training had no effect on total moves or percent alternation during either of the testing days in Y-maze ($F(3,35)/(3,36) < 2.642$, $P > 0.05$, for all comparisons) (Table 2). In passive avoidance there were no group differences in the latency to enter the dark compartment during the training day ($P > 0.05$) (Table 2). Apamin 0.02 mg/kg administered before the training day increased the difference between the entry latency during the testing and training day ($P = 0.017$). In contrast, apamin administered after the daily training had no effect on passive avoidance ($P > 0.05$) (Table 2).

3.2. Medial septal-lesioned groups; apamin administered before the training; I

3.2.1. Water maze

A comparison between the sham-lesioned group and the medial septal-lesioned-vehicle group showed a clear impairment in platform finding ($P = 0.000$) (Fig. 2a) and escape length ($F(1,17) = 23.77$, $P = 0.000$) (Fig. 2b) during the first 5 days. The 0.06 mg/kg dose of apamin decreased the escape length significantly compared to the medial septal-lesioned-vehicle group ($F(1,15) = 14.44$, $P = 0.006$). Apamin 0.06 mg/kg also increased the number of found platforms ($P = 0.018$ vs. medial septal-lesioned-vehicle group). However, apamin 0.06 mg/kg did not reverse the navigation failure present in medial septal-lesioned mice completely, as the group's performance was also impaired when compared with the sham-lesioned group (number of found platforms: $P = 0.001$)). Escape length, however, was not impaired ($F(1,16) = 1.00$, $P > 0.05$). The apamin 0.2 mg/kg had no effect on escape length ($F(1,15) = 0.31$, $P > 0.05$) or the ability to find the platform ($P > 0.05$) compared to the medial septal-lesioned-vehicle group. There were no group differences in swimming speed during the first 5 days (group: $F(3,31) = 2.19$, $P > 0.05$) (Sham: 21.5 ± 3.5; vehicle: 19.2 ± 3.0; 0.06 mg/kg: 17.8 ± 4.0; 0.2 mg/kg: 18.6 ± 2.0; group mean ± S.D. cm/s) between the groups. On the sixth day, during the spatial bias test, no group differences were observed in counter crossings ($F(3,31) = 0.507$, $P > 0.05$) (Sham: 6.10 ± 2.73; vehicle: 5.00 ± 1.32; 0.06 mg/kg: 5.25 ± 2.87; 0.2 mg/kg: 5.00 ± 1.69; group mean ± S.D.).

During the platform reversal, the vehicle- and apamin 0.2 mg/kg treated medial septal-lesioned mice were not as effective in escaping from the pool compared to the sham-lesioned group: there were differences in the number of found platforms (vehicle or apamin 0.2 mg/kg treated medial septal-lesioned vs. sham-lesioned group: $P = 0.000$) (Fig. 2a) and in the escape length ((group: $F(3,31) = 11.65$, $P = 0.000$); vehicle treated medial septal-lesioned vs. sham-lesioned group: ($F(1,17) = 19.73$, $P = 0.001$); apamin 0.2 mg/kg treated medial septal-lesioned vs. sham-lesioned group: ($F(1,16) = 24.38$, $P = 0.001$)) (Fig. 2b). However, apamin 0.06 mg/kg treatment decreased the escape length ($F(1,15) = 23.80$, $P = 0.000$) and increased the probability of platform finding ($P = 0.000$) in medial septal-lesioned mice. Indeed, there was no significant difference between the 0.06 mg/kg treated medial septal-lesioned group and the sham-lesioned group in escape length ($F(1,16) = 0.27$, $P > 0.05$) or in the number of found platforms ($P > 0.05$). There were no group differences in swimming speed during the platform reversal trials (group: $F(3,31) = 0.71$, $P > 0.05$) (Sham: 21.0 ± 4.6; vehicle: 20.0 ± 2.8; 0.06 mg/kg: 18.3 ± 6.3; 0.2 mg/kg: 21.0 ± 2.4; group mean ± S.D. cm/s) between any of the groups. On the eighth day, during the spatial bias test, no group differences were observed in counter crossings

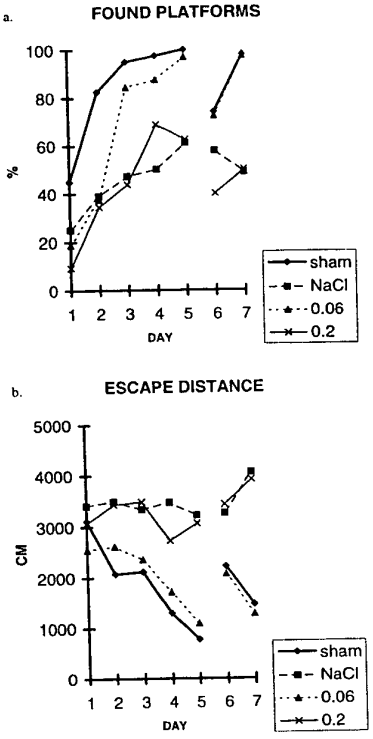

Fig. 2. Administration of apamin 0.06 mg/kg 30 min before the daily training alleviated the navigation failure present in medial septal-lesioned mice during both reference memory and reversal learning days by increasing the percentage of found platforms (a) and decreasing the escape length (cm) (b). In both panels, the *X*-axis indicates the reference memory training days 1–5 (fixed platform location) and reversal learning days 6–7 (reversal of the platform location). The values are daily group means.

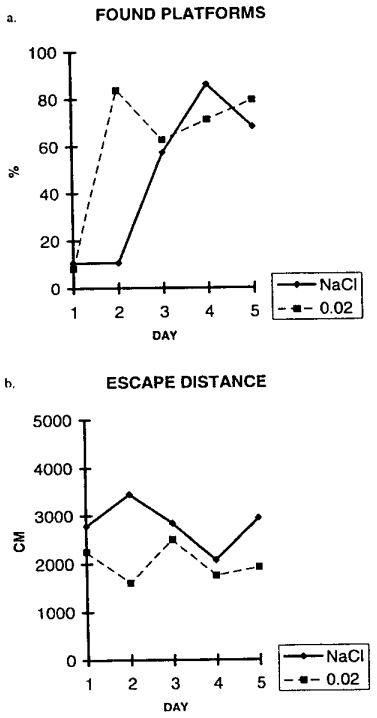

Fig. 3. Administration of apamin 0.02 mg/kg 30 min before the daily training alleviated the navigation failure present in medial septal-lesioned mice during reference memory training days by increasing the percentage of found platforms (a) and decreasing the escape length (cm) (b). In both panels, the *X*-axis indicates the reference memory training days 1–5 (fixed platform location). The values are daily group means.

($F(3,31) = 3.01$, $P = 0.045$, Scheffe's test: $P > 0.05$) (Sham: 6.60 ± 1.90; vehicle: 4.00 ± 1.80; 0.06 mg/kg: 5.13 ± 3.23; 0.2 mg/kg: 4.13 ± 1.13; group mean $\pm$ S.D.).

3.2.2. Y-maze and passive avoidance

During the first day in Y-maze all the medial septal-lesioned groups made significantly less total moves than the sham-lesioned group ($F(3,31) = 9.432$, $P = 0.000$). However, the percentage alternation was not affected ($F(3,31) = 0.899$, $P > 0.05$) (Table 2). During the second day in Y-maze there were no longer any group differences in total moves or percent alternation ($F(3,31) < 2.252$, $P > 0.05$) (Table 2).

The major proportion of medial septal-lesioned mice refused to enter the dark compartment already on the training day of passive avoidance test. The latency was greatest in medial septal-lesioned-vehicle group ($P = 0.001$ vs. sham-lesioned) and medial septal-lesioned-apamin 0.2 mg/kg group ($P = 0.002$ vs. sham-lesioned). The apamin 0.06 mg/kg treatment decreased the latencies on the training day compared to the medial septal-lesioned-vehicle group ($P = 0.021$) (Table 2). After the testing day, it was observed that there were no group differences in the difference between the latencies to enter the dark compartment on the testing day and the training day ($P > 0.05$) (Table 2).

3.3. Medial septal-lesioned mice; apamin administered before the training; II

3.3.1. Water maze

Administration of apamin 0.02 mg/kg increased the number of mice that found the platform ($P = 0.021$) (Fig. 3a) and it also decreased the escape length ($F(1,11) = 5.98$, $P = 0.033$) (Fig. 3b). There were no group differences in swimming speed ($F(1,11) = 0.41$, $P > 0.05$) (vehicle: 17.0 ± 3.1; 0.02 mg/kg: 15.6 ± 4.8; group mean $\pm$ S.D. cm/s). There were no group differences in counter crossings ($F(1,11) = 0.406$, $P > 0.05$) (vehicle: 5.00 ± 2.24; 0.02 mg/kg: 4.17 ± 2.48; group mean $\pm$ S.D.) during the bias assessment measured on the sixth day of the water maze training.

3.4. Medial septal-lesioned mice; apamin administered after the training

3.4.1. Water maze

Administration of apamin had no effect on the number of found platforms ($P > 0.05$) (Fig. 4a). There was an overall group difference in escape length (group: $F(2,21)$

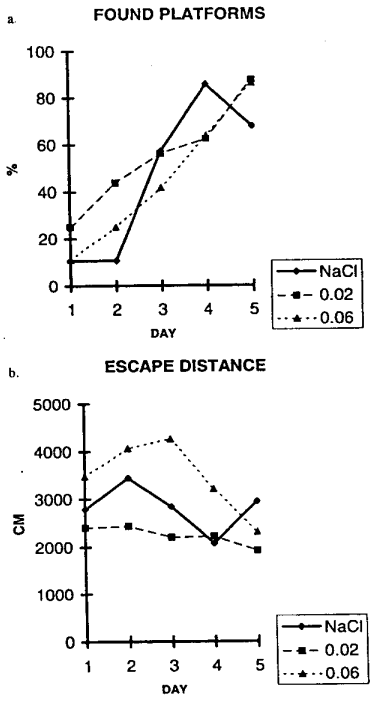

Fig. 4. Administration of apamin 0.02 and 0.06 mg/kg immediately after the daily training did not affect the number of found platforms (a) or escape length (cm) (b). In both panels, the *X*-axis indicates the reference memory training days 1–5 (fixed platform location). The values are daily group means.

= 4.38, $P = 0.026$) (Fig. 4b), but neither of the apamin-treated groups differed significantly from the vehicle group. In addition, the apamin 0.06 mg/kg group swam faster than the medial septal-lesioned-vehicle group ($F(1,14) = 12.31$, $P = 0.003$) (vehicle: 17.0 ± 3.1; 0.02 mg/kg: 16.9 ± 5.0; 0.06 mg/kg: 21.5 ± 2.0; group mean ± S.D. cm/s). There were no group differences in counter crossings ($F(2,21) = 1.225$, $P > 0.05$) (vehicle: 5.00 ± 2.24; 0.02 mg/kg: 3.50 ± 2.73; 0.06 mg/kg: 4.89 ± 1.27; group mean ± S.D.) during the bias assessment measured on the sixth day of the water maze training.

3.5. Histology

The locations of the lesions in medial septal-lesioned mice were confirmed by studying the cresyl fast violet -stained sections (Fig. 5a). The decrease of acetylcholine-

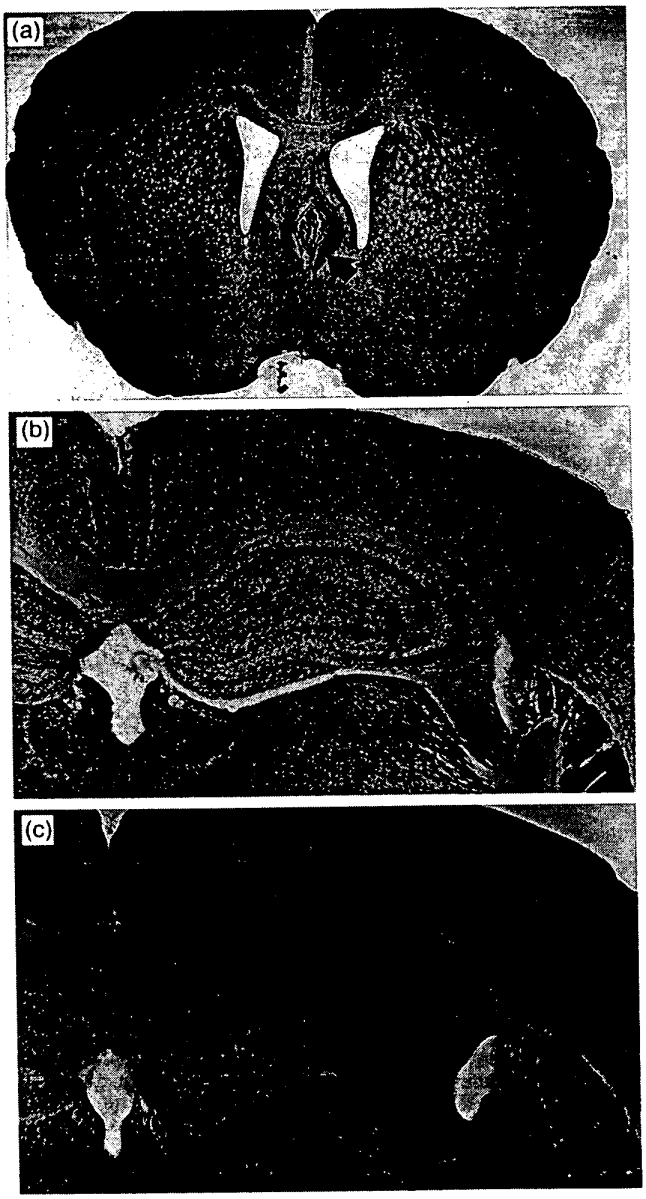

Fig. 5. (a) Cresyl violet staining of a coronal section containing medial septal-lesion site. An arrow indicates the location of the lesion. (b) Acetylcholinesterase staining of a coronal hippocampal section of an intact mouse. (c) Acetylcholinesterase staining of a coronal hippocampal section of an medial septal-lesioned mouse.

containing fibers in hippocampus was confirmed by acetylcholinesterase staining (Fig. 5, panels b and c).

4. Discussion

We described that in intact mice administration of apamin (0.02–0.2 mg/kg) before or after the training had no effect on water maze or Y-maze performance, but apamin 0.02 mg/kg at one dose administered before the training increased passive avoidance entry latency during the testing trial.

Previously, it has been shown that apamin could facilitate memory processing in a appetitively-motivated bar-pressing response task in intact mice. In the report of Messier et al., administration of apamin before the training at a dose of 0.2 mg/kg accelerated the acquisition of a bar-pressing response, but also increased the bar-pressing rates. Doses of 0.1 and 0.4 mg/kg were not effective. Administration of apamin at a dose of 0.2 mg/kg after the training also facilitated the memory process (Messier et al., 1991). In another article by Deschaux et al. (1997), apamin improved learning in an object recognition task in intact rats at a dose of 0.4 mg/kg. Doses of 0.1 mg/kg and 0.2 mg/kg were not effective, and apamin was also ineffective when administered after the training (Deschaux et al., 1997). We observed that apamin 0.02 mg/kg administered before the training trial increased passive avoidance entry latency. However, several non-mnemonic factors, such as altered sensitivity to foot shock, may affect passive avoidance performance. Indeed, the effects of apamin on pain threshold has not been studied and it is possible that the increased testing trial entry latency may have resulted from non-cognitive factors. One explanation for the failure of apamin to alter water maze and Y-maze performance might be, that these tests were too easy for intact mice, i.e., there may have been a ceiling effect. On the other hand, the tests used in this and previous studies probably impose different mnemonic demands, which could also explain the lack of effect of apamin in intact mice in our study. Indeed, water maze measures spatial reference memory and Y-maze contains a spatial working memory component. In contrast, the previous studies by Messier et al. (1991) and Deschaux et al. (1997) employed tests that do not require spatial memory.

We report here, that pretraining injections of apamin can markedly stimulate water maze behaviour of medial septal-lesioned mice. The effective doses were 0.06 mg/kg and 0.02 mg/kg. The 0.2 mg/kg dose, however, was ineffective, which may be a reflection of the possible toxic side-effects (Lallement et al., 1995). The lack of any effect of injections of apamin after the daily training trials on performance in Morris water maze raises the possibility that apamin does not enhance formation of spatial memory, but influences some other factor which modulates escape performance, such as anxiety, arousal, attention or motor behaviour. Indeed, the effects of apamin on these functions are largely unexplored. However, some of the present results tentatively suggest that apamin can stimulate cognitive processes in medial septal-lesioned mice.

First, the effects of apamin on locomotor activity and accuracy of the learning performance did not occur in the same behavioural tests used in this study. Apamin had no effect on swimming speed in water maze, suggesting that changes in motor activity do not account for the beneficial effect of apamin on spatial navigation. In contrast, apamin actually decreased the hypoactivity of medial septal-lesioned mice in Y-maze and passive avoidance tests, but produced no obvious cognitive improvement in these tests.

Second, we observed that the learning curves of apamin and vehicle treated mice started from the same level, but the drug treated group had a steeper learning curve. Indeed, an increase in the slope of the learning curve is classically interpreted as an improvement of memory formation. In addition, apamin treatment alleviated the defect observed during platform reversal in medial septal-lesioned mice, showing that the effect is not limited to one learning event in the spatial memory test. However, retrieval of previously learned spatial information was not stimulated by apamin treatment in medial septal-lesioned mice. Furthermore, apamin had no effect on spontaneous alternation behavior, a primitive measure of working memory, in Y-maze or passive avoidance functions, suggesting that the mechanisms underlying acquisition of spatial reference memory engrams may be especially amenable to the modulation of the function of Ca^{2+}-dependent K^+ channels.

The bias assessments on days 6 and 8 showed no significant differences between any of the sham-lesioned or medial septal-lesioned groups, even though there was a clear difference in platform finding and escape length. This may be due to a different search strategy of mice compared to rats who generally show a close correlation between reduced escape length and the bias performance (Morris, 1984; Riekkinen et al., 1997). Indeed, we have found that in rats a medial septal-lesion increases escape distance and reduces bias, and metrifonate, a cholinesterase inhibitor, can alleviate both changes (Riekkinen et al., 1997). In contrast, in mice, a medial septal lesion increased only escape distance, but had no effect on bias (Ikonen et al., unpublished). Furthermore, metrifonate reduced escape distance, but had no effect on spatial bias in mice (Ikonen et al., unpublished results). Therefore, it is possible that mice are not as sensitive as rats in developing bias in the water maze.

In conclusion, apamin alleviated the acquisition defect during reference memory testing in medial septal-lesioned mice and it had no effect on inhibitory avoidance or spontaneous alternation behavior in the Y-maze. The present and previous results (Deschaux et al., 1997; Messier et al., 1991) indicate that blockade of Ca^{2+}-dependent K^+ channels may facilitate reference memory function.

Acknowledgements

This work was supported by the Academy of Finland. The authors wish to thank Ewen McDonald, PhD, for revising the language of the manuscript.

References

Bowen, D.M., Francis, P.T., Pangalos, M.N., Stephens, P.H., Procter, A.W., Chessell, I.P., 1992. 'Traditional' pharmacotherapy may succeed in Alzheimer's disease. Trends Neurosci. 15, 84–85.

Deschaux, O., Bizot, J.C., Goyffon, M., 1997. Apamin improves learning in an object recognition task in rats. Neurosci. Lett. 222, 159–162.

Dragunow, M., Abraham, W.C., Goulding, M., Mason, S.E., Robertson, H.A., Faull, R.L., 1989. Long-term potentiation and the induction of c-*fos* mRNA and proteins in the dentate gyrus of unanesthetized rats. Neurosci. Lett. 10, 274–280.

Dreyer, F., 1990. Peptide toxins and potassium channels. Rev. Physiol. Biochem. Pharmacol. 115, 93–136.

Dunnett, S.B., Fibiger, H.C., 1993. Role of forebrain cholinergic systems in learning and memory: relevance to the cognitive deficits of aging and Alzheimer's dementia. Prog. Brain Res. 98, 413–420.

Dunnett, S.B., Everitt, B.J., Robbins, T.W., 1991. The basal forebrain-cortical cholinergic system: interpreting the functional consequences of excitotoxic lesions. Trends Neurosci. 14, 494–501.

Fibiger, H.C., 1991. Cholinergic mechanisms in learning, memory and dementia: a review of recent evidence. Trends Neurosci. 14, 220–223.

Gehlert, D.R., Gackenheimer, S.L., 1993. Comparison of the distribution of binding sites for the potassium channel ligands apamin, charybdotoxin and iodoglyburide in the rat brain. Neuroscience 52, 191–205.

Habermann, E., 1984. Apamin. Pharmacol. Ther. 25, 255–270.

Hagan, J.J., Morris, R.G.M., 1988. The cholinergic hypothesis of memory: a review of animal experiments. In: Iversen, L.L., Iversen, S.D., Snyder, S.H. (Eds.), Psychopharmacology of the Aging Nervous System. Plenum, New York, pp. 237–323.

Hedreen, J.C., Bacon, S.J., Price, D.L., 1985. A modified histochemical technique to visualize acetylcholinesterase-containing axons. J. Histochem. Cytochem. 33, 134–140.

Heurteaux, C., Messier, C., Destrade, C., Lazdunski, M., 1993. Memory processing and apamin induce immediate early gene expression in mouse brain. Mol. Brain Res. 3, 17–22.

Kawai, T., Watanabe, M., 1986. Blockade of Ca-activated K conductance by apamin in rat sympathetic neurons. Br. J. Pharmacol. 87, 225–232.

Lallement, G., Fosbraey, P., Baille le Crom, V., Tatersall, J.E.H., Blanchet, G., Wetherell, J.R., Rice, P., Passingham, S.L., Sentenac-Roumanou, H., 1995. Compared toxicity of potassium channel blockers, apamin and dendrotoxin. Toxicology 104, 47–52.

Lazdunski, M., Romey, G., Schmid-Antomarchi, H., Renaud, J.-F., Mourre, C., Hughes, M., Fosset, M., 1988. The apamin-sensitive Ca^{2+}-dependent K^+ch annel: molecular properties, differentiation, involvement in muscle disease, and endogenous ligands in mammalian brain. In: Baker, P.F. (Ed.), Handbook of Experimental Pharmacology, Vol. 83. Springer, Berlin, pp. 135–145.

Matthews, R.T., Lee, W.L., 1991. A comparison of extracellular and intracellular recordings from medial septum/diagonal band neurons in vitro. Neuroscience 42, 451–462.

Messier, C., Mourre, C., Bontempi, B., Sif, J., Lazdunski, M., Destrade, C., 1991. Effect of apamin, a toxin that inhibits Ca^{2+}-dependent K^+ channels, on learning and memory processes. Brain Res. 551, 322–326.

Morris, R., 1984. Developments of a water-maze procedure for studying spatial learning in the rat. J. Neurosci. Meth. 11, 47–60.

Mourre, C., Hugues, M., Lazdunski, M., 1986. Quantitative autoradiographic mapping in rat brain of the receptor of apamin, a polypeptide toxin specific for one class of Ca^{2+}-dependent K^+ channels. Brain Res. 382, 239–249.

Riekkinen Jr., P. Sirviö, J., Riekkinen, P., 1990. The effects of THA on medial septal lesion-induced memory defects. Pharmacol. Biochem. Behav. 36, 237–241.

Riekkinen Jr., P. Schmidt, B., Stefanski, R., Kuitunen, J., Riekkinen, M., 1996. Metrifonate improves spatial navigation and avoidance behaviour in scopolamine-treated, medial septum-lesioned and aged rats. Eur. J. Pharmacol. 309, 121–130.

Riekkinen Jr., P. Schmidt, B., Riekkinen, M., 1997. Behavioral characterisation of metrifonate-improved acquisition of spatial information in medial septum-lesioned rats. Eur. J. Pharmacol. 323, 11–19.

Strong, P.N., 1990. Potassium channel toxins. Pharmacol. Ther. 46, 137–162.

The Journal of Neuroscience, December 1, 2002, 22(23):10163–10171

Small Conductance Ca^{2+}-Activated K^+ Channels Modulate Synaptic Plasticity and Memory Encoding

Robert W. Stackman,[2] Rebecca S. Hammond,[2] Eftihia Linardatos,[2] Aaron Gerlach,[1] James Maylie,[3] John P. Adelman,[1] and Thanos Tzounopoulos[1,2]

[1]Vollum Institute, Departments of [2]Behavioral Neuroscience and [3]Obstetrics and Gynecology, Oregon Health and Science University, Portland, Oregon 97239-3098

Activity-dependent changes in neuronal excitability and synaptic strength are thought to underlie memory encoding. In hippocampal CA1 neurons, small conductance Ca^{2+}-activated K^+ (SK) channels contribute to the afterhyperpolarization, affecting neuronal excitability. In the present study, we examined the effect of apamin-sensitive SK channels on the induction of hippocampal synaptic plasticity in response to a range of stimulation frequencies. In addition, the role of apamin-sensitive SK channels on hippocampal-dependent memory encoding and retention was also tested. The results show that blocking SK channels with apamin increased the excitability of hippocampal neurons and facilitated the induction of synaptic plasticity by shifting the modification threshold to lower frequencies. This facilitation was NMDA receptor (NMDAR) dependent and appeared to be postsynaptic. Mice treated with apamin demonstrated accelerated hippocampal-dependent spatial and nonspatial memory encoding. They required fewer trials to learn the location of a hidden platform in the Morris water maze and less time to encode object memory in an object-recognition task compared with saline-treated mice. Apamin did not influence long-term retention of spatial or nonspatial memory. These data support a role for SK channels in the modulation of hippocampal synaptic plasticity and hippocampal-dependent memory encoding.

Key words: synaptic plasticity; Ca^{2+}-activated K^+ channels; excitability; hippocampus; spatial memory; object memory

In hippocampal pyramidal neurons, action potentials are followed by an afterhyperpolarization (AHP) with three kinetic components. The predominant components, the medium AHP (mAHP) and slow AHP (sAHP), are attributable to the activation of small conductance Ca^{2+}-activated K^+ (SK) channels (Blatz and Magleby, 1986; Lancaster and Nicoll, 1987; Storm, 1990; Sah, 1996; Stocker et al., 1999). In addition to their different kinetics, the mAHP and the sAHP can be pharmacologically distinguished because apamin blocks the mAHP but not the sAHP (Kohler et al., 1996; Sah and Clements, 1999; Stocker et al., 1999). Apamin, a peptide derived from bee venom, is a highly selective blocker of SK channels, having no other known targets (Garcia et al., 1991). In CA1 neurons, synaptic activation may induce Ca^{2+} influx through NMDA receptors (NMDARs) (Alford et al., 1993; Kovalchuk et al., 2000), as well as through voltage-gated Ca^{2+} channels (Magee and Johnston, 1995). Synaptic activation of a Ca^{2+}-dependent K^+ current resembling the I_{sAHP} reduces postsynaptic excitability in response to high-frequency synaptic input (Lancaster et al., 2001).

Multiple forms of synaptic plasticity occur at the Schaffer collateral CA1 synapses, including long-term potentiation (LTP) and long-term depression (LTD) (Malenka and Nicoll, 1993). Essential for these processes is the influx of Ca^{2+} through NMDARs and the consequent rise in cytosolic Ca^{2+} (Lynch et al., 1983; Brocher et al., 1992; Malenka et al., 1992; Mulkey and Malenka, 1992). The magnitude of the rise in cytosolic Ca^{2+}, as determined by the degree and pattern of NMDAR activation, distinguishes whether a synapse undergoes LTP or LTD. Trains of afferent stimuli capable of inducing synaptic plasticity cause a summation of EPSPs that generate action potentials. The consequent increases in intracellular Ca^{2+} may activate SK channels; thus SK channels may represent a mechanism for modulating the induction of synaptic plasticity. Using a single stimulus frequency (100 Hz for 1 sec or 5 Hz for 3 min) (Behnisch and Reymann, 1998; Norris et al., 1998; Foster, 1999), the magnitude of LTP induced in the CA1 region was increased by extracellular application of apamin. The present experiments investigated whether SK channels modulate the threshold for synaptic plasticity as defined by the frequency–response function (Bear, 1995) and the mechanism through which such a modulation may occur. By using a wide range of stimulation frequencies, the results show that SK channel activity modulated the threshold for the induction of synaptic plasticity through a postsynaptic mechanism that required NMDAR activation.

SK channel blockade has been shown to (1) facilitate hippocampal-independent learning (Messier et al., 1991; Fournier et al., 2001) and (2) enhance spatial memory in hippocampal-lesioned mice but not in intact mice (Ikonen et al., 1998; Ikonen and Riekkinen, 1999). Differences in behavioral paradigm and the precise memory process addressed complicate the literature concerning the cognitive effects of apamin in rodents. Based on our electrophysiological findings, hippocampal-dependent tests were specifically modified to examine the effects of apamin on the

Received May 10, 2002; revised Sept. 24, 2002; accepted Sept. 24, 2002.

This work was supported by a grant from the Medical Research Foundation of Oregon (T.T.) and by grants from the National Institutes of Health (J.M., J.P.A.). We thank Drs. Craig Jahr, Laurence Trussell, and members of their laboratories for helpful discussions. We also thank Sophie Davis (Oregon Health and Science University/Portland State University Saturday Academy 2001 summer high school science apprenticeship program) for help with behavioral testing and Laura Tull, Dr. Anastassios Tzingounis, and Dr. Jacques Wadiche for helpful comments on this manuscript.

Correspondence should be addressed to Dr. Thanos Tzounopoulos, Auditory Neuroscience, L-335A, Oregon Hearing Research Center, Oregon Health and Science University, 3181 Southwest Sam Jackson Park Road, Portland, OR 97239-3098. E-mail: tzounopo@ohsu.edu.

initial stages of memory encoding. The data demonstrate that apamin facilitated spatial and nonspatial memory encoding in C57BL/6 mice.

MATERIALS AND METHODS

Electrophysiology

Hippocampal slices were prepared from 3- to 6-week-old male C57BL/6NHsd mice (Harlan Sprague Dawley, Indianapolis, IN). Animals were anesthetized with halothane and decapitated. The cerebral hemispheres were quickly removed and placed in a partially frozen solution of artificial CSF (ACSF) (in mM): 119 NaCl, 2.5 KCl, 1.2 $MgSO_4$, 2.5 $CaCl_2$, 1 $NaHPO_4$, 26.2 $NaHCO_3$, and 10 glucose and equilibrated with 95% O_2 and 5% CO_2. Hippocampi were removed, placed on an agar block, and transferred to a slicing chamber containing a similarly partially frozen solution. Transverse hippocampal slices (300–500 μm thick) were cut with a Vibratome tissue slicer, transferred into a humidified holding chamber, and allowed to recover for ≥1 hr before recordings were performed. The following drugs were used: apamin (Calbiochem, La Jolla, CA) and D-2 amino-5-phosphonovaleric acid (D-APV) (Tocris Cookson, Ellisville, MO). Extracellular field potentials were recorded in the stratum radiatum using electrodes (3–6 MΩ) filled with 3 M NaCl. For whole-cell recordings, CA1 pyramidal neurons were visualized with a water-immersion objective (40×; Zeiss, Thornwood, NY) using a microscope equipped with infrared/differential interference contrast optics (Zeiss Axioskop 2FS) and a CCD camera (Sony, Tokyo, Japan). Whole-cell recording pipettes were fabricated from TW150F-4 thin-wall borosilicate glass (World Precision Instruments, Sarasota, FL) and had resistances of 1.5–3 MΩ. Pipettes were filled with an intracellular solution containing (in mM): 140 $KMeSO_4$, 8 NaCl, 1 $MgCl_2$, 10 HEPES, 2 Mg-ATP, 0.4 Na_2-GTP, and 20 μM EGTA, pH 7.3, 290 mOsm. Slices were continuously perfused with ACSF. Whole-cell, patch-clamp currents were recorded with an Axopatch 200A amplifier (Axon Instruments, Foster City, CA), digitized using an ITC-16 analog-to-digital converter (InstruTech, Port Washington, NY), and transferred to a computer using Pulse software (Heka Elektronik, Lambrecht/Pfalz, Germany). CA1 neurons were voltage clamped at −55 mV, and I_{AHP} tail currents were evoked by a depolarizing voltage command to +20 mV for 200 msec followed by a return to −55 mV. Experiments on control slices were interleaved with those on experimental slices. Data were collected and analyzed online (10 kHz sampling rate) using IGOR (WaveTech, Lake Oswego, OR) and a program kindly donated by Dr. Greg Hjelmstad (University of California San Francisco, San Francisco, CA). The maximal initial slope of the field EPSP was measured to monitor the strength of synaptic transmission, minimizing contamination by voltage-dependent events. Summary graphs were obtained by normalizing each experiment according to the average value of all points on the 10 min baseline, aligning the points with respect to the start of the (LTP and LTD) induction protocol, dividing each experiment into 1 min bins, and averaging these across experiments. The amount of potentiation or depression of the synaptic response was measured 40–50 min after conditioning. Data are expressed as mean ± SEM, as a percentage of the baseline. Student's *t* test and two-factor ANOVA were used to determine significance between groups of data; $p < 0.05$ was considered significant. Experiments were included in the data analysis only when LTP could be generated at the end of the experimental manipulation, ensuring that the occurrence of short-term potentiation or LTD was attributable to the experimental manipulation.

Morris water maze

To assess hippocampal-dependent spatial learning and memory, naive male C57BL/6NHsd mice (4–6 weeks of age) were trained in a Morris water maze (Silva et al., 1998; Cho et al., 1999). Before the start of behavioral testing, mice were habituated over a 3 d period to daily handling and intraperitoneal injection. Over the following 2 d, all mice received nonspatial habituation trials (one trial per day). During these trials, a clear Plexiglas platform (13 cm diameter) was placed in the center of a white polyethylene pool (60 cm high, 109 cm diameter), and floor-to-ceiling curtains were drawn around the pool to block the animals' use of extra-maze cues. The platform was 1 cm below the surface of the water, and the water was rendered opaque by the addition of nontoxic white Tempra paint. Each mouse was placed on the platform for 60 sec and then released into the pool at four locations adjacent to the platform and allowed to swim and climb onto the platform.

Spatial training. After nonspatial habituation, mice were trained on the spatial (hippocampal-dependent) version of the water maze task. Training comprised 24 trials (four trials per day) during which the platform remained submerged 1 cm below the water surface in a fixed position in the center of one quadrant of the pool. During a given trial, the mouse was introduced into the pool at one of four possible start points (north, south, west, and east) and allowed 60 sec to swim to the platform. The order of start points varied in a pseudorandom manner for each mouse every day. After remaining on the platform for 30 sec, the mouse was placed into a holding cage for a 45 sec intertrial interval. Throughout water maze testing, the water temperature was maintained at 22–23°C. Each mouse received intraperitoneal apamin (0.4 mg/kg, 10 ml/kg; Calbiochem) or 0.9% saline (10 ml/kg) 30 min before the first training trial of each day. This dose of apamin was defined in pilot studies conducted to determine a dose that was behaviorally effective but that induced no motor or convulsive effects.

Spatial memory testing. After the fourth, 12th, and 20th training trials, a probe test was conducted in which each mouse received a 30 sec free swim in the pool with the platform removed. Twenty-four hours after the final training trial (24th trial), each mouse received a 60 sec probe test of long-term retention. The behavior of the mice during training and probe tests was recorded with a computerized video tracking system (EthoVision 2.2; Noldus, Leesburg, VA) and analyzed to determine the amount of time spent in each of the four quadrants of the water maze.

Object recognition

To assess the effects of apamin on nonspatial hippocampal-dependent memory, naive male C57BL/6NHsd mice (4–6 weeks of age) were tested in an object-recognition memory task (Vnek and Rothblat, 1996; Clark et al., 2000). Before object recognition testing, all mice were habituated to intraperitoneal injection and to the open-field arena (38 × 38 × 64 cm high) for 5 min each day for 3 d. During a subsequent sample session, two identical novel objects [Duplo or Lego blocks (Lego Company, Billund, Denmark), toys, etc.] were placed into opposite corners (southwest and northeast) of the open-field arena, and the mouse was allowed to explore the objects. Pilot studies revealed that C57BL/6 mice averaged 38 sec of exploration of either sample object during a 5 min sample session. For the present study, the object recognition task was modified to explicitly examine the influence of apamin on object memory encoding. To manipulate encoding, mice were allowed to explore the sample objects until either 19 sec (minimal training) or 38 sec (extensive training) of object exploration had been accumulated. Twenty-four hours after the sample session, a test session was conducted during which each mouse was placed back into the arena containing one of the familiar objects and a novel object for 5 min. The spatial position of the novel object was counterbalanced so that one-half of the mice experienced the novel object in the southwest corner of the open field, whereas the other half of the mice experienced the novel object in the northeast corner. After each session, all objects were cleaned with 10% ethanol to reduce the possibility that mice were imparting some odor cue to the objects that would influence object exploratory behavior during a subsequent test session. Pilot studies were conducted to select objects that elicited equivalent degrees of exploration in mice. This is necessary to verify that naive mice exhibited no inherent preference for one object over the other.

The behavior of each mouse was recorded using the EthoVision system and scored to determine the amount of time spent exploring each of the objects during each session. Object exploration was defined as any time that the mouse's head was oriented toward the object, was within 2–3 cm of the object, and its vibrissas were moving. Object recognition memory was quantified by measuring the difference in exploration times between the novel and familiar object. A novel object preference index, a ratio of the amount of time spent exploring the novel object over the total time spent exploring both objects, was used to measure recognition memory. A novel object preference ratio of >0.5 indicates that the mouse spent more time exploring the novel object than the familiar one.

RESULTS

Apamin blocks SK channels underlying the mAHP and increases excitability

CA1 neurons express an apamin-sensitive I_{mAHP} (Fig. 1*A*) thought to be mediated by apamin-sensitive SK channels (Kohler et al., 1996; Stocker et al., 1999). Action potentials recorded in response to current injections showed that apamin (100 nM) increased the number of action potentials discharged in CA1

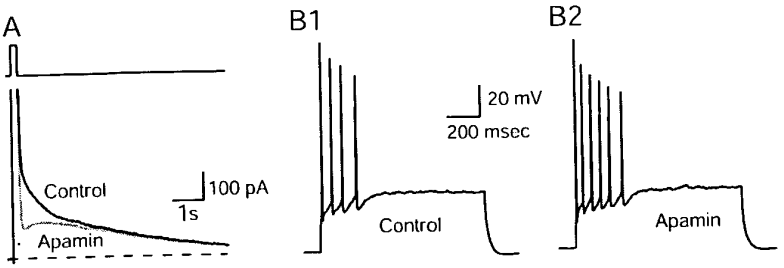

Figure 1. Blockade of the apamin-sensitive afterhyperpolarization (mAHP) increases excitability. *A*, I_{AHPs} were evoked in the whole-cell configuration by a 200 msec depolarizing pulse to +20 mV followed by a return to the −55 mV holding potential. I_{AHPs} were obtained in the presence and absence of apamin (100 nM). After application of apamin, the medium-duration component (I_{mAHP}) of the tail current was selectively inhibited. *Dashed line* indicates zero current. *B*, Apamin increased the number of action potentials. *B1*, Response of a pyramidal neuron to a 1 sec depolarizing current pulse. *B2*, Response of the same neuron to the same depolarizing current pulse in the presence of apamin (control cells fired an average ± SEM of 4.7 ± 1.2 action potentials/depolarizing pulse, which increased to 6.7 ± 1.7 with apamin; $n = 5$; $p = 0.04$; paired Student's t test).

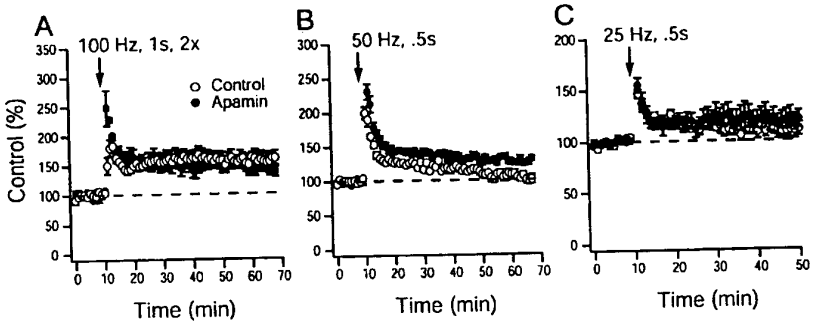

Figure 2. Apamin block of SK channel activity enhances plasticity induced by high-frequency stimulation. *A*, A 100 Hz, 1 sec tetanus in control and apamin (100 nM)-treated slices (164 ± 7%, $n = 9$ slices per 6 animals for controls; 165 ± 6%, $n = 10$ slices per 6 animals for apamin; $p > 0.05$; unpaired Student's t test). *B*, A 50 Hz, 0.5 sec stimulation protocol in control and apamin (100 nM)-treated slices (106 ± 4%, $n = 12$ slices per 8 animals for control slices, 125 ± 3%, $n = 13$ slices per 8 animals for apamin-treated slices; $p < 0.05$; unpaired Student's t test). *C*, A 25 Hz, 0.5 sec stimulation protocol in control and apamin (100 nM)-treated slices (109 ± 9%, $n = 8$ slices per 6 animals for controls; 120 ± 6%, $n = 8$ slices per 6 animals for apamin; $p > 0.05$; unpaired Student's t test). Control and apamin-treated slices were interleaved. Synaptic strength was measured as the initial slope of the recorded field EPSP. *Dashed line* indicates baseline response in *A–C*.

neurons (Fig. 1*B*). Control cells fired an average ± SEM of 4.7 ± 1.2 action potentials per depolarizing pulse (Fig. 1*B1*), which was increased to 6.7 ± 1.7 in the presence of apamin (Fig. 1*B2*) ($n = 5$; $p = 0.04$; paired Student's t test). This result indicates that blockade of apamin-sensitive SK channels increases excitability. Such changes in excitability may influence the threshold for the induction of synaptic plasticity.

Blocking SK channels facilitates the induction of synaptic plasticity

To investigate the role of SK channels on the induction of synaptic plasticity at CA1 synapses, stimulation protocols that evoke LTP or LTD were delivered to mouse hippocampal brain slices in the presence or absence of apamin. Figure 2*A* shows the effect of apamin (100 nM) application on the ability of high-frequency stimulation (100 Hz applied twice for 1 sec, separated by 10 sec) to generate LTP. Equal extents of LTP were observed in control (164 ± 7%; $n = 9$ slices per 6 animals) and apamin-treated (165 ± 6%; $n = 10$ slices per 6 animals) slices, showing that apamin does not alter the ability of high-frequency stimulation to induce robust LTP ($p > 0.05$; unpaired Student's t test). After a 50 Hz, 0.5 sec stimulus, significantly more LTP was induced in the presence of apamin (125 ± 3%, $n = 13$ slices per 8 animals for apamin-treated slices; 106 ± 4%, $n = 12$ slices per 8 animals for control slices; $p < 0.05$; unpaired Student's t test) (Fig. 2*B*). Using a 25 Hz, 0.5 sec stimulus, LTP was not different in control and apamin-treated slices (120 ± 6%, $n = 8$ slices per 6 animals for apamin-treated slices; 109 ± 9%, $n = 8$ slices per 6 animals for control slices; $p > 0.05$; unpaired Student's t test) (Fig. 2*C*).

To determine whether apamin affects the threshold for induction of synaptic plasticity, its effects on lower stimulation frequencies were examined. A 10 Hz stimulation for 900 pulses resulted in LTD in control slices (77 ± 6%; $n = 10$ slices per 6 animals), whereas apamin-treated slices did not show changes in synaptic strength (101 ± 7%; $n = 9$ slices per 5 animals; $p < 0.05$; unpaired Student's t test) (Fig. 3*A*). In addition, 5-Hz stimulation for 900 pulses resulted in LTD in apamin-treated slices (85 ± 5%; $n = 9$ slices per 5 animals) but did not affect long-lasting changes in synaptic strength in control slices (103 ± 4%; $n = 10$ slices per 6 animals; $p < 0.05$; unpaired Student's t test) (Fig. 3*B*). These results suggest that apamin alters the frequency–response relationship (Bear, 1995) for the induction of synaptic plasticity. The modification threshold is the level of postsynaptic response at which the sign of the synaptic modification reverses from LTD to LTP (Bienenstock et al., 1982). The smooth transition from LTD to LTP may be demonstrated by systematically varying the frequency of conditioning stimulation for a given number of pulses. The frequency–response relationships for control and apamin-treated slices are presented in Figure 3*C* and demonstrate that blockade of SK channels with apamin shifts the frequency–response function to the lower frequencies, facilitating the induction of synaptic plasticity.

Blocking SK channels does not affect neurotransmitter release

To investigate whether the apamin-induced shift in the frequency–response function at CA1 synapses involves presynaptic or postsynaptic changes, the effects of apamin on paired-pulse facilitation, post-tetanic potentiation, and short-term depression were investigated.

Paired-pulse facilitation, an increased second response to two stimuli applied in rapid succession, is thought to reflect an increase in the probability of neurotransmitter release (Katz and Miledi, 1968). Paired-pulse facilitation was tested at interstimulus

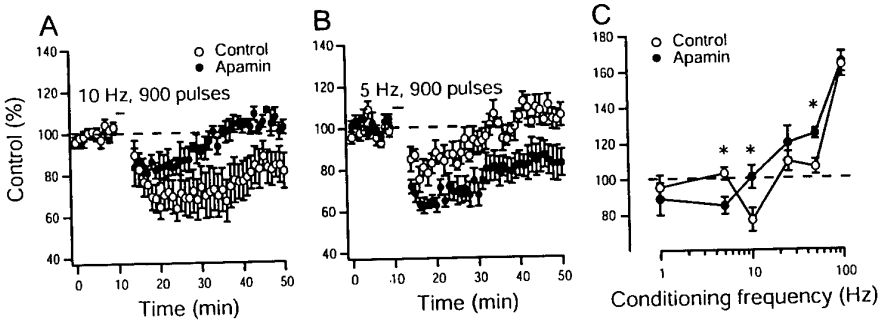

Figure 3. Apamin block of SK channel activity shifts the synaptic modification threshold to lower frequencies. Induction of synaptic plasticity by 10 Hz, 900 pulse stimulation in control slices (77 ± 6%; n = 10 slices per 6 animals) and apamin (100 nM)-treated slices (101 ± 7%; n = 9 slices per 5 animals; $p < 0.05$; unpaired Student's t test) (*A*) and 5 Hz, 900 pulse stimulation protocol in control slices (103 ± 4%; n = 8 slices per 5 animals) and apamin (100 nM)-treated slices (85 ± 5%; n = 9 slices per 5 animals; $p < 0.05$; unpaired Student's t test) (*B*). *Dashed line* indicates baseline response. *C*, Frequency–response relationship for the induction of LTP and LTD in controls and experiments from slices in which apamin (100 nM) was applied. The mean effect of 900 pulses of conditioning stimulation delivered at various frequencies to the Shaffer collaterals on the synaptic response measured 40–50 min after conditioning is shown. *$p < 0.05$ versus respective control data point; Student's t test. *Dashed line* indicates the transition between LTD and LTP.

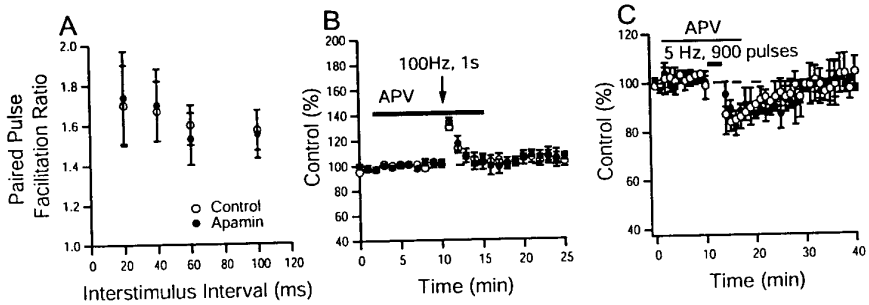

Figure 4. SK channels do not have presynaptic effects in CA1. *A*, Paired-pulse facilitation (*PPF*), measured as the ratio of the second response to the first, was plotted as a function of interstimulus interval for controls and in the presence of apamin ($n > 8$ for all interstimulus intervals). No significant differences were detected ($p > 0.05$; paired Student's t test). *B*, Time course of post-tetanic potentiation elicited by 100 Hz, 1 sec tetanus in control and apamin-treated slices. Post-tetanic potentiation (peak enhancement in controls, 132 ± 6% of baseline, n = 9 slices per 4 animals; peak enhancement in apamin, 134 ± 5% of baseline, n = 9 slices per 4 animals) was not different between groups ($p > 0.05$; unpaired Student's t test). *C*, Time course of short-term depression elicited by 5 Hz, 900 pulse stimulation in control and apamin-treated slices (80 ± 7% of baseline, n = 6 slices per 3 animals; peak depression in apamin, 82 ± 5% of baseline, n = 6 slices per 3 animals). No significant differences were detected between groups ($p > 0.05$; paired Student's t test). Synaptic strength was measured as the initial slope of the recorded field EPSP. *Solid line* in *B* and *C* indicates the duration of D-APV application.

intervals ranging from 20 to 100 msec and was not significantly altered by application of apamin ($p > 0.05$; paired Student's t test; $n > 8$ for all interstimulus intervals) (Fig. 4*A*), suggesting that apamin does not alter neurotransmitter release.

Post-tetanic potentiation, a slow decay of the postsynaptic responses after repetitive stimulation has been terminated, presumably reflects the slow decay of elevated presynaptic Ca^{2+} levels induced by the tetanic stimulus (Zucker, 1989). The effects of apamin on post-tetanic potentiation were examined using a 100 Hz, 1 sec tetanus delivered in the presence of D-APV (100 μM), an NMDA receptor antagonist. The time course of post-tetanic potentiation was not different between control and apamin-treated slices, nor were differences detected in the peak enhancement achieved in the presence or absence of apamin (control, 132 ± 6%, n = 9 slices per 4 animals; apamin treated, 134 ± 5%, n = 9 slices per 5 animals; $p > 0.05$; unpaired Student's t test) (Fig. 4*B*).

Short-term depression was also examined using a 5 Hz, 900 stimuli tetanus delivered in the presence of D-APV (100 mM). This same protocol had revealed differences between control and apamin-treated slices when performed in the absence of D-APV (Fig. 3*B*). In the presence of D-APV (Fig. 4*C*), the magnitude and time course of depression were not different between control slices (peak depression, 80 ± 7%, n = 9 slices per 4 animals) and apamin-treated slices (peak depression, 82 ± 5%, n = 9 slices per 5 animals; $p > 0.05$; unpaired Student's t test). The lack of effect of apamin on paired-pulse facilitation, post-tetanic potentiation, and short-term depression suggests that apamin does not affect presynaptic events but rather alters NMDAR-dependent postsynaptic events to shift the threshold for the induction of synaptic plasticity in CA1 synapses.

Blocking SK channels accelerates hippocampal-dependent spatial memory encoding

The results presented above indicate that apamin facilitates the induction of synaptic plasticity in the CA1 region of the hippocampus. It was hypothesized that apamin might also alter hippocampal-dependent memory assessed in the Morris water maze, a task considered to require the activation of NMDARs and synaptic plasticity in the hippocampus (Morris et al., 1982; Tsien et al., 1996). Considering the finding that apamin shifted the threshold for the induction of synaptic plasticity (Fig. 3*C*), it was predicted that apamin would exert its greatest influence during the initial stages of spatial memory encoding. Specifically, the effects of systemic apamin were examined using a version of the Morris water-maze task modified to explicitly assess the encoding of spatial memory. The rationale being that if synaptic plasticity is more easily induced in the presence of apamin, fewer trials may be required to encode spatial memory in apamin-treated mice. Naive mice received apamin (0.4 mg/kg, i.p.; n = 10) or 0.9% saline (n = 9) 30 min before daily training for 6 d (four trials per day) in the water maze task. The platform location remained fixed throughout all training trials. Immediately after the fourth, 12th, and 20th training trials, each mouse received a 30 sec probe test. These interpolated probe tests assess the development of a spatial bias for the training quadrant of the pool at an

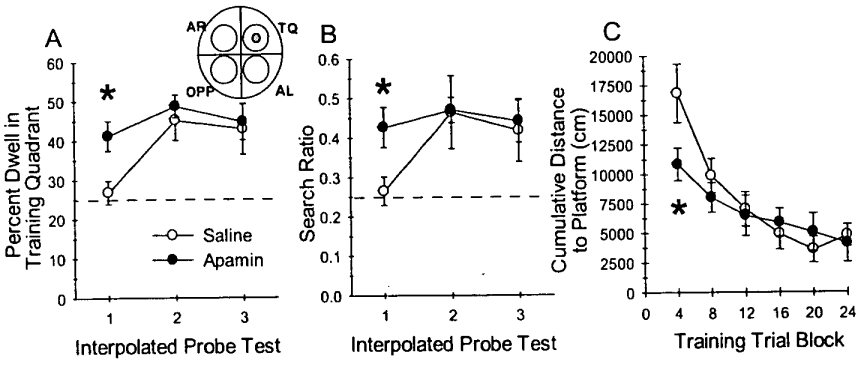

Figure 5. Apamin block of SK channels facilitates the encoding of spatial memory. *A*, A modified Morris water maze task was used to examine the effects of apamin on encoding of spatial memory. Mice were trained for four trials per day for 6 d, and 30 sec probe tests were presented immediately after the fourth, 12th, and 20th trial. Mean ± SEM percentage of time spent dwelling (*Percent Dwell*) in the training quadrant during the interpolated probe tests revealed that mice treated with 0.4 mg/kg apamin ($n = 10$) spent significantly more time in the training quadrant during the first probe test than saline-treated ($n = 9$) control mice (*$p < 0.009$ vs saline-treated mice on probe test 1; planned comparison Student's t test). The *dashed line* at 25% represents chance performance. *AL*, Adjacent left; *AR*, adjacent right; *OPP*, opposite; *TQ*, training quadrant. *B*, Mean ± SEM search ratio reflects the accuracy with which mice search in the correct location within the training quadrant of the pool. Search ratio is computed as the number of times the animal crosses into the zone (see *circular regions of inset diagram*) encompassing the platform (*shaded zone*) divided by the total number of crossings into all four zones. The *dashed line* at 0.25 represents chance performance during the probe tests or the lack of spatial bias for any particular pool location. Apamin-treated mice exhibited a significantly higher search ratio than saline-treated mice during the first probe test (*$p < 0.02$ vs saline-treated mice on probe test 1; planned comparison Student's t test). Measures of the percentage of time spent dwelling in the training quadrant or search ratio from the second or third probe tests were equivalent between the two groups, indicating that there were no group differences in platform search behavior after more training. *C*, Mean ± SEM cumulative distance to platform measures of saline- and apamin-treated mice plotted in blocks of four training trials. This measure indicates the proximity of the mice to the platform during each training trial. Consistent with the data from probe test 1, apamin-treated mice swam in closer proximity to the platform during the first four trial block of training than saline-treated mice (*$p < 0.04$; *post hoc* Tukey multiple comparisons test).

early (probe 1), intermediate (probe 2), and late (probe 3) stage of spatial memory encoding. Apamin treatment accelerated the development of a spatial bias for the training quadrant during the first interpolated probe test (probe 1), as shown in Figure 5*A*. Planned comparisons analyses revealed that apamin-treated mice spent significantly more time in the training quadrant than saline-treated mice (mean ± SEM; apamin, 41.1 ± 3.8%; saline, 26.8 ± 2.9%; $t_{(17)} = -2.94$; $p = 0.009$). In addition, apamin-treated mice exhibited more accurate search behavior as indicated by search ratio (Fig. 5*B*), computed as the number of crossings into a circular zone encompassing the platform divided by the total number of crossings into all four zones (Fig. 5*B*, *inset diagram*) (apamin, 0.43 ± 0.05; saline, 0.26 ± 0.04; $t_{(17)} = -2.52$; $p = 0.02$). Saline-treated mice required 12 training trials to develop this degree of preference (probe 2). Thus, after minimal training (just four trials), apamin-treated mice exhibited significant spatial memory of the training quadrant, whereas control mice exhibited a chance level of performance. There were no additional differences in performance on probes 2 and 3 between apamin- and saline-treated mice, indicating that after 12 training trials, the saline-treated mice had acquired the memory for platform location and were performing as accurately as apamin-treated mice. Spatial memory encoded by apamin-treated mice was stable throughout the training session, because there was no difference in training-quadrant preference across the three interpolated probe tests. Two-factor, repeated-measures (treatment × four trial block) ANOVA on cumulative distance to platform measures revealed a significant treatment × four trial block interaction ($F_{(4,68)} = 2.53$; $p < 0.05$) and a significant effect of four trial block ($F_{(4,68)} = 15.75$; $p < 0.001$). Tukey multiple comparisons tests revealed a significant difference between apamin- and saline-treated mice in cumulative distance to platform on the first four trial block (Fig. 5*C*). The cumulative distance to platform is a score of the proximity of the mouse to the platform during training and is a more sensitive measure of spatial behavior than escape latency (Gallagher et al., 1993). The difference in cumulative distance measures between apamin- and saline-treated mice reflects more accurate platform search behavior by the apamin-treated mice, a finding that is consistent with the observed differences in spatial search behavior during probe 1. An identical analysis of escape latency data found a significant effect of four trial block ($F_{(4,68)} = 8.50$; $p < 0.001$) but no treatment × four trial block interaction ($F_{(4,68)} = 0.44$; $p > 0.5$) and no significant effect of treatment ($F_{(4,68)} = 0.54$; $p > 0.5$). Apamin treatment did not cause any overt influence on swimming, and swim speeds were not different between groups ($F_{(1,17)} = 0.29$; $p > 0.5$). Analyses restricted to the data from the first four training trials also indicated no significant differences in escape latencies ($t_{(17)} = 0.33$; $p > 0.05$) or swim speed ($t_{(17)} = 0.04$; $p > 0.05$). Collectively, these results suggest that apamin-mediated blockade of SK channels facilitated the encoding of hippocampal-dependent spatial memory.

Data from the probe test given 24 hr after the final training trial were examined to test whether memory encoded under SK channel blockade would be differentially retained. Both groups of mice exhibited a spatial bias for searching in the training quadrant during the 24 hr retention probe test. There were no differences between saline- and apamin-treated mice during the final probe trial with regard to the percentage of time spent dwelling in the training quadrant (mean ± SEM; saline, 41.6 ± 4.6; apamin, 38.1 ± 4.3; $t_{(17)} = 0.57$; $p > 0.6$) or with regard to the search ratio (saline, 0.43 ± 0.05; apamin 0.38 ± 0.05; $t_{(17)} = 0.64$; $p > 0.5$). Together with the data of Figure 5*A–C*, it appears that apamin-treated mice encoded the spatial memory of the platform location with less training than the saline-treated mice. However, once encoded, there was no difference in retention of the spatial memory between apamin- and saline-treated mice.

Blocking SK channels accelerates hippocampal-dependent nonspatial memory encoding.

To further examine the role of SK channels in hippocampal memory, the effects of apamin on a nonspatial object-recognition task were examined. This task assesses the encoding and retention of memory for an object and is sensitive to lesions of the hippocampus (Vnek and Rothblat, 1996; Clark et al., 2000) and to manipulation of hippocampal NMDARs (Tang et al., 1999).

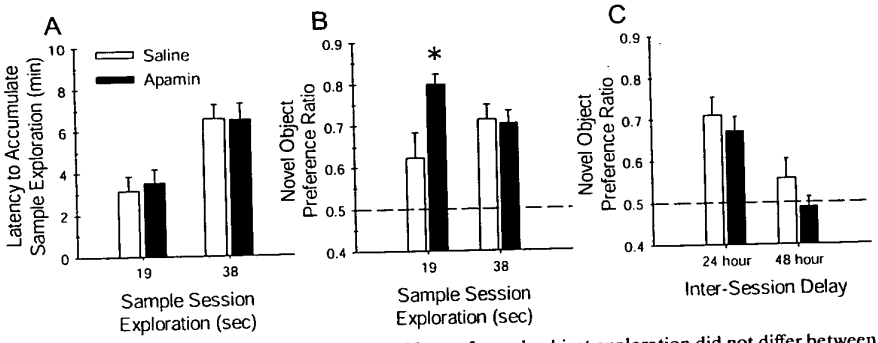

Figure 6. Apamin block of SK channel activity facilitates the encoding of nonspatial object memory but does not influence the retention of object memory. Object-recognition memory was quantified by computing the novel object preference ratio, the amount of time spent exploring the novel object during the test session divided by the total time spent exploring both the familiar and novel object. *A*, The object recognition task was modified to test the influence of apamin on object memory encoding. As described in Materials and Methods, during the sample session, saline- and apamin-treated mice were restricted to either 19 sec (minimal training) or 38 sec (extensive training) of sample object exploration. The amount of time required to accumulate either 19 or 38 sec of sample object exploration did not differ between apamin- and saline-treated mice (p values >0.05; unpaired Student's t test). *B*, Restricting the amount of object exploration during the sample session to 19 sec weakens the degree of preference exhibited by the mouse during a test session 24 hr later. This is illustrated by the lower novel object preference ratio of the saline-treated mice ($n = 9$) limited to 19 sec of sample object exploration. However, apamin (0.4 mg/kg)-treated mice ($n = 10$) that were limited to only 19 sec of sample object exploration exhibited a significantly greater novel object preference during the 24 hr test session ($*p < 0.04$ vs saline-treated mice permitted 19 sec of object exploration; planned comparison Student's t test). When apamin (0.4 mg/kg)-treated ($n = 10$) and saline-treated ($n = 9$) mice were permitted 38 sec of sample object exploration, there was no difference in novel object preference ratio during the 24 hr test session. Each *dashed line* at 0.5 represents chance performance or a lack of discrimination between the novel and familiar object. *C*, Object memory retention decays over a similar time course in apamin- and saline-treated mice. Both apamin- and saline-treated mice exhibited similar strong preference for the novel object during a 24 hr retention test; mean ± SEM novel object preference ratios were not significantly different. Four days later, the same mice received a second sample session with two new objects. When tested for retention 48 hr later, both apamin- and saline-treated mice failed to show a strong preference for the novel object over the familiar object. These data indicate that apamin does not affect the retention of object memory.

Given that apamin-treated mice developed a significant spatial memory for the platform location after minimal water-maze training, it was hypothesized that apamin would influence the encoding of object memory in a similar manner. Pilot studies indicated that during a 5 min sample session, C57BL/6J mice typically spend an average of 38 sec exploring each sample object. To examine the influence of apamin on object memory encoding, the amount of sample object exploration was manipulated. Mice were allowed to explore the sample objects until they had accumulated object exploration times of either 19 sec (minimal training) or 38 sec (extensive training). The results obtained for spatial memory encoding led to our prediction that apamin would facilitate object memory retention in mice limited to 19 sec of sample object exploration compared with respective saline-treated mice.

Naive C57BL/6NHsd mice received apamin (0.4 mg/kg, i.p.) or 0.9% saline 30 min before the sample session. Each mouse was placed into the arena containing two identical novel objects. Depending on group assignment, the mouse was removed from the arena after exploring either sample object for 19 sec (minimal training) or 38 sec (extensive training). During the sample session, there was no significant difference between saline- and apamin-treated mice with regard to the time required to reach the respective 19 or 38 sec sample object exploration limit ($t_{(17)} = -1.31$ and 0.04, respectively; p values of >0.05) (Fig. 6*A*), indicating that all mice exhibited the same curiosity and motivation. Object memory retention was assessed during a test session 24 hr later, in which each mouse was allowed to explore the arena containing one of the familiar objects from the sample session and a novel object. Saline-treated mice limited to 19 sec of sample object exploration exhibited a weaker preference for the novel object during the test session compared with mice permitted 38 sec of sample object exploration (Fig. 6*B*). Planned comparisons analysis revealed that apamin-treated mice limited to 19 sec of sample object exploration exhibited a stronger preference for the novel object compared with the respective saline-treated mice ($t_{(17)} = -2.17$; $p = 0.04$) (Fig. 6*B*). These data suggest that apamin is capable of facilitating object memory encoding. There was no difference in novel object preference ratio between saline- and apamin-treated mice permitted 38 sec of sample object exploration ($t_{(17)} = -0.11$; $p > 0.05$), indicating that both groups exhibited equivalent object memory retention. In accordance with our findings of apamin-treated mice in the Morris water-maze task, these findings suggest that apamin block of SK channels facilitates the encoding of nonspatial memory, perhaps by reducing the threshold for memory formation.

The retention of object memory decays faster in hippocampal-lesioned rodents (Vnek and Rothblat, 1996; Clark et al., 2000) and is sensitive to genetic manipulation of the hippocampal NMDAR (Tang et al., 1999). Hippocampal-lesioned rats fail to retain object memory over a 24 hr delay (Clark et al., 2000) but are able to retain object memory over a 5 min delay (Mumby et al., 2002). The influence of systemic apamin on the rate of decay of object memory retention was examined in a second cohort of C57BL/6NHsd mice. During a sample session, apamin- (0.4 mg/kg, i.p.) and saline-treated mice were exposed to two identical sample objects for 5 min. Both groups exhibited a similar preference for the novel object during the 24 hr test session, as shown in Figure 6*C*, indicating that apamin did not influence memory retention at 24 hr, consistent with the 38 sec data of Figure 6*B*. Four days later, the same groups were exposed to a second set of sample objects and then tested for retention 48 hr later. As depicted in Figure 6*C*, neither group exhibited a significant preference for the novel object at the 48 hr test session, suggesting that object memory decayed over the same rate between the two groups. These data indicate that apamin did not influence object memory retention.

DISCUSSION

The present study demonstrates that blockade of synaptically activated SK channels increases excitability and decreases the threshold for the induction of hippocampal synaptic plasticity via a postsynaptic mechanism that requires the activation of NMDARs. The reduced threshold for induction of synaptic plasticity is associated with facilitated memory encoding. This enhancement is correlated with changes in the induction of synaptic plasticity but is not necessarily attributable to these changes,

because there is no way to rule out the effects of apamin on other brain structures that can influence hippocampal function.

Neural circuits derive flexibility from activity-driven bidirectional modification of synaptic strength (Sejnowski, 1977; Bienenstock et al., 1982). An important characteristic of this process is the threshold for synaptic modification (Bear, 1995), which is defined by the frequency–response function for the induction of synaptic plasticity. As postsynaptic activity increases, the threshold for LTD is reached first, and an additional increase leads to a transition from LTD to LTP. This transition represents the synaptic modification threshold (Bear, 1995). A prominent model for the regulation of the synaptic modification threshold proposes that the direction of altered synaptic efficacy, potentiation, or depression is determined by the level of postsynaptic Ca^{2+} during neural activity (Lisman, 1989; Artola and Singer, 1993; Malenka and Nicoll, 1993). The rise in Ca^{2+} within the dendritic spine is the critical trigger for synaptic plasticity. Stronger depolarization allows more Ca^{2+} to enter and leads to synaptic potentiation (Lisman, 1989; Artola and Singer, 1993; Bliss and Collingridge, 1993; Cummings et al., 1996; Malenka and Nicoll, 1999), whereas weaker depolarization leads to less Ca^{2+} influx and synaptic depression (Mulkey and Malenka, 1992; Dudek and Bear, 1993). Therefore, any manipulation that influences the magnitude or dynamics of Ca^{2+} increase within dendritic spines may profoundly influence the form of the resulting synaptic plasticity.

Synaptic activation of the channels underlying the I_{sAHP} (Lancaster et al., 2001; Martin et al., 2001) regulates synaptic efficacy and may influence the threshold for synaptic plasticity, as hypothesized by previous studies (Sah and Bekkers, 1996). Our results showed that application of apamin caused a shift of the synaptic modification threshold to lower frequencies, an effect that is consistent with facilitated induction of synaptic plasticity. Apamin-sensitive SK channels underlie the mAHP in CA1 neurons, which peaks ~200 msec after the action potential (Sah and Clements, 1999; Stocker et al., 1999), a time course that may enable the mAHP to influence neuronal discharge activity, and the integration of synaptic events as the rate of afferent stimulation increases toward the threshold for synaptic plasticity (5–20 Hz). These are precisely the stimulation frequencies around which apamin exerted its significant effects on the induction of synaptic plasticity.

Our results suggest that SK channel activity modulates the induction of synaptic plasticity that requires postsynaptic depolarization and NMDAR activation. Postsynaptic depolarization induced by repetitive synaptic stimulation raises intracellular Ca^{2+} levels through voltage-gated Ca^{2+} channels or NMDARs, permitting the activation of SK channels. By hyperpolarizing the postsynaptic membrane, SK channels decrease excitability and modulate the activation of NMDARs, which involves voltage-dependent removal of the Mg^{2+} block (Mayer et al., 1987). By affecting the degree of NMDAR activation and the subsequent Ca^{2+} entry, SK channels may modulate the induction of synaptic plasticity. Our experiments suggest that SK channels are dendritically localized. Although direct evidence for the distribution of SK channels in the dendrites is currently unavailable, it has been suggested that apamin-sensitive SK channels are located predominantly in proximal and distal dendrites of motor neurons (Cangiano et al., 2002). In addition, Ca^{2+}-activated K^+ channels have been reported in the dendrites of mammalian neurons (Andreasen and Lambert, 1995; Sah and Bekkers, 1996; Schwindt and Crill, 1997).

Synaptic plasticity is believed to represent, at least in part, the cellular mechanisms responsible for learning and memory. It is generally accepted that some form of an increase in synaptic efficacy in the hippocampus is necessary for encoding spatial memory in the water maze task (Moser et al., 1998). Whether such memory formation in the hippocampus is dependent on LTP or LTD has been difficult to establish (Holscher, 1997; Jeffery, 1997; Shors and Matzel, 1997). In the present study, blockade of SK channels increases excitability, reduces the threshold for hippocampal synaptic plasticity, and facilitates hippocampal memory encoding. Systemically administered apamin crosses the blood–brain barrier (Habermann, 1984), and high densities of apamin-sensitive SK channels are present in limbic regions, including the hippocampus (Mourre et al., 1987; Gehlert and Gackenheimer, 1993; Stocker and Pedarzani, 2000). Apamin-treated mice acquired a spatial memory for the water maze platform location after just four training trials (minimal training), whereas saline-treated mice required as many as 12 trials to demonstrate spatial memory acquisition. In the object recognition task, apamin-treated mice exhibited a significantly stronger test session preference for the novel object than saline-treated mice when limited to 19 sec of sample object exploration (minimal training). The parallel between the reduction of the threshold for synaptic plasticity and the improved memory encoding after minimal spatial or nonspatial training suggests a correlation between the facilitation of the induction of synaptic plasticity and memory encoding. The amount of induced plasticity cannot be equated with the rate of learning, because control and apamin-treated slices showed the same amount of LTP and LTD. However, the rate of learning seems to be dependent on the threshold for the induction of synaptic plasticity.

Previous studies indicate that apamin enhances spatial memory in mice with lesions of the hippocampal formation but have failed to detect an influence of apamin on memory retention in intact mice after extensive training (Ikonen et al., 1998; Ikonen and Riekkinen, 1999). Moreover, it was proposed recently that there are differences in apamin sensitivity between mice and rats, with rats being relatively insensitive to the cognitive effects of apamin (van der Staay et al., 1999). However, this claim is not substantiated by recent findings. Independent laboratories have demonstrated that in rats, apamin enhances the induction of synaptic plasticity (Behnisch and Reymann, 1998; Norris et al., 1998) and facilitates nonspatial memory (Deschaux et al., 1997; Fournier et al., 2001). Our data suggest that apamin exerts its influence on an early stage of memory encoding, an effect that may not have been detected given the approaches used previously. This indicates that apamin facilitated memory after minimal spatial or nonspatial training. Apamin did not have a significant effect on memory retention in mice after extensive spatial training, consistent with previous reports of the effects of apamin in mice and rats (Ikonen et al., 1998; Ikonen and Riekkinen, 1999; van der Staay et al., 1999).

From our behavioral data, no distinction can be made between an effect of apamin that leads to enhanced memory formation and that of an enhanced processing of the sensory input that precedes the formation of memory. However, the results suggest that it is unlikely that the enhancing effects of apamin are a consequence of sensory, motor, or attentional influences. If apamin was to influence sensory or attentional mechanisms, then apamin treatment would have enhanced object memory retention in both groups of mice, those limited to 19 sec of sample exploration as well as those allowed 38 sec of sample exploration. The beneficial

effect of apamin on spatial memory encoding in the Morris water maze cannot be attributed to enhanced motor function, because no differences in swim speed between apamin- and saline-treated mice were observed.

Collectively, the data from electrophysiological and behavioral studies indicate that blockade of SK channels by apamin increases excitability, shifts the threshold for the induction of synaptic plasticity, and facilitates hippocampal-dependent memory. The behavioral significance of this apamin-induced increase in excitability is to facilitate the processing of to-be-remembered information. The behavioral studies do not indicate whether the apamin-mediated enhancement in memory is caused by a facilitation of the induction of LTP or LTD. However, the shift in the threshold for synaptic plasticity produced by apamin could represent a mechanism for ensuring that there is coincident stimulation of hippocampal NMDARs leading to an enhancement of synaptic efficacy during the initial stages of learning. Learning-induced reduction of the AHP has been shown to underlie learning and memory in other behavioral paradigms. A potentiation of EPSPs and a reduction in the mAHP and sAHP currents is associated with classical conditioning of the eye-blink response in rabbits (Disterhoft et al., 1988; LoTurco et al., 1988; Coulter et al., 1989) and with olfactory operant conditioning in rats (Saar et al., 1998). Single-unit recording studies of hippocampal neurons from behaving rabbits during eye-blink conditioning trials have revealed increases in neuronal firing rates that are specific to learning (Berger et al., 1983; McEchron and Disterhoft, 1999). Therefore, the AHP is a negative regulator of learning, and reduction of the AHP by apamin appears to facilitate learning and memory. Together with the results presented here, it appears that apamin-sensitive SK channels represent a neural mechanism capable of regulating hippocampal-dependent memory.

REFERENCES

Alford S, Frenguelli BG, Schofield JG, Collingridge GL (1993) Characterization of Ca^{2+} signals induced in hippocampal CA1 neurones by the synaptic activation of NMDA receptors. J Physiol (Lond) 469:693–716.

Andreasen M, Lambert JD (1995) The excitability of CA1 pyramidal cell dendrites is modulated by a local Ca^{2+}-dependent K^+-conductance. Brain Res 698:193–203.

Artola A, Singer W (1993) Long-term depression of excitatory synaptic transmission and its relationship to long-term potentiation. Trends Neurosci 16:480–487.

Bear MF (1995) Mechanism for a sliding synaptic modification threshold. Neuron 15:1–4.

Behnisch T, Reymann KG (1998) Inhibition of apamin-sensitive calcium dependent potassium channels facilitate the induction of long-term potentiation in the CA1 region of rat hippocampus in vitro. Neurosci Lett 253:91–94.

Berger TW, Rinaldi PC, Weisz DJ, Thompson RF (1983) Single-unit analysis of different hippocampal cell types during classical conditioning of rabbit nictitating membrane response. J Neurophysiol 50:1197–1219.

Bienenstock EL, Cooper LN, Munro PW (1982) Theory for the development of neuron selectivity: orientation specificity and binocular interaction in visual cortex. J Neurosci 2:32–48.

Blatz AL, Magleby KL (1986) Single apamin-blocked Ca-activated K^+ channels of small conductance in cultured rat skeletal muscle. Nature 323:718–720.

Bliss TV, Collingridge GL (1993) A synaptic model of memory: long-term potentiation in the hippocampus. Nature 361:31–39.

Brocher S, Artola A, Singer W (1992) Intracellular injection of Ca^{2+} chelators blocks induction of long-term depression in rat visual cortex. Proc Natl Acad Sci USA 89:123–127.

Cangiano L, Wallen P, Grillner S (2002) Role of apamin-sensitive K_{Ca} channels for reticulospinal synaptic transmission to motoneuron and for the afterhyperpolarization. J Neurophysiol 88:289–299.

Cho YH, Friedman E, Silva AJ (1999) Ibotenate lesions of the hippocampus impair spatial learning but not contextual fear conditioning in mice. Behav Brain Res 98:77–87.

Clark RE, Zola SM, Squire LR (2000) Impaired recognition memory in rats after damage to the hippocampus. J Neurosci 20:8853–8860.

Coulter DA, LoTurco JJ, Kubota M, Disterhoft JF, Moore JW, Alkon DL (1989) Classical conditioning reduces amplitude and duration of calcium-dependent afterhyperpolarization in rabbit hippocampal pyramidal cells. J Neurophysiol 61:971–981.

Cummings JA, Mulkey RM, Nicoll RA, Malenka RC (1996) Ca^{2+} signaling requirements for long-term depression in the hippocampus. Neuron 16:825–833.

Deschaux O, Bizot JC, Goyffon M (1997) Apamin improves learning in an object recognition task in rats. Neurosci Lett 222:159–162.

Disterhoft JF, Golden DT, Read HL, Coulter DA, Alkon DL (1988) AHP reductions in rabbit hippocampal neurons during conditioning correlate with acquisition of the learned response. Brain Res 462:118–125.

Dudek SM, Bear MF (1993) Bidirectional long-term modification of synaptic effectiveness in the adult and immature hippocampus. J Neurosci 13:2910–2918.

Foster TC (1999) Involvement of hippocampal synaptic plasticity in age-related memory decline. Brain Res Brain Res Rev 30:236–249.

Fournier C, Kourrich S, Soumireu-Mourat B, Mourre C (2001) Apamin improves reference memory but not procedural memory in rats by blocking small conductance Ca^{2+}-activated K^+ channels in an olfactory discrimination task. Behav Brain Res 121:81–93.

Gallagher M, Burwell R, Burchinal M (1993) Severity of spatial learning impairment in aging: development of a learning index for performance in the Morris water maze. Behav Neurosci 107:618–626.

Garcia ML, Galvez A, Garcia-Calvo M, King VF, Vazquez J, Kaczorowski GJ (1991) Use of toxins to study potassium channels. J Bioenerg Biomembr 23:615–646.

Gehlert DR, Gackenheimer SL (1993) Comparison of the distribution of binding sites for the potassium channel ligands [^{125}I]apamin, [^{125}I]charybdotoxin and [^{125}I]iodoglyburide in the rat brain. Neuroscience 52:191–205.

Habermann E (1984) Apamin. Pharmacol Ther 25:255–270.

Holscher C (1997) Long-term potentiation: a good model for learning and memory? Prog Neuropsychopharmacol Biol Psychiatry 21:47–68.

Ikonen S, Riekkinen Jr P (1999) Effects of apamin on memory processing of hippocampal-lesioned mice. Eur J Pharmacol 382:151–156.

Ikonen S, Schmidt B, Riekkinen Jr P (1998) Apamin improves spatial navigation in medial septal-lesioned mice. Eur J Pharmacol 347:13–21.

Jeffery KJ (1997) LTP and spatial learning–where to next? Hippocampus 7:95–110.

Katz B, Miledi R (1968) The role of calcium in neuromuscular facilitation. J Physiol (Lond) 195:481–492.

Kohler M, Hirschberg B, Bond CT, Kinzie JM, Marrion NV, Maylie J, Adelman JP (1996) Small-conductance, calcium-activated potassium channels from mammalian brain. Science 273:1709–1714.

Kovalchuk Y, Eilers J, Lisman J, Konnerth A (2000) NMDA receptor-mediated subthreshold Ca^{2+} signals in spines of hippocampal neurons. J Neurosci 20:1791–1799.

Lancaster B, Nicoll RA (1987) Properties of two calcium-activated hyperpolarizations in rat hippocampal neurones. J Physiol (Lond) 389:187–203.

Lancaster B, Hu H, Ramakers GM, Storm JF (2001) Interaction between synaptic excitation and slow afterhyperpolarization current in rat hippocampal pyramidal cells. J Physiol (Lond) 536:809–823.

Lisman J (1989) A mechanism for the Hebb and the anti-Hebb processes underlying learning and memory. Proc Natl Acad Sci USA 86:9574–9578.

LoTurco JL, Coulter DA, Alkon DL (1988) Enhancement of synaptic potentials in rabbit CA1 pyramidal neurons following classical conditioning. Proc Natl Acad Sci USA 85:1672–1676.

Lynch G, Larson J, Kelso S, Barrionuevo G, Schottler F (1983) Intracellular injections of EGTA block induction of hippocampal long-term potentiation. Nature 305:719–721.

Magee JC, Johnston D (1995) Synaptic activation of voltage-gated channels in the dendrites of hippocampal pyramidal neurons. Science 268:301–304.

Malenka RC, Nicoll RA (1993) NMDA-receptor-dependent synaptic plasticity: multiple forms and mechanisms. Trends Neurosci 16:521–527.

Malenka RC, Nicoll RA (1999) Long-term potentiation–a decade of progress? Science 285:1870–1874.

Malenka RC, Lancaster B, Zucker RS (1992) Temporal limits on the rise in postsynaptic calcium required for the induction of long-term potentiation. Neuron 9:121–128.

Martin ED, Araque A, Buno W (2001) Synaptic regulation of the slow Ca^{2+}-activated K^+ current in hippocampal CA1 pyramidal neurons: implication in epileptogenesis. J Neurophysiol 86:2878–2886.

Mayer ML, MacDermott AB, Westbrook GL, Smith SJ, Barker JL (1987) Agonist- and voltage-gated calcium entry in cultured mouse spinal cord neurons under voltage clamp measured using arsenazo III. J Neurosci 7:3230–3244.

McEchron MD, Disterhoft JF (1999) Hippocampal encoding of non-spatial trace conditioning. Hippocampus 9:385–396.
Messier C, Mourre C, Bontempi B, Sif J, Lazdunski M, Destrade C (1991) Effect of apamin, a toxin that inhibits Ca^{2+}-dependent K^+ channels, on learning and memory processes. Brain Res 551:322–326.
Morris RG, Garrud P, Rawlins JN, O'Keefe J (1982) Place navigation impaired in rats with hippocampal lesions. Nature 297:681–683.
Moser EI, Krobert KA, Moser MB, Morris RG (1998) Impaired spatial learning after saturation of long-term potentiation. Science 281:2038–2042.
Mourre C, Cervera P, Lazdunski M (1987) Autoradiographic analysis in rat brain of the postnatal ontogeny of voltage-dependent Na^+ channels, Ca^{2+}-dependent K^+ channels and slow Ca^{2+} channels identified as receptors for tetrodotoxin, apamin and (−)-desmethoxyverapamil. Brain Res 417:21–32.
Mulkey RM, Malenka RC (1992) Mechanisms underlying induction of homosynaptic long-term depression in area CA1 of the hippocampus. Neuron 9:967–975.
Mumby DG, Gaskin S, Glenn MJ, Schramek TE, Lehmann H (2002) Hippocampal damage and exploratory preferences in rats: memory for objects, places, and contexts. Learn Mem 9:49–57.
Norris CM, Halpain S, Foster TC (1998) Reversal of age-related alterations in synaptic plasticity by blockade of L-type Ca^{2+} channels. J Neurosci 18:3171–3179.
Saar D, Grossman Y, Barkai E (1998) Reduced after-hyperpolarization in rat piriform cortex pyramidal neurons is associated with increased learning capability during operant conditioning. Eur J Neurosci 10:1518–1523.
Sah P (1996) Ca^{2+}-activated K^+ currents in neurones: types, physiological roles and modulation. Trends Neurosci 19:150–154.
Sah P, Bekkers JM (1996) Apical dendritic location of slow afterhyperpolarization current in hippocampal pyramidal neurons: implications for the integration of long-term potentiation. J Neurosci 16:4537–4542.
Sah P, Clements JD (1999) Photolytic manipulation of $[Ca^{2+}]_i$ reveals slow kinetics of potassium channels underlying the afterhyperpolarization in hippocampal pyramidal neurons. J Neurosci 19:3657–3664.
Schwindt PC, Crill WE (1997) Modification of current transmitted from apical dendrite to soma by blockade of voltage- and Ca^{2+}-dependent conductances in rat neocortical pyramidal neurons. J Neurophysiol 78:187–198.
Sejnowski TJ (1977) Storing covariance with nonlinearly interacting neurons. J Math Biol 4:303–321.
Shors TJ, Matzel LD (1997) Long-term potentiation: what's learning got to do with it? Behav Brain Sci 20:597–655.
Silva AJ, Giese KP, Federov NB, Frankland PW, Kogan JH (1998) Molecular, cellular, and neuroanatomical substrates of place learning. Neurobiol Learn Mem 70:44–61.
Stocker M, Pedarzani P (2000) Differential distribution of three Ca^{2+}-activated K^+ channel subunits, SK1, SK2, and SK3, in the adult rat central nervous system. Mol Cell Neurosci 15:476–493.
Stocker M, Krause M, Pedarzani P (1999) An apamin-sensitive Ca^{2+}-activated K^+ current in hippocampal pyramidal neurons. Proc Natl Acad Sci USA 96:4662–4667.
Storm JF (1990) Potassium currents in hippocampal pyramidal cells. Prog Brain Res 83:161–187.
Tang YP, Shimizu E, Dube GR, Rampon C, Kerchner GA, Zhuo M, Liu G, Tsien JZ (1999) Genetic enhancement of learning and memory in mice. Nature 401:63–69.
Tsien JZ, Huerta PT, Tonegawa S (1996) The essential role of hippocampal CA1 NMDA receptor-dependent synaptic plasticity in spatial memory. Cell 87:1327–1338.
van der Staay FJ, Fanelli RJ, Blokland A, Schmidt BH (1999) Behavioral effects of apamin, a selective inhibitor of the SK_{Ca}-channel, in mice and rats. Neurosci Biobehav Rev 23:1087–1110.
Vnek N, Rothblat LA (1996) The hippocampus and long-term object memory in the rat. J Neurosci 16:2780–2787.
Zucker RS (1989) Short-term synaptic plasticity. Annu Rev Neurosci 12:13–31.

sium concentrations (22) and reactivity to specific antibodies (26), are not shared by U2AF^{65}. Finally, studies reporting protein-protein interactions among SR proteins failed to detect interactions between the U2AF^{65} RS region and other splicing factors (23, 27). Taken together, these observations suggest that there are two distinct classes of RS domains.

The orchestrated formation and disruption of short RNA-RNA helices is a common theme in pre-mRNA splicing (28) and probably in other processes that involve RNA. Here we have described a mechanism by which a spliceosomal RNA-RNA base-pairing interaction can be regulated by a protein.

REFERENCES AND NOTES

1. M. J. Moore, C. C. Query, P. A. Sharp, in *The RNA World*, R. F. Gesteland and J. F. Atkins, Eds. (Cold Spring Harbor Laboratory Press, Cold Spring Harbor, NY, 1993), p. 303.
2. R. Parker, P. G. Siciliano, C. Guthrie, *Cell* **49**, 229 (1987); J. Y. Wu and J. L. Manley, *Genes Dev.* **3**, 1553 (1989); Y. Zhuang and A. M. Weiner, *ibid.*, p. 1545.
3. P. E. Hodges and J. D. Beggs, *Curr. Biol.* **4**, 264 (1994).
4. B. Ruskin, P. D. Zamore, M. R. Green, *Cell* **52**, 207 (1988); P. D. Zamore and M. R. Green, *Proc. Natl. Acad. Sci. U.S.A.* **86**, 9243 (1989).
5. P. D. Zamore, J. G. Patton, M. R. Green, *Nature* **355**, 609 (1992).
6. C. G. Burd and G. Dreyfuss, *Science* **265**, 615 (1994).
7. J. Valcárcel, R. Singh, P. D. Zamore, M. R. Green, *Nature* **362**, 171 (1993).
8. R. Singh, J. Valcárcel, M. R. Green, *Science* **268**, 1173 (1995).
9. Modifications in the RS region did not affect binding to the Py tract (12) (see also Fig. 2B), as expected from previous studies (5, 8).
10. R. K. Gaur, J. Valcárcel, M. R. Green, *RNA* **1**, 407 (1995).
11. M. J. Moore and P. A. Sharp, *Science* **256**, 992 (1992).
12. J. Valcárcel and M. R. Green, unpublished observations.
13. D. A. Wassarman and J. A. Steitz, *Science* **257**, 1918 (1992).
14. Interestingly, the region in U6 that forms base pairs with U2 is immediately upstream of a pyrimidine stretch [T.-P. Hausner, L. M. Giglio, A. M. Weiner, *Genes Dev.* **4**, 2146 (1990)], suggesting that U2AF^{65} could bind to this sequence to modulate the U2-U6 interaction. Alternatively, this effect could be due to the general annealing activity associated with the U2AF^{65} RS region (18).
15. C. C. Query, M. J. Moore, P. A. Sharp, *Genes Dev.* **8**, 587 (1994).
16. Even protein-protein interaction motifs composed predominantly of a single amino acid, such as acidic transcription activation and proline-rich SH3 domains, contain additional types of residues also critical for activity [S. J. Triezenberg, *Curr. Opin. Genet. Dev.* **5**, 190 (1995); T. Pawson and J. Schlessinger, *Curr. Biol.* **3**, 434 (1993)].
17. P. Zuo and J. L. Manley, *Proc. Natl. Acad. Sci. U.S.A.* **91**, 3363 (1994).
18. C.-G. Lee, P. D. Zamore, M. R. Green, J. Hurtwitz, *J. Biol. Chem.* **268**, 13472 (1993).
19. M. R. Green, *Annu. Rev. Genet.* **20**, 671 (1986); C. W. J. Smith and B. Nadal-Ginard, *Cell* **56**, 749 (1989).
20. M. Feughelman *et al.*, *Nature* **175**, 834 (1955).
21. B. Calnan *et al.*, *Science* **252**, 1167 (1991).
22. A. M. Zahler, W. S. Lane, J. A. Stolk, M. B. Roth, *Genes Dev.* **6**, 837 (1992).
23. J. Wu and T. Maniatis, *Cell* **75**, 1061 (1993); J. Kohtz *et al.*, *Nature* **368**, 119 (1994); H. Amrein, M. L. Hedley, T. Maniatis, *Cell* **76**, 735 (1994).
24. P. Zuo and J. L. Manley, *EMBO J.* **12**, 4727 (1993).
25. J. F. Cáceres and A. R. Krainer, *ibid.*, p. 4715.
26. M. B. Roth, A. M. Zahler, J. A. Stolk, *J. Cell Biol.* **115**, 587 (1991).
27. Y. Ono, M. Ohno, Y. Shimura, *Mol. Cell. Biol.* **14**, 7611 (1994); J. Fleckner and M. R. Green, unpublished observations.
28. H. Madhani and C. Guthrie, *Annu. Rev. Genet.* **28**, 1 (1994).
29. Buffer D: 20 mM Hepes (pH 8.0), 0.2 mM EDTA, 20% glycerol, 0.05% NP-40, and 1 mM dithiothreitol.
30. Plasmid pMINX [M. Zillmann *et al.*, *Mol. Cell. Biol.* **8**, 814 (1988)] was used to generate pPy-MINX (pre-mRNA positions 165 to 177 substituted by AUCCAGGAAUUCUAAUACGACUCACUAU) and pbp^m.MINX (pre-mRNA positions 150 to 160 substituted by UAUGAUAGUGA). The corresponding pre-mRNAs were generated by in vitro transcription of Bam HI–digested templates.
31. Plasmids pT7U2 [A. M. Kleinschmidt *et al.*, *Nucleic Acids Res.* **17**, 4817 (1989)], pT7U2ΔBPRS (deletion of U2 snRNA positions 37 to 42), and pHU1A [J. R. Patton, R. J. Patterson, T. Pederson, *Mol. Cell. Biol.* **7**, 4030 (1987)] were used to transcribe U2 snRNA (positions 1 to 71), ΔBPRS, and U1 snRNA, respectively.
32. Abbreviations for the amino acid residues are as follows: A, Ala; C, Cys; D, Asp; E, Glu; F, Phe; G, Gly; H, His; I, Ile; K, Lys; L, Leu; M, Met; N, Asn; P, Pro; Q, Gln; R, Arg; S, Ser; T, Thr; V, Val; W, Trp; and Y, Tyr.
33. RS (U2AF^{35}): positions 561 to 723 of U2AF^{35} cDNA [M. Zhang *et al.*, *Proc. Natl. Acad. Sci. U.S.A.* **89**, 8769 (1992)]. RS (SF2): positions 887 to 1039 of ASF/SF2 cDNA [H. Ge *et al.*, *Cell* **66**, 373 (1991); A. R. Krainer *et al.*, *ibid.*, p. 383].
34. U2AF^{65} Δ(1–55) was prepared by deletion of a Bam HI–Xma I fragment from pGEX3X-U2AF^{65} (5) and religation after Klenow treatment. U2AF^{65} Δ(1–63) has been described (5). U2AF^{65} Δ(1–94) was prepared by inserting a U2AF^{65} cDNA fragment encoding amino acids 94 to 475, flanked by Bam HI and Eco RI, into the same sites in pGEX-2T [D. B. Smith and K. S. Johnson, *Gene* **67**, 31 (1988)]. Digestion of this construct with Bam HI was used to obtain all the RS mutant derivatives.
35. Inserts were obtained by annealing complementary oligodeoxyribonucleotides corresponding to sequences encoding the RS repeats or mutant derivatives.
36. U2AF^{65} was cloned in plasmid pGEX-CS [T. D. Parks *et al.*, *Anal. Biochem.* **216**, 413 (1994)] to generate a GST-U2AF^{65} fusion with a TEV protease cleavage site between the two polypeptides. The fusion protein was expressed in bacteria, purified, and cleaved with TEV protease as described by Parks *et al.* (*ibid.*).
37. M. Mirfakhrai and A. M. Weiner, *Nucleic Acids Res.* **21**, 3591 (1993).
38. Reactions (20 μl) containing 75% buffer D (29), 75 mM KCl, 10 fmol of adenovirus-major-late (AdML) promotor derived pre-mRNAs (30), 50 fmol of U2 snRNA, ΔBPRS or U1 snRNA (31), recombinant U2AF^{65} or derivatives (50 ng/μl), psoralen (20 μg/ml), and pGEM3 plasmid (47 ng/μl) were irradiated at 25°C with 366-nm ultraviolet light (UVP Inc. lamp, at a distance of 3.5 cm from the samples) for 30 min. Under these conditions, U2AF^{65} promoted interactions between U2 snRNA and a variety of pre-mRNAs from *Drosophila* to human genes.
39. Primer extension mapping of psoralen cross-links has been shown to give rise to more than one primer extension stop from a single cross-link [G. Ericson and P. Wollenzien, *Anal. Biochem.* **174**, 215 (1988); J. Teare and P. Wollenzien, *Nucleic Acids Res.* **18**, 855 (1990)].

40. We thank M. Jacobson and T. Pederson for the U1 snRNA clone, L. Chiang and J. Kielty for technical support, T. O'Toole for secretarial assistance, and F. Gebauer, K. Neugebauer, and members of the Green lab for advice and comments on the manuscript. Supported by European Molecular Biology Organization and Spanish Ministerio de Educación y Ciencia fellowships to J.V., Leukemia Society of America postdoctoral and special fellowships to R.S., and a grant from the National Institutes of Health to M.R.G.

25 June 1996; accepted 30 July 1996

Small-Conductance, Calcium-Activated Potassium Channels from Mammalian Brain

M. Köhler, B. Hirschberg, C. T. Bond, J. M. Kinzie, N. V. Marrion, J. Maylie, J. P. Adelman*

Members of a previously unidentified family of potassium channel subunits were cloned from rat and human brain. The messenger RNAs encoding these subunits were widely expressed in brain with distinct yet overlapping patterns, as well as in several peripheral tissues. Expression of the messenger RNAs in *Xenopus* oocytes resulted in calcium-activated, voltage-independent potassium channels. The channels that formed from the various subunits displayed differential sensitivity to apamin and tubocurare. The distribution, function, and pharmacology of these channels are consistent with the SK class of small-conductance, calcium-activated potassium channels, which contribute to the afterhyperpolarization in central neurons and other cell types.

Action potentials in vertebrate neuronsare followed by an afterhyperpolarization (AHP) that may persist for several seconds and may have profound consequences for the firing pattern of the neuron. The AHP has several components. The fast component (fAHP) helps to repolarize the action potential and regulates spike interval, whereas subsequent slow components (sAHP) underlie spike-frequency adaptation (*1–5*).

Each component of the AHP is kinetically distinct and is mediated by different Ca^{2+}-activated K^+ channels. The large-conductance (100 to 200 pS), voltage- and Ca^{2+}-activated K^+ channels (BK channels) underlie the fAHP (*6*, *7*), which develops rapidly (1 to 2 ms) and decays within tens

of milliseconds. The channels underlying the sAHP are SK channels, which differ from BK channels in that they are more Ca^{2+}-sensitive, are activated in a voltage-independent manner, and have a smaller unit conductance (*8*, *9*). The sAHP varies considerably in different cell types, activating slowly (10 to 1000 ms), and it may decay over several seconds (*6*, *9*–*11*).

The fAHP is blocked by low concentrations of external tetraethylammonium and charybdotoxin, in accord with the pharmacology of BK channels (*6*, *7*, *12*). In contrast, the sAHP is insensitive to these agents but exhibits one or the other of two classes of behavior regarding sensitivity to the bee venom peptide toxin apamin. In hippocampal pyramidal neurons the sAHP is insensitive to apamin (*4*), whereas in hippocampal interneurons it is blocked by nanomolar concentrations of the toxin (*13*).

Voltage-independent, apamin-sensitive K^+ channels activated by submicromolar concentrations of Ca^{2+} have been described for peripheral cell types, including skeletal muscle (*14*), gland cells (*15*, *16*), and T lymphocytes (*17*). These channels have unitary conductances of 5 to 20 pS. Apamin-insensitive SK channels have also been reported (*8*). Thus, SK channels make up a subfamily of Ca^{2+}-activated K^+ channels that play key physiological roles in many cell types. We present here the molecular structures for a class of K^+ channel subunits with six transmembrane domains. The characteristics of the expressed channels define this class as SK channels.

A sequence with homology to the pore region of cloned K^+ channels was detected in a database search (*18*) and was used as a probe on cDNA libraries. Three full-length coding sequences were isolated, one from human (hSK1) and two from rat (rSK2, rSK3) brain, and a partial clone, rSK1, representing the rat homolog of hSK1. The sequences predict proteins of 561 (hSK1), 580 (rSK2), and 553 (rSK3) amino acids (Fig. 1A). Hydrophobicity analysis predicts six transmembrane segments with the NH_2- and COOH-termini residing inside the cell (Fig. 1B). The sequences are highly conserved across their transmembrane cores (80 to 90% identity) but diverge in sequence and length within their NH_2- and COOH-terminal domains. The fourth predicted membrane-spanning domain contains three positively charged amino acids, separated by six and seven residues. Multiple consensus targets for phosphorylation by several protein kinases are found in all clones; however, each clone contains potential phosphorylation sites not conserved among all members. There are no conserved N-linked glycosylation sites (NXXS/T) (*19*) in predicted extracellular domains and no consensus nucleotide or Ca^{2+} binding domains (E-F hands). Although related in topology to voltage-dependent K^+ channels, including a P region and S4 segment, the clones reside on a distinct evolutionary branch within the K^+ channel superfamily (Fig. 1C).

Sequences distinct for each of the rat clones were used as probes for in situ hybridizations on sections prepared from rat brain (*20*). The mRNAs are broadly distributed throughout the central nervous system, in characteristic but overlapping patterns (Fig. 2, A through C). The rSK1 and rSK2 probes were also used on Northern (RNA) blots prepared with mRNA isolated from total brain and several peripheral tissues. The rSK1 probe detected mRNAs of different sizes in brain (3.2 kb) and heart (4.4 kb), whereas the rSK2 mRNA was detected in brain and adrenal gland as two bands of 2.2 and 2.4 kb (Fig. 2D) (*21*).

In vitro–synthesized mRNAs were injected into *Xenopus* oocytes, and two-electrode, voltage-clamp recordings were performed 2 to 5 days later (*22*). Voltage protocols failed to evoke currents different

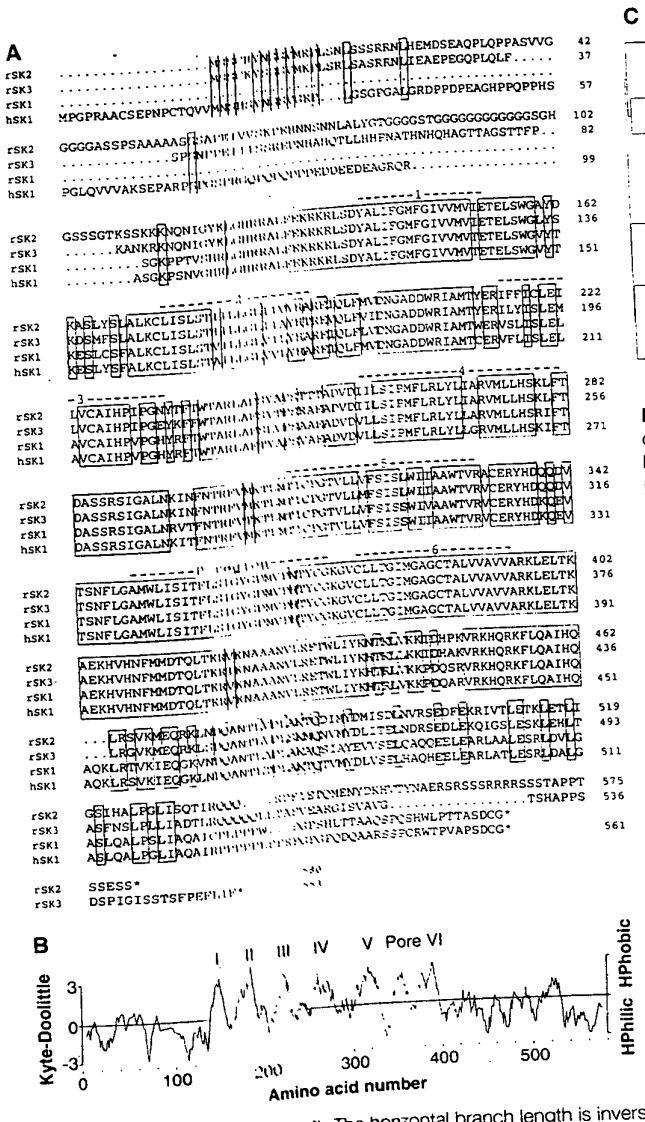

Fig. 1. (**A**) Amino acid sequences (*19*) predicted for hSK1, rSK2, rSK3, and the partial clone, rSK1. Alignments were generated by eye; dots represent gaps introduced to optimize the alignment. The six predicted transmembrane domains and the pore region are overlined. Residues that are conserved among all of the clones are boxed. Amino acid numbers for the full-length coding sequences are given on the right. The GenBank accession numbers for these sequences are as follows: rSK2, U69882; hSK1. U69883; rSK3, U69884; and rSK1, U69885. The asterisks indicate stop codons. (**B**) Hydropathy plot for rSK2 calculated from the algorithm of Kyte and Doolittle with an amino acid window of nine residues. HPhobic, hydrophobic; HPhilic, hydrophilic. (**C**) Dendrogram of representative mammalian members of the K^+ channel superfamily (*23*). The horizontal branch length is inversely proportional to the similarity between sequences.

M. Köhler, B. Hirschberg, C. T. Bond, J. M. Kinzie, N. V. Marrion, J. P. Adelman, Vollum Institute, L-474, Oregon Health Sciences University, 3181 Southwest Sam Jackson Road, Portland, OR 97201, USA.
J. Maylie, Department of Obstetrics and Gynecology, Oregon Health Sciences University, Portland, OR 97201, USA.
*To whom correspondence should be addressed.

from control oocytes. Because of the similar mRNA distribution in brain of rSK2 and mGluR1a, a metabotropic glutamate receptor (*23*, *24*), mGluR1a mRNA was injected with or without the SK mRNAs. The application of glutamate to oocytes expressing only mGluR1a evoked a transient inward current due to activation of endogenous Ca^{2+}-activated Cl^- channels after the release of intracellular Ca^{2+} (Fig. 3A) (*23*, *24*). In oocytes coexpressing mGluR1a with rSK2, application of glutamate evoked the same Cl^- current, which was followed by an outward current (Fig. 3B). Similar results were obtained with rSK3 and hSK1. Intracellular injection of the Ca^{2+} chelator EGTA (~10 mM, final concentration) (*25*) abolished both current responses evoked by subsequent application of glutamate (Fig. 3C), indicating that both components are Ca^{2+}-activated. The ion selectivity of rSK2 was examined in oocytes injected with only the rSK2 mRNA (*26*). The current activated by injection of Ca^{2+} (~1 mM final concentration) reversed near the K^+ reversal potential in ND96 solution. The reversal potential of the currents shifted with increasing extracellular K^+ with a slope of 55.4 mV for a 10-fold change in K^+ concentration (2 to 20 mM K^+, substituted for Na^+), confirming that the channels are selective for K^+ over Na^+.

Macroscopic currents were also recorded

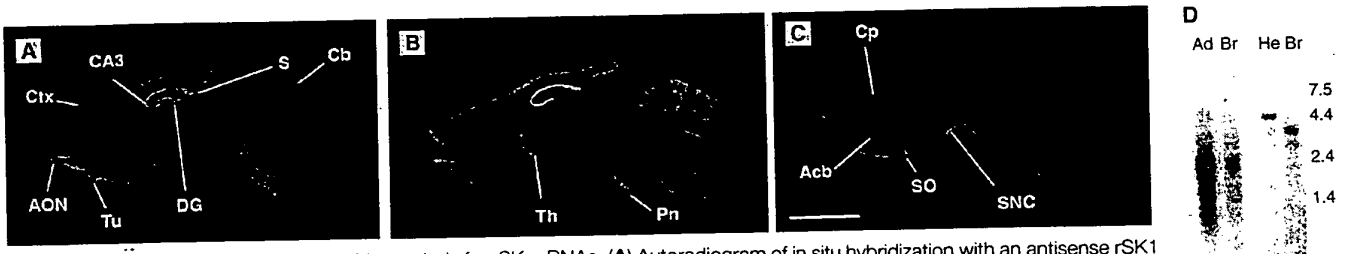

Fig. 2. In situ hybridization and Northern blot analysis for rSK mRNAs. (**A**) Autoradiogram of in situ hybridization with an antisense rSK1 RNA probe. Hybridization was found in the hippocampus (CA3), the dentate gyrus (DG), the subiculum (S), the anterior olfactory nucleus (AON) and olfactory tubercle (Tu), the cerebellum (Cb), and the cortex (Ctx). (**B**) Autoradiogram of in situ hybridization with an antisense rSK2 RNA probe. Of the SK mRNAs, rSK2 mRNA was the most widely expressed and was highest in the hippocampus (not labeled), with lower levels of expression in the olfactory bulb and the anterior olfactory nucleus, the granular layer of the cerebellum (not labeled), the reticular nucleus of the thalamus (Th), and the pontine nucleus (Pn). (**C**) Autoradiogram of in situ hybridization with an antisense rSK3 RNA probe. Hybridization was seen in the lateral septum and ventral tegmental area, the olfactory tubercle (not labeled), the caudate-putamen (Cp), the nucleus accumbens (Acb), the supraoptic nucleus (SO), many nuclei of the thalamus and hypothalamus (not labeled), and the substantia nigra pars compacta (SNC). Scale bar, 5 mm. (**D**) Northern blot analysis of rSK1 and rSK2 mRNAs. Polyadenylated [poly(A)$^+$] mRNA (3 μg) from rat whole brain, heart, lung, spleen, adrenal gland, liver, kidney, and skeletal muscle was prepared as a Northern blot and probed with riboprobes specific for either rSK1 (right) or rSK2 (left); rSK1 mRNA was detected in rat brain (Br) and heart (He), and rSK2 mRNA was detected in brain and adrenal gland (Ad). Neither rSK1 nor rSK2 mRNA was detected from lung, liver, kidney, thymus, spleen, or skeletal muscle. Molecular sizes are indicated in kilobases.

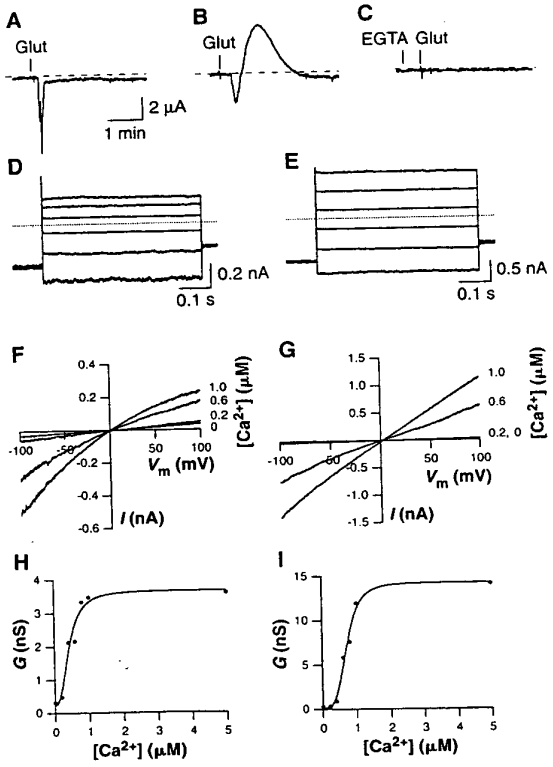

Fig. 3. Expression of rSK2 and hSK1 in *Xenopus* oocytes. In (A) through (C), the metabotropic glutamate (Glut) receptor mGluR1a was expressed with or without rSK2 in *Xenopus* oocytes. Whole cell currents were measured from oocytes superfused with ND96 solution 2 to 3 days after mRNA injection. The holding potential was −80 mV. (**A**) Addition of glutamate (1 mM) to an oocyte injected with mGluR1a mRNA alone evoked a transient Ca^{2+}-activated Cl^- current. Similar results were obtained in six other oocytes injected with mGluR1a. (**B**) Addition of glutamate (1 mM) to oocytes coinjected with mGluR1a and rSK2 mRNA evoked the transient Ca^{2+}-activated Cl^- current observed with mGluR1a-injected oocytes, followed by a large transient outward current. Similar results were obtained in 14 other oocytes coinjected with mGlu1a and rSK2. (**C**) Injection of EGTA (final concentration, ~10 mM) abolished the response to subsequent addition of glutamate in oocytes coinjected with mGluR1a and rSK2 mRNA. Similar results were obtained in three other oocytes coinjected with mGluR1a and rSK2. (**D** and **E**) Currents evoked by voltage steps from inside-out macropatches excised from an oocyte expressing rSK2 (D) or hSK1 (E). With 5 μM Ca^{2+} in the intracellular solution, the membrane was stepped from a holding potential of −80 mV to test potentials between −100 and 100 mV and then repolarized to −50 mV. Currents activated instantaneously and showed no inactivation during the 500-ms test pulses. (**F** and **G**) Current traces (*I*) elicited by 2.5-s voltage ramps (V_m) from −100 to 100 mV from inside-out macropatchs excised from oocytes expressing rSK2 (F) or hSK1 (G). The traces were obtained in the presence of the indicated concentrations of intracellular Ca^{2+}; current amplitudes increased as the Ca^{2+} concentration was increased. (**H** and **I**) The relation between Ca^{2+} concentration and response obtained from the patches shown above for rSK2 (H) or hSK1 (I) channels. The slope conductance, *G*, at the reversal potential is plotted as a function of Ca^{2+} concentration. The data were fitted with the Hill equation, yielding a $K_{0.5}$ of 0.43 μM and 0.71 μM and a Hill coefficient of 4.8 and 3.9 for rSK2 and hSK1, respectively.

from excised patches (27). Application of Ca^{2+} to the cytoplasmic face of inside-out macropatches from oocytes expressing rSK2 or hSK1 evoked substantial currents that were not detected in the absence of Ca^{2+}, nor were they detected from control oocytes. Voltage steps to potentials between −100 and 100 mV evoked time-independent currents (Fig. 3, D and E) that were not obviously voltage-dependent. The Ca^{2+} sensitivity of rSK2 and hSK1 was determined. Currents evoked by voltage ramps from an inside-out macropatch were dependent on the concentration of Ca^{2+} on the intracellular face of the membrane (Fig. 3, F and G). The slope conductance at the reversal potential was plotted as a function of Ca^{2+} concentration, and the data points were fitted with the Hill equation (Fig. 3, H and I). For rSK2 the average $K_{0.5}$ (concentration for half-maximal activation) for Ca^{2+} was 0.63 ± 0.23 μM (n = 8), and for hSK1 it was 0.70 ± 0.06 μM (n = 4). The steep dependence on Ca^{2+} seen from the plots was reflected by a Hill coefficient of 4.81 ± 1.46 for rSK2 and 3.90 ± 0.45 for hSK1, which suggests that at least four Ca^{2+} ions were involved in channel gating. These results identify this family as Ca^{2+}-activated K^+ channels.

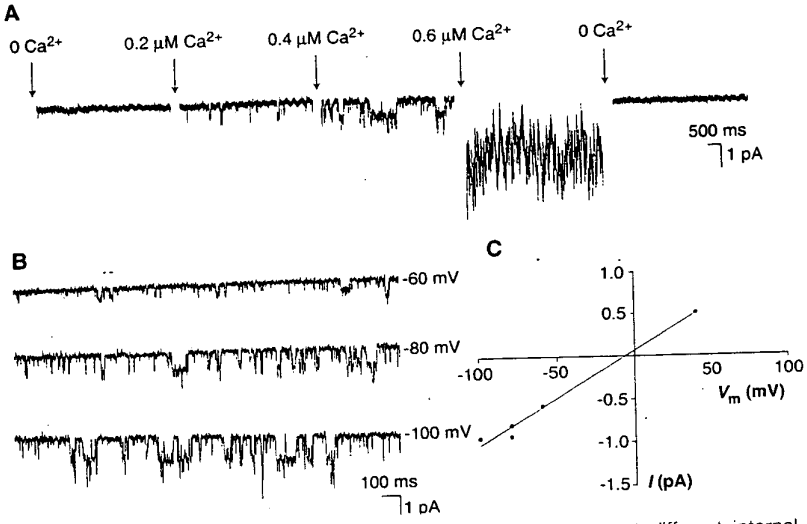

Fig. 4. Single-channel recordings of rSK2. (**A**) Continuous recording at different internal Ca^{2+} concentrations from a representative inside-out patch containing rSK2 channels. Addition of 0.2 μM Ca^{2+} elicited openings to a single amplitude. Increasing Ca^{2+} to 0.4 μM increased channel activity, and openings to several levels are apparent. Upon addition of 0.6 μM Ca^{2+}, channel activity increased such that discrete amplitudes could not be resolved. Channel activity ceased when Ca^{2+} was removed. Gaps represent breaks in the continuously acquired recording. The baseline (zero current level) of the segment recorded in 0.6 μM Ca^{2+} has been aligned by eye. For display, data were digitally filtered at 300 Hz. (**B**) Channel activity from a representative patch recorded in the presence of 0.4 μM Ca^{2+} at −60, −80, and −100 mV. The patch contained more than one channel, and double openings are apparent. For display, traces were digitally filtered at 300 Hz. (**C**) Single-channel current-voltage relation for the patch presented in (B). Data points were derived from the fitting of amplitude histograms at each membrane potential. Linear regression yielded a single-channel conductance of 10.8 pS, with a reversal at −6 mV.

Activation of SK channels underlies the sAHP in central neurons. Distinguishing features of endogenous SK channels are their activation by submicromolar Ca^{2+}, lack of voltage-dependent gating, and unit conductance (8, 14, 16). The sAHP in many neurons is blocked by picomolar concentrations of apamin, whereas in others it is not affected. Cloned members of this family exhibit these features. Indeed, the pattern of in situ hybrid-

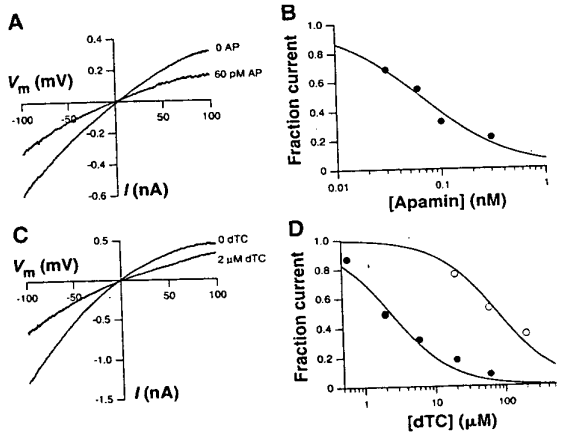

Fig. 5. Pharmacology of rSK2 and hSK1. (**A** and **C**) Macroscopic rSK2 currents were recorded in 5 μM Ca^{2+} from inside-out macropatches with either 0 or 60 pM apamin (AP) (A) or 0 or 2 μM *d*-tubocurare (dTC) (C) in the extracellular solution. (**B** and **D**) Dose-response curves for block by external apamin [shown in (B) for rSK2] or *d*-tubocurare [shown in (D) for rSK2, closed circles, and hSK1, open circles]. Block was determined from multiple inside-out macropatches with or without drug. Each data point represents the fractional current (drug per control) at −100 mV from the average of six control patches and six subsequent patches with drug. Currents were elicited by voltage ramps as in (A). The continuous lines represent nonlinear least squares fits to the data for a 1:1 stoichiometry, giving a K_i of 63 pM for AP and 2.4 μM (rSK1) or 76.2 μM (hSK1) for dTC.

ization for rSK2 mRNA is coincident with the pattern of radiolabeled apamin binding in rat brain (*32*).

The cloned SK subunits contain no significant amino acid homology to other cloned K^+ channel subunits except for a 12-residue stretch within the putative pore domain. Hydrophobicity plots predict that these subunits contain six transmembrane domains, a topology shared with members of the voltage-gated class of K^+ channels (*33*). Like the cyclic nucleotide–gated channels, the cloned SK channels contain an S4 domain with positively charged residues but are not gated in a voltage-dependent manner (*34*). It has been proposed that the charged residues in the S4 segment may form salt bridges with other residues in different regions of the channel, imparting structural stability, even when the charged residues do not participate in voltage sensing (*35*, *36*). In some cells, such as hippocampal pyramidal neurons, the sAHP is regulated by transmitters that act through protein kinases (*8*, *37*). Although it is unclear whether the kinases influence the sAHP through direct phosphorylation of native SK channels or through intermediary effectors, the primary sequences for all of the cloned SK subunits contain many potential phosphorylation sites.

Several hypotheses have been advanced to account for the differences in the sAHP among different cell types (*11*, *29*). The complement of expressed SK subunits, their subcellular distribution, and regulation all may be responsible for differences in the sAHP after an action potential. The shared characteristics of the SK channels responsible for the sAHP were faithfully recapitulated by the clones presented here. The molecular mechanisms underlying variability in sAHPs will likely be understood as this K^+ channel family is further characterized.

REFERENCES AND NOTES

1. J. R. Hotson and D. A. Prince, *J. Neurophysiol.* **43**, 409 (1980).
2. B. Gustaffson and H. Wigstrom, *Brain Res.* **206**, 462 (1981).
3. Y. Yarom, M. Sugimori, R. Ilinas, *Neuroscience* **16**, 719 (1985).
4. B. Lancaster and P. R. Adams, *J. Neurophys.* **55**, 1268 (1986).
5. R. A. Nicoll, *Science* **241**, 545 (1988).
6. B. Lancaster and R. A. Nicoll, *J. Physiol. (London)* **389**, 187 (1987).
7. F. Viana, D. A. Bayliss, A. J. Berger, *J. Neurophysiol.* **69**, 2150 (1993).
8. B. Lancaster, R. A. Nicoll, D. J. Perkel, *J. Neurosci.* **11**, 23 (1991).
9. P. Sah, *J. Neurophysiol.* **74**, 1772 (1995).
10. J. F. Storm, *J. Physiol. (London)* **409**, 171 (1989).
11. B. Lancaster and R. S. Zucker, *ibid.* **475**, 229 (1994).
12. A. Butler, S. Tsunoda, D. P. McCobb, A. Wei, L. Salkoff, *Science* **261**, 221 (1993).
13. L. Zhang and C. J. McBain, *J. Physiol. (London)* **488**, 661 (1995).
14. A. L. Blatz and K. L. Magleby, *Trends Neurosci.* **10**, 463 (1987).
15. A. Tse and B. Hille, *Science* **255**, 462 (1992).
16. Y. B. Park, *J. Physiol. (London)* **481**, 555 (1994).
17. S. Grissmer, R. S. Lewis, M. D. Cahalan, *J. Gen. Physiol.* **99**, 63 (1992).
18. A BLAST search of the expressed sequence tag (EST) database, using the query sequence FXSIPXXXWWAXVTMTTVGYGDMXP (*19*) and allowing for mismatches, retrieved known K^+ channel sequences and GenBank entry M62043. Oligonucleotides corresponding to nucleotides 6 to 36 (sense) and 258 to 287 (antisense) of M62043 were synthesized (Genosys), radiolabeled with polynucleotide kinase (BRL) and ^{32}P-labeled adenosine triphosphate (DuPont Biotechnology Systems), and used to screen ~10^6 recombinant phage from the human hippocampal cDNA library [40% formamide; 1 M NaCl, 1% SDS, 37°C; washed with 1× standard saline citrate (SSC) (150 mM NaCl, 15 mM sodium citrate, pH 7.2) 50°C]. We purified double positively hybridizing phage by rescreening at reduced densities. The cDNA inserts were subcloned into M13, and the nucleotide sequences were determined with T7 DNA polymerase (Sequenase, United States Biochemical). A fragment of this clone containing the pore domain (amino acids 325 to 522) was radiolabeled with random primers (Boehringer) and used to screen a rat brain cDNA library (30% formamide, 1 M NaCl, 1% SDS, 37°C; washed with 2× SSC, 50°C). Positively hybridizing phage were purified and the nucleotide sequences of the inserts determined. We performed computer analyses using the GCG software suite (Genetics Computer Group; version 8.1). We generated the dendrogram using the PILEUP multiple sequence analysis program with full-length coding sequences for the listed subunits. The gap penalty was 3, and the gap extension penalty was 0.5. Specific members of subfamilies, and their accession numbers are as follows: K_v1 ($hK_v1.1$; L02750); K_v2 (mshab; M64228); K_v3 ($mK_v3.3$; X60796); K_v4 (mshal; M64226); $K_{ir}1$ (RomK1; X72341); $K_{ir}2$ (Irk1; X73052) $K_{ir}3$ (Girk1; U01071); $K_{ir}4$ ($K_{ir}4.1$/Bir10; X83585); $K_{ir}5$ ($K_{ir}5.1$/Bir9; X83581); $K_{ir}6$ ($K_{ir}6.1$/uKatp; D42145); hK_vCa (hslo; U11717); and mK_vCa (mslo; L16912).
19. Abbreviations for the amino acid residues are as follows: A, Ala; C, Cys; D, Asp; E, Glu; F, Phe; G, Gly; H, His; I, Ile; K, Lys; L, Leu; M, Met; N, Asn; P, Pro; Q, Gln; R, Arg; S, Ser; T, Thr; V, Val; W, Trp; Y, Tyr, and X, unknown.
20. Care and handling of adult female Sprague-Dawley rats were in accordance with institutional guidelines. Rats were deeply anesthetized with pentobarbital and perfused transcardially with ice-cold saline and then with ice-cold 4% paraformaldehyde in 0.1 M sodium borate (pH 9.5). The brains were removed quickly and fixed overnight at 4°C in 4% paraformaldehyde in borate buffer (pH 9.5) containing 10% sucrose. Cryostat microtome sections (25 μm) were mounted onto gelatin- and poly-L-lysine–coated glass slides and incubated for 15 min in 4% paraformaldehyde in 0.1 M phosphate-buffered saline (PBS), washed twice in 0.1 M PBS, and treated for 30 min at 37°C in proteinase K (10 mg/ml) in 100 mM tris, 50 mM EDTA (pH 8) and then with 0.0025% acetic anhydride (w/w) in 0.1 M triethanolamine at room temperature. The sections were then washed in 2× SSC, dehydrated in increasing concentrations of ethanol, and vacuum-dried at room temperature. Templates for probe synthesis represented sequences unique to each of the clones. ^{35}S-labeled antisense cRNA probe was heated to 65°C for 5 min and diluted to 10^7 cpm/ml in hybridization buffer: 66% formamide, 260 mM NaCl, 1.3× Denhardt solution (13 mM tris, pH 8.0, 1.3 mM EDTA, 13% dextran sulfate). Sections in the hybridization mixture were covered with siliconized glass cover slips and sealed with DPX mountant. After the slides had been incubated at 58°C for 20 hours, they were soaked in 4× SSC to remove cover slips, then rinsed in 4× SSC (four times, 5 min each) before treatment with ribonuclease A (20 mg/ml for 30 min at 37°C). The slides were then rinsed in decreasing concentrations of SSC containing 1 mM dithiothreiotol (DTT) to a final stringency of 0.1× SSC, 1 mM DTT for 30 min at 65°C. After the sections had been dehydrated in increasing concentrations of ethanol, they were vacuum-dried and exposed to DuPont Cronex-4 x-ray film for 7 days. The film was scanned by a Microtek ScanMaker 1850S at a resolution of 728 pixels per centimeter, and the images were analyzed with Image v1.55 software (NIH) and Photoshop (Adobe).
21. Total RNA was extracted [J. M. Chirgwin, A. E. Przybyla, R. J. MacDonald, W. J. Rutter, *Biochemistry* **18**, 5294 (1979)] from rat brain, adrenal gland, thymus, spleen, skeletal muscle, heart, kidney, liver, and lung of 3-week-old Sprague-Dawley rats. Polyadenylated [poly(A)$^+$] mRNA was purified by oligo d(T) cellulose chromatography (Collaborative Research), and 3 μg from each tissue was prepared as a Northern blot by electrophoresis through a 1% agarose-formaldehyde gel and transfer to Genescreen (DuPont Biotechnology Systems) nylon membranes. Antisense riboprobes were synthesized from linearized DNA templates with ^{32}P-labeled uridine triphosphate (DuPont Biotechnology Systems). Blots were hybridized in 50% formamide, 5% SDS, 400 mM $NaPO_4$ (pH 7.2), 1 mM EDTA at 60°C for 12 hours; then they were washed in 0.05× SSC at 65°C and visualized with a PhosphorImager 445 SI (Molecular Dynamics) after 15 hours.
22. In vitro mRNA synthesis and oocyte injections were performed as described in [J. P. Adelman *et al.*, *Neuron* **9**, 209 (1992)]. *Xenopus* care and handling were in accordance with institutional guidelines. Frogs underwent no more than two surgeries, separated by at least 3 weeks, and well-established techniques were used for the surgeries. Frogs were anesthetized with an aerated solution of the ethyl ester of 3-aminobenzoic acid. Oocytes were studied 2 to 5 days after injection with 2 ng of mRNA. We measured whole cell currents using a two-electrode voltage clamp with a CA-1 amplifier interfaced to a Macintosh Quadra 650 computer. Data were simultaneously acquired through Pulse (Heka Electronik) at 500 Hz and Chart (AD Instruments) at 10 Hz. During recording, oocytes were continuously superfused with ND96 solution containing 96 mM NaCl, 2 mM KCl, 1.8 mM $CaCl_2$, 1 mM $MgCl_2$, 5 mM Hepes (pH 7.5 with NaOH) at room temperature. To minimize Cl^- currents, some oocytes were soaked and studied in Cl^--free ND96 solution (96 mM sodium gluconate, 2 mM potassium gluconate, 2.7 mM calcium gluconate, 1-mM magnesium gluconate, 5 mM Hepes, pH 7.5 with NaOH).
23. K. M. Houamed *et al.*, *Science* **349**, 760 (1991).
24. M. Masu, Y. Tanabe, K. Tsuchida, R. Shigemoto, S. Nakanishi, *Nature* **349**, 760 (1991).
25. After establishment of the two-electrode voltage clamp, the oocyte was impaled with a third electrode containing 200 mM EGTA, pH adjusted to 7.2 with KOH. We monitored the input resistance during impalement to ensure oocyte viability. At the indicated time, 50 nl of the EGTA solution was injected into the oocyte. If we assume an oocyte volume of 1 μl, the predicted final concentration of EGTA was 10 mM.
26. Two days after injection, the oocytes were soaked for >24 hours in Cl^--free ND96 solution to minimize Cl^- currents. In the two-electrode recording mode, currents were activated by injection of 5 nl of 200 mM $CaCl_2$ through a third electrode, resulting in a final intracellular concentration of ~1 mM Ca^{2+}. This procedure resulted in a longer lasting activation of the K^+ current than that activated by glutamate in oocytes coinjected with mGluR1a and rSK2.
27. Oocytes were injected as described for two-electrode, voltage-clamp recordings. At 2 to 9 days after injection, inside-out macropatches were excised into an intracellular solution containing 116 mM potassium gluconate, 4 mM KCl, 10 mM Hepes (pH 7.25, adjusted with KOH) supplemented with $CaCl_2$ or EGTA or both. To obtain nominally Ca^{2+}-free solution, we added 1 mM EGTA. Alternatively, $CaCl_2$ was added to the cytoplasmic solution to give free Ca^{2+} concentrations (1 to 10 μM). In this case, the proportion of Ca^{2+} binding to gluconate was determined by a computer program (CaBuf) (we used a stability constant for calcium gluconate of 15.9 M^{-1}) [R. M. C. Dawson, D. C. Elliot, W. H. Elliot, K. M. Jones, *Data for Biochemical Research* (Oxford Univ. Press, New York, 1969)]. To obtain Ca^{2+} concentra-

tions below 1 μM, we added 5 mM EGTA to the cytoplasmic solution and added $CaCl_2$ as calculated using the CaBuf program and published stability constants [A. Fabiato and F. Fabiato, *J. Physiol. (London)* **75**, 463 (1979)]. For experiments in which Mg^{2+} was added to the cytoplasmic solution, $MgCl_2$ was added to the total concentrations stated in the text. Under these conditions, binding of Mg^{2+} to gluconate is negligible (stability constant, 1.7 M^{-1}). Electrodes were pulled from thin-walled, filamented borosilicate glass (World Precision Instruments) and filled with 116 mM potassium gluconate, 4 mM KCl, 10 mM Hepes (pH 7.25). Electrode resistance was typically 2 to 5 megohms. Membrane patches were voltage-clamped with an Axopatch 200A amplifier (Axon Instruments). The data were low-pass–Bessel filtered at 2 kHz and were acquired with Pulse software (Heka Electronik). In the analysis we used Pulse, Kaleidograph (Abelbeck), or IGOR (Wavemetrics) software. All experiments were performed at room temperature from a holding potential of −80 mV. Voltage ramps (2.5 s) from −100 to 100 mV were acquired at a sampling frequency of 500 Hz. The currents recorded from macropatches showed small inward rectification in the absence of cytoplasmic cations other than K^+ and Ca^{2+} (5 μM). In the hippocampus, SK channels exhibit significant inward rectification in the presence of intracellular Mg^{2+} (*8*). When different concentrations of Mg^{2+} (0.1 to 3 mM) were added to the intracellular face of inside-out patches, outward currents were reduced. Apamin was from Calbiochem, and *d*-tubocurare was from Research Biochemicals International.

28. Solutions used were the same as for macropatch recordings. Electrodes were pulled from Corning 7052 glass (Garner) and had resistances of 9 to 13 megohms. Data were filtered at 1 kHz (Bessel), acquired at 10 kHz with Pulse (Heka Electronik), and stored directly on a Macintosh Quadra 650. Single channels were analyzed with MacTac (SKALAR Instruments). The "50% threshold" technique was used to estimate event amplitudes. The threshold was adjusted for each opening, and each transition was inspected visually before being accepted. Amplitude histograms were constructed using MacTacfit (SKALAR Instruments), and the single channel conductance was determined from a Gaussian distribution. Channel open probability was estimated from *NP*(o), the product of the open probability multiplied by the number of channels; *NP*(o) was calculated as the sum of the (dwell time multiplied by level number) divided by the total time, and *N* was estimated as the number of simultaneously open channels at 0.4 μM Ca^{2+}.

29. P. Sah and E. M. McLachlan, *J. Neurophysiol.* **68**, 1834 (1992).
30. A. R. Artalejo, A. G. Garcia, E. Neher, *Pfluegers Arch.* **423**, 97 (1993).
31. N. J. Dun, Z. G. Jiang, N. Mo, *J. Physiol. (London)* **375**, 499 (1986).
32. D. R. Gelhert, *Neuroscience* **52**, 191 (1993).
33. L. Y. Jan and Y. N. Jan, *Nature* **345**, 672 (1990).
34. E. H. Goulding, G. R. Tibbs, S. A. Siegelbaum, *ibid.* **372**, 369 (1994).
35. S. R. Durell and H. R. Guy, *Biophys. J.* **62**, 238 (1992).
36. D. M. Papazian *et al.*, *Neuron* **14**, 1293 (1995).
37. P. Pedarzani and J. F. Storm, *Pfluegers Arch.* **431**, 723 (1996).

38. We thank M. Litt for assistance with database searches, J. Saugstad and G. Westbrook for early experiments with mGluR1a, and B. Bean for helpful and enthusiastic discussions. We thank G. Westbrook for supplying the mGluR1a clone and C. Miller for supplying the charybdotoxin. M.K. was supported by a grant from the DRG, B.H. by an NIH cardiology training grant, and J.M.K. by a National Research Service Award grant. This work was supported by NIH grants to J.M. and J.P.A.

2 May 1996; accepted 29 July 1996

A Cyclin-Dependent Kinase–Activating Kinase (CAK) in Budding Yeast Unrelated to Vertebrate CAK

F. Hernan Espinoza, Alison Farrell, Hediye Erdjument-Bromage, Paul Tempst, David O. Morgan*

Progress through the cell cycle is governed by the cyclin-dependent kinases (CDKs), the activation of which requires phosphorylation by the CDK-activating kinase (CAK). In vertebrates, CAK is a trimeric enzyme containing CDK7, cyclin H, and MAT1. CAK from the budding yeast *Saccharomyces cerevisiae* was identified as an unusual 44-kilodalton protein kinase, Cak1, that is only distantly related to CDKs. Cak1 accounted for most CAK activity in yeast cell lysates, and its activity was constant throughout the cell cycle. The *CAK1* gene was essential for cell viability. Thus, the major CAK in *S. cerevisiae* is distinct from the vertebrate enzyme, suggesting that budding yeast and vertebrates may have evolved different mechanisms of CDK activation.

The activation of CDKs requires association with a cyclin subunit and phosphorylation by CAK at a conserved threonine residue (*1*). The major CAK activity in vertebrate and starfish cells is a heterotrimer composed of CDK7, cyclin H, and MAT1 (*2–4*). The homologous CDK-cyclin complex in fission yeast also has CAK activity (*5*). However, in the budding yeast *Saccharomyces cerevisiae*, the closest CDK7 homolog (Kin28) does not have CAK activity (*6*, *7*), and the enzyme responsible for CDK activation in this organism is unknown.

To explore the nature of CAK in budding yeast, we used conventional chromatographic methods to purify the major CAK activity in yeast lysates (Fig. 1). We measured CAK activity by testing the ability of column fractions to activate the histone H1 kinase activity of purified human CDK2–cyclin A complexes, which are more readily prepared in large quantities than are yeast Cdc28-cyclin complexes. Peak fractions also activated Cdc28-Clb2 (*8*). We estimate that CAK activity was purified over 1000-fold after six chromatographic steps. In the last steps of purification, CAK activity comigrated with a single protein of ~44 kD on polyacrylamide gels (p44) (Fig. 1, B and C). We were unable to purify p44 to homogeneity; however, in multiple preparations, p44 was the only protein that consistently copurified with CAK activity, suggesting that p44 alone was responsible for the activity. This conclusion is supported by results from gel filtration analysis of CAK activity in crude yeast lysates (*8*) or partially purified CAK preparations (Fig. 1A), in which the apparent molecular size of native CAK was ~45 kD.

Tryptic peptides from p44 were subjected to mass spectrometry and amino acid sequencing. Comparison of peptide sequences with the *Saccharomyces* Genomic Database (Stanford University) revealed that the amino acid sequences of two peptides matched predicted sequences in a previously uncharacterized open reading frame, YFL029c, on chromosome VI (*9*). In addition, the masses of these two peptides, as well as those of two additional peptides from p44, matched the theoretical masses of tryptic peptides in the predicted sequence of YFL029c (Fig. 2). The YFL029c open reading frame encodes a protein with sequence similarity to protein kinases and a molecular size of 42,183 daltons. We conclude that this open reading frame encodes p44, which we call Cak1.

Cak1 is only distantly related to other protein kinases. Its closest known relative in any species is yeast Cdc28, with which it shares limited similarity (~23% identity) (Fig. 2). It is even less similar to yeast Kin28 (17% identity) and is therefore not closely related to the CDK7 subfamily. Cak1 is also distinct from most other protein kinases in that it lacks a highly conserved NH_2-terminal cluster of glycine residues that contributes to the adenosine triphosphate (ATP) binding site (*10*). Cak1 has large amino acid inserts between conserved kinase subdomains. On the basis of studies of protein kinase structure (*11*, *12*), we predict that these inserts are located in loops between conserved secondary

F. H. Espinoza, A. Farrell, D. O. Morgan, Department of Physiology and Department of Biochemistry and Biophysics, University of California, San Francisco, CA 94143–0444, USA.
H. Erdjument-Bromage and P. Tempst, Molecular Biology Program, Memorial Sloan-Kettering Cancer Center, New York, NY 10021, USA.
*To whom correspondence should be addressed.

Pflügers Arch - Eur J Physiol (2001) 441:544–550
DOI 10.1007/s004240000447

ORIGINAL ARTICLE

Morten Grunnet · Bo S. Jensen · Søren-Peter Olesen
Dan A. Klaerke

Apamin interacts with all subtypes of cloned small-conductance Ca^{2+}-activated K^+ channels

Received: 16 May 2000 / Received after revision: 29 August 2000 / Accepted: 31 August 2000 / Published online: 21 November 2000

Abstract The purpose of the present study was to examine how apamin interacts with the three cloned subtypes of small-conductance Ca^{2+}-activated K^+ channels (hSK1, rSK2 and rSK3). Expression of the SK channel subtypes in *Xenopus laevis* oocytes resulted in large outward currents (0.5–5 μA) after direct injection of Ca^{2+}. In all three cases the Ca^{2+}-activated K^+ currents could be totally inhibited by 500 nM apamin. Dose–response curves revealed a subtype-specific affinity for the apamin-induced inhibition with IC_{50} values of 704 pM and 196 nM (biphasic) for hSK1, 27 pM for rSK2 and 4 nM for rSK3. Consistent with these results, membranes prepared from oocytes expressing the SK channel subtypes bound ^{125}I-labelled apamin with distinct dissociation constants (K_d values) of approx. 390 pM for hSK1, 4 pM for rSK2 and 11 pM for rSK3. These results show that apamin binds to and blocks all three subtypes of cloned SK channels, and the distinct values for IC_{50} and K_d suggest that apamin may be useful for determining the expression pattern of SK channel subtypes in native tissue.

Keywords ^{125}I-apamin · Inhibition · SK1 · SK2 · SK3 · *Xenopus laevis* oocytes

Introduction

Small-conductance, Ca^{2+}-activated K^+ channels (SK channels) are characterized by a low single-channel conductance (<20 pS) and voltage-independent activation by Ca^{2+} in the submicromolar concentration range [3]. SK channels have been identified in numerous excitatory and non-excitatory tissues, such as the central nervous system (CNS) [4, 10, 18, 25, 29], skeletal muscle cells [3], intestinal smooth muscle [2], adrenal chromaffin cells [21], T-lymphocytes [5], hepatocytes [22] and epithelia [23, 33], indicating that these channels are important for the function of many cell types. In particular, in neurones, currents originating from SK channels are thought to be responsible for the slow afterhyperpolarization (sAHP) following an action potential [10, 18, 20, 25, 26, 28, 34]. In many cases [20, 24, 28, 34], but not all [4, 19, 25, 29], the sAHP's are reportedly blocked by the peptidyl toxin apamin, which is an 18-amino-acid toxin from the venom of the honey bee [8].

Three highly homologous subtypes (SK1, SK2 and SK3) of small-conductance Ca^{2+}-activated K^+ channels have been cloned [15]. The cloned SK channels show a high degree of homology to another recently cloned K^+ channel type, the intermediate-conductance, Ca^{2+}-activated K^+ channel [12, 14], but share little homology with other K^+ channel families except in part of the pore region [15]. Heterologously expressed SK channel subtypes exhibit distinct pharmacological properties. Tubocurarine blocks SK1 channels 30-fold less effectively than SK2 [15], and it has been claimed that SK1 channels are insensitive to apamin, whereas apamin blocks SK2 channels in subnanomolar concentrations [13, 15]. This has led to the suggestion that expression of the SK1 subtype could be responsible for the apamin-insensitive, Ca^{2+}-dependent sAHP's in the brain [9, 13].

However, recently it was shown that SK1 channels expressed in mammalian cell lines are blocked by apamin [27, 30] and it was suggested that the apamin sensitivity of SK1 channels could depend on the expression system employed. The purpose of the present study was to examine the interaction of apamin with SK1, SK2 and SK3 channels after expression in *Xenopus laevis* oocytes. Our data show that apamin not only blocks all three subtypes of SK channels with different affinities, but also that all subtypes are receptors for ^{125}I-labelled apamin binding after expression in *Xenopus laevis* oocytes. These findings question the suggestion that SK1 channels are responsible for the apamin-insensitive currents seen in native tissue.

M. Grunnet · B.S. Jensen · S.-P. Olesen · D.A. Klaerke (✉)
Department of Medical Physiology, The Panum Institute,
University of Copenhagen, Blegdamsvej 3,
2200 Copenhagen N, Denmark
e-mail: d.klaerke@mfi.ku.dk
Tel.: +45-35-327569, Fax: +45-35-327526

Materials and methods

Molecular biology

To obtain robust expression in *Xenopus laevis* oocytes cDNA's coding for hSK1, rSK2 and rSK3 were subcloned into pBF, an oocyte expression vector which contains the 5′ and 3′ untranslated regions from the *Xenopus laevis* β-globin as well as a poly-A segment. For in vitro transcription, the plasmids were linearized downstream of the poly-A segment and mRNA was synthesized from the SP6 RNA polymerase promoter using the mCAP mRNA capping kit (Stratagene, La Jolla, Calif., USA). mRNA's were phenol/chloroform extracted, ethanol precipitated and dissolved in Tris/EDTA (TE) buffer to a concentration of approximately 0.1 μg/μl. The integrity of the transcripts was confirmed by agarose gel electrophoresis, and mRNA was stored at –80°C until injection.

Expression in *Xenopus laevis* oocytes

Female *Xenopus laevis* frogs were anaesthetized for 15–20 min in 2 g/l Tricain (3-aminobenzoic acid ethyl ester, Sigma A-5040) before an ovarian lobe was removed from the abdominal cavity through a small (1 cm) insertion. Oocytes were defolliculated enzymatically by incubation in 1% collagenase (Boehringer Mannheim, 1088831) and 0.1% trypsin inhibitor (Sigma T-2011) in Kulori medium (90 mM NaCl, 1 mM KCl, 1 mM $MgCl_2$, 1 mM $CaCl_2$, 5 mM HEPES-Tris, pH 7.4) for 1 h followed by five washes in Kulori containing 0.1% BSA (Sigma A-6003), and incubation for 1 h in a hypertonic phosphate buffer (100 mM K_2HPO_4, pH 6.5). Subsequently, stage V and VI oocytes were selected, washed five times in Kulori and kept overnight at 19°C before injection with 50 nl of mRNA (approx. 5 ng) using a Nanoject microinjector (Drummond, USA). Injected and non-injected oocytes were kept in Kulori at 19°C before electrophysiological measurements or membrane preparation.

Electrophysiology

Currents through expressed SK channels were measured using the two-electrode voltage-clamp technique. Oocytes were impaled with a current electrode and a voltage-clamp electrode pulled from borosilicate glass capillaries on a vertical patch electrode puller (List Medical, Germany). Both electrodes had a tip resistance of 0.8–2 MΩ when filled with 1 M KCl and were connected to a two-electrode voltage-clamp amplifier (Warner, USA). The clamp voltage was controlled by a custom-built voltage generator. Ramps were generated from –80 to 80 mV in steps of 20 mV with a duration of 1 s. During the experiments, oocytes were placed in a small chamber (volume: 200 μl) connected to a continuous flow system (flow: 6 ml/min). The bath solution was a modified Kulori medium with a low Cl^- concentration (5 mM) containing Cl^- channel inhibitors [50 μM 4,4-diisothiocyanatostilbene 2,2-disulfonic acid (DIDS), 50 μM niflumic acid, 50 μM *N*-phenylanthranilic acid]. To activate expressed SK channels, $CaCl_2$ (9.2 nl, 100 mM) was injected during the experiment using the Nanoject injector.

Preparation of membranes from *Xenopus laevis* oocytes

For membrane preparation, batches of 60–80 oocytes injected with SK1, SK2, SK3 or non-injected oocytes were homogenized in 10% sucrose dissolved in homogenization buffer [600 mM KCl, 5 mM 3-(*N*-morpholino) propanesulfonic acid (MOPS), 100 μM phenyl methyl sulfonyl flouride (PMSF), 1 μM pepstatin A, 1 μM *p*-aminobenzamide, aprotinine (1 μg/ml) and leupeptin (1 μg/ml) pH 6.8] in a volume of 10 μl/oocyte with 10 strokes at 1000 rpm in a glass/Teflon homogenizer (Braun-Melsungen) at 0°C. The homogenate was placed on top of a step gradient consisting of 7 ml 50% sucrose and 3.5 ml 20% sucrose in homogenization buffer and centrifuged at 67,000 *g* for 30 min at 4°C in a Beckman SW 40 rotor. The interface (between 20% and 50% sucrose) was collected and subjected to centrifugation at 84,000 *g* for 30 min at 4°C in a Beckman Ti 70.1 rotor. The supernatant was discarded, and the pellet resuspended in 200 μl 300 mM sucrose, 100 mM KCl, 5 mM MOPS pH 6.8 and stored at – 80°C until use.

Binding assay

Binding of ^{125}I-labelled apamin was measured essentially as previously described [6, 16]. In short, the incubation with the ligand was carried out in 0.5 ml medium (10 mM KCl, 10 mM NaCl, 20 mM Tris-HCl, 0.1% BSA pH 8.4) in polystyrene tubes. Non-specific binding was defined in the presence of 500 nM apamin, and incubation was carried out at 4°C for 1–3 h. Toxin was always added directly to the incubation medium to avoid adsorption phenomena. The protein concentration of the vesicles was between 0.6 and 50 μg/ml. At the end of the incubation, the samples were rapidly filtered through Toyo Advantec GC 50 glass fibre filters [presoaked for ≥60 min in 0.3% (w/v) polyethylenimine] on Millipore 1002530 filter apparatus, followed by two washes with ice-cold buffer consisting of 150 mM NaCl, 20 mM Tris-HCl pH 7.4 (3 ml per wash). In each experiment, double or triplicate assays were routinely performed and the data averaged.

Analysis of data

Dose–response studies

The results were subject to either a one-site competition analysis using the equation:

$$Y = I - \frac{I_{max}[X]}{IC_{50} + [X]}$$

where Y=relative current in %, X=logarithm of apamin concentration, I_{max}=maximal current in the absent of apamin, IC_{50}=is the apamin concentration required for half-maximal current inhibition, or a two-site competition analysis using the equation:

$$Y = I - \frac{I_{max(1)}[X]}{IC_{50(1)} + [X]} - \frac{I_{max(2)}[X]}{IC_{50} + [X]}$$

Binding studies

The results from saturation binding experiments were subject to a Michaelis–Menten analysis where the equilibrium dissociation constant (K_d) and the maximal receptor concentration (B_{max}) were determined using the one-site binding equation:

$$Y = \frac{B_{max}[X]}{K_d + [X]}$$

where Y=receptor concentration, X=logarithm of radioligand concentration, B_{max}=maximal binding and K_d is the concentration of radioligand required to reach half-maximal binding.

The data from saturation experiments were transformed into Scatchard plots, and the B_{max} and K_d values determined from this linear regression were approximately identical to the values determined from the one-site binding equation.

Results

Expression of small-conductance Ca^{2+}-activated K^+ channels in *Xenopus laevis* oocytes

To activate expressed SK channels, $CaCl_2$ was injected directly into the oocytes with the membrane potential clamped at 5 mV. In oocytes injected with mRNA coding

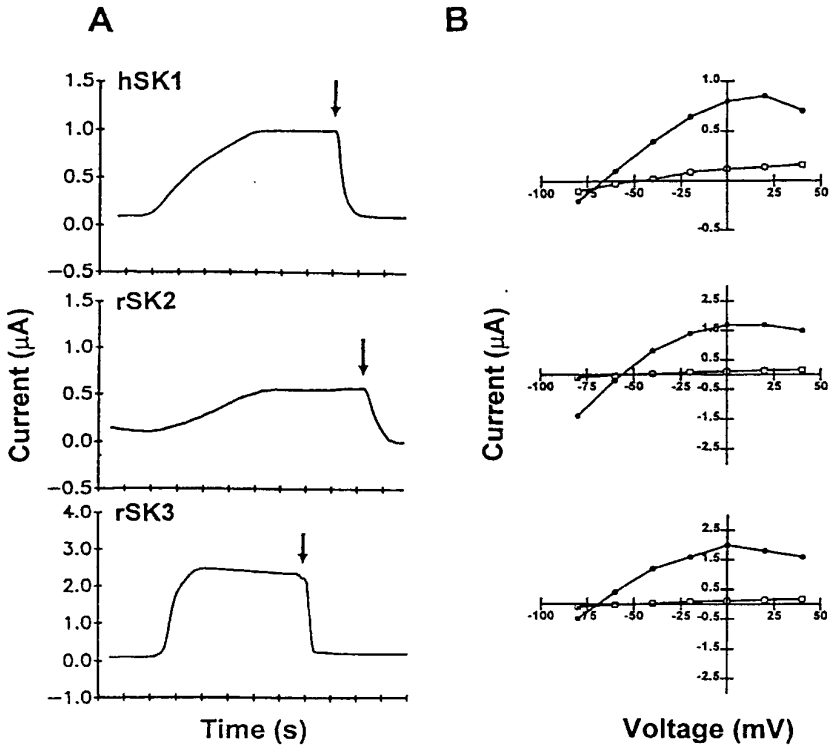

Fig. 1A, B Expression of SK channels in *Xenopus laevis* oocytes. **A** The result of two-electrode voltage-clamp measurements from oocytes injected with mRNA coding for hSK1, rSK2 and rSK3 or non-injected oocytes (control). At time 0, 9.2 nl of 100 mM $CaCl_2$ was injected directly into the oocytes resulting in an estimated increase in total intracellular Ca^{2+} of 0.9 mM. After the expressed SK channels had been activated 500 nM apamin was added to the bath (*arrow*). The membrane potential was clamped at 5 mV and the traces show the measured whole-cell current as a function of time. **B** The corresponding current–voltage relationship for oocytes expressing hSK1, rSK2 and rSK3 before (□) and after (●) $CaCl_2$ injection. The figure shows one typical experiment for each channel subtype out of a total of more that 50 experiments

for hSK1, rSK2 or rSK3, the Ca^{2+} injection resulted after a short delay in a large outward current, typically in the range of from 0.5 to 5 μA (Fig. 1A). The delay between the Ca^{2+} injection and the onset of the outward current varied from oocyte to oocyte, and was not related to the SK channel subtype expressed. This delay might reflect the intracellular diffusion rate for Ca^{2+}, and the variability could be due to the position of the injection pipette in the oocyte cytoplasm. The Ca^{2+}-induced currents were stable for at least 5 min (data not shown), and could for all three channel types be totally inhibited by 500 nM apamin applied to the outside of the oocytes (Fig. 1A).

Figure 1B shows the whole cell current–voltage (*I–V*) relationship for SK-expressing oocytes in experiments similar to those shown in Fig. 1A. Before Ca^{2+} injection, the *IV* curves were not different from those of non-injected oocytes (data not shown), confirming that SK channels expressed in oocytes are not active at resting levels of intracellular Ca^{2+}. Injection of Ca^{2+} resulted in an inwardly rectifying current with a reversal potential of approx. −60 to −70 mV, which is close to the calculated reversal potential for K^+, and thus consistent with the opening of SK channels.

In initial experiments, where 95 mM Cl^- was present in the external medium and Cl^- channel blockers were absent, the injection of Ca^{2+} activated endogenous Cl^- channels in addition to the expressed SK channels. To eliminate this problem, all experiments were done in the presence of Cl^- channel inhibitors and in a medium with a low Cl^- concentration (5 mM). Under these conditions neither the injection of Ca^{2+} nor the addition of apamin had any effect on the current measured at a membrane potential of 5 mV in control oocytes (data not shown), indicating that the Ca^{2+}-induced currents in RNA-injected oocytes are solely mediated by expressed SK channels. In contrast to the in-side-out patch-clamp method, which does not allow direct addition of apamin to the extracellular side, or right-side-out patch-clamp measurements, which have recently been reported as unsuitable for studying the effect of apamin [13], the whole-cell two-electrode voltage-clamp method as presented here constitutes a convenient system for studying the effect of extracellular apamin.

Sensitivity of SK channels to apamin

The effect of exposure to increasing concentrations of apamin was examined in oocytes expressing SK channels. It is evident that the sensitivity to apamin and the fit of the dose–response curves differ significantly between the three subtypes of SK channels (Fig. 2). For rSK2 and rSK3, the dose–response curves could be fitted to a one-site competition equation with IC_{50} values of 27±4 pM and 4±1 nM, respectively. For hSK1, however, the best fit was obtained using a two-site competition equation, resulting in two apparent IC_{50}'s for apamin inhibition, one with a relatively high affinity (IC_{50}=704±27 pM) and another with an approx. 250-fold lower affinity (IC_{50}=196±69 nM).

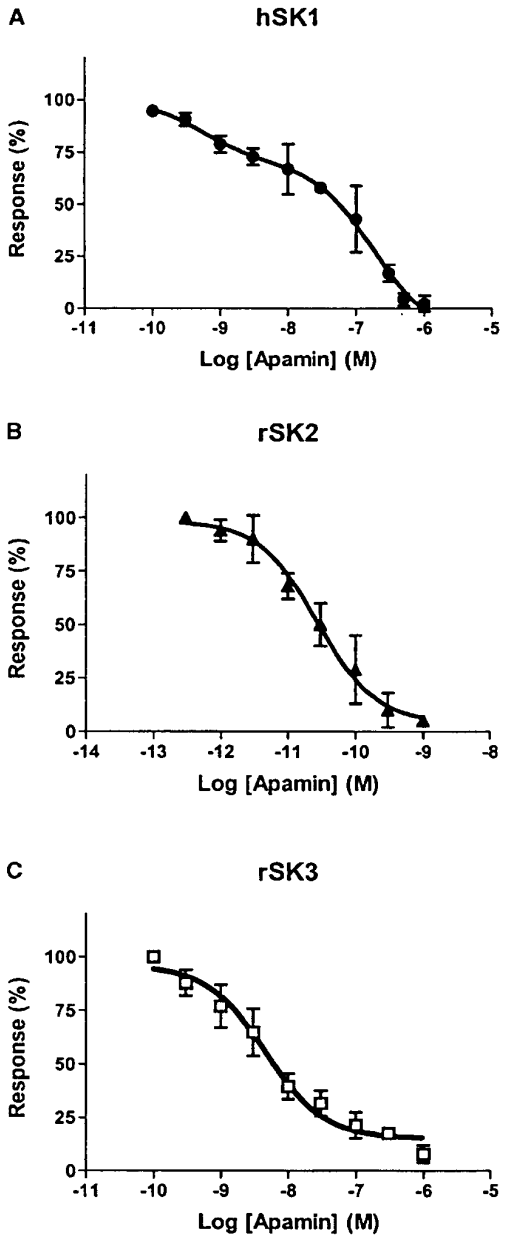

Fig. 2A–C Concentration-dependent inhibition of SK currents by apamin. *Xenopus laevis* oocytes expressing hSK1, rSK2 and rSK3 channels were voltage-clamped at a holding potential of 5 mV and the SK channels were activated by direct injection of $CaCl_2$ as shown in Fig. 1 before exposure to increasing concentrations of apamin from the outside (bath). At each concentration of apamin the whole-cell current was allowed to stabilize (approx. 30 s), before the degree of inhibition was measured. The figure shows the current at the indicated concentrations of apamin as a percentage of control current (no addition) for oocytes expressing hSK1 (**A**), rSK2 (**B**) and rSK3 (**C**) channels. Each curve shows the results (±SE) of four independent experiments. For rSK2 and rSK3 channels the data points were best fitted to a sigmoidal dose–response curve, whereas data points for hSK1 were best fitted to a two-site competition equation (regression coefficients are ≥0.98)

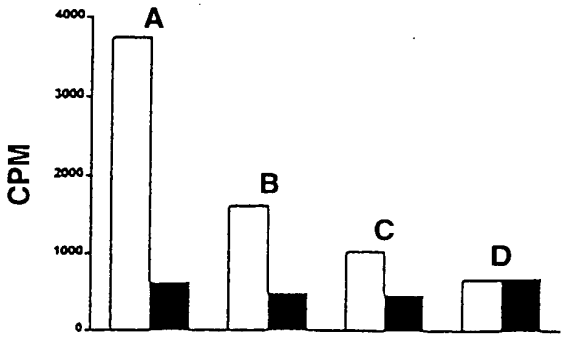

Fig. 3 Binding of ^{125}I-labelled apamin to plasma membranes from *Xenopus laevis* oocytes. Plasma membranes from oocytes expressing rSK2 [3.0 µg (**A**), 1.2 µg (**B**) and 0.6 µg (**C**)] and plasma membranes from non-injected oocytes (20 µg, **D**) were incubated for 1 h at 4°C with 5 pM of ^{125}I-labelled apamin in the absence (*open bars*) or presence (*closed bars*) of excess amounts of unlabelled apamin (500 nM). Binding was determined as described in Materials and methods. The results are given as mean of measurements in duplicate

Binding of ^{125}I-labelled apamin to cloned SK channels

Apamin can be radiolabeled with ^{125}I with practically full preservation of its biological activity [11], and ^{125}I-labelled apamin has been used in a large number of studies to detect apamin binding proteins (for review, see [7, 11]). However, it is not clear whether apamin binds to all SK channel subtypes and, in particular, the affinity with which ^{125}I-labelled apamin binds to the individual subtypes is not known.

To clarify this matter, membranes were prepared from batches of oocytes expressing each of the SK channel subtypes as well as from non-injected oocytes. Figure 3 shows an initial experiment, measuring ^{125}I-labelled apamin binding to different amounts of membranes prepared from oocytes expressing rSK2 and to membranes from non-injected oocytes. For the membranes from SK2-expressing oocytes, the specific binding constitutes approx. 80% of the total binding, and depends strictly on the amount of membranes. The membranes prepared from the non-injected oocytes show no specific binding of ^{125}I-labelled apamin, demonstrating that the oocytes do not express an endogenous apamin receptor.

When membranes prepared from oocytes expressing each of the three SK channel subtypes were incubated with increasing concentrations of ^{125}I-labelled apamin, from 10 times below to approx. 10 times above the K_d value, the toxin associated in a concentration-dependent manner. The specific binding, determined as the difference between the total binding and the non-specific binding, was for all three membrane preparations a saturable function of the ^{125}I-labelled apamin concentration (Fig. 4). Transformation of the data into Scatchard plots resulted in straight lines, suggesting that ^{125}I-labelled apamin interacts with a single class of receptor sites in each of the membrane fractions. The apparent K_d values

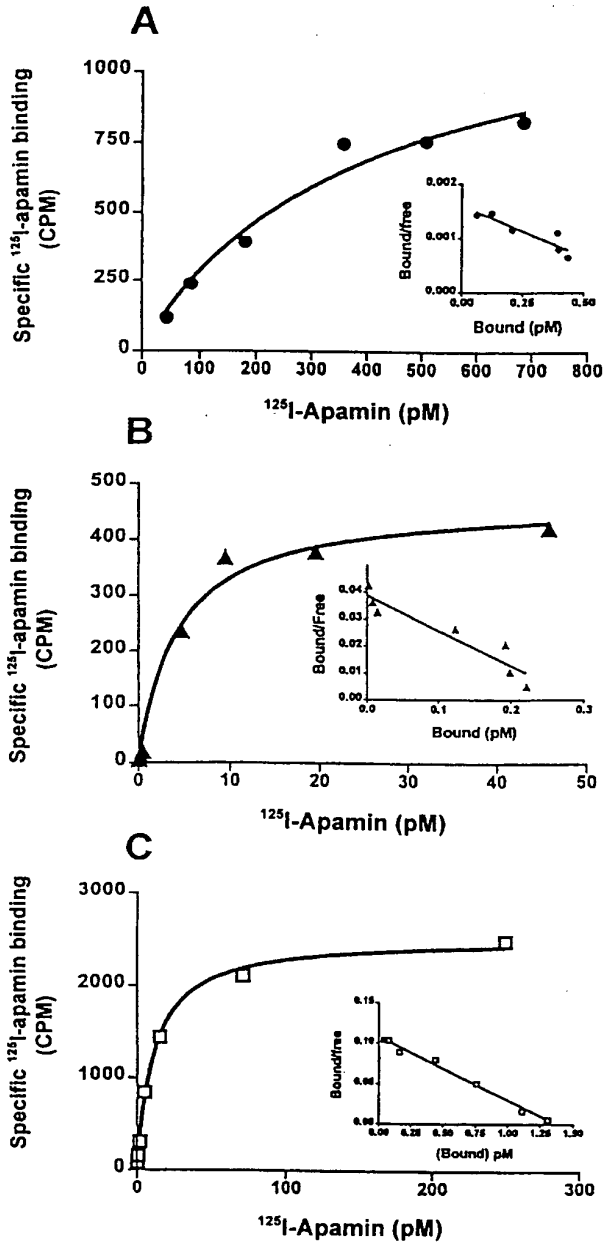

Fig. 4A–C Saturation of ^{125}I-labelled apamin binding to SK channel subtypes. Plasma membrane vesicles from oocytes expressing hSK1 (**A**, 50 µg protein/sample), rSK2 (**B**, 0.5 µg protein/sample) and rSK3 (**C**, 10 µg protein/sample) were incubated with the indicated amounts of ^{125}I-labelled apamin at 4°C for 3 h to reach equilibrium before specific binding was determined as described in Materials and methods. Data points are the mean of duplicates or triplicates. The *insets* show the Scatchard analysis by linear transformation of the respective data points. The calculated equilibrium dissociation constants (K_d) are given in Table 1

Table 1 Calculated IC_{50} and K_d values for apamin's interaction with cloned SK channel subtypes

SK channel subtype	IC_{50} (1)	IC_{50} (2)	K_d
hSK1	704±27 pM	196±69 nM	390±120 pM
rSK2	27±4 pM	–	4±1 pM
rSK3	4±1 nM	–	11±1 pM

for ^{125}I-labelled apamin binding to hSK1, rSK2 and rSK3 were 390 pM, 4 pM and 11 pM, respectively. K_d values calculated from the curve fit (one-site binding equation) did not differ from the K_d values obtained from the Scatchard transformation. To avoid using very large amounts of radioactivity, the saturation curves for SK1, which has a relatively low affinity for apamin, was not continued to complete saturation. However, we believe that the presented data are sufficient to give a reasonable estimation of the K_d value for ^{125}I-labelled apamin binding to SK1.

Discussion

The present study shows that apamin inhibits and binds to hSK1, rSK2 and rSK3 channels with distinct values of half maximal inhibition (IC_{50}) and dissociation constant (K_d). The significant differences between the apparent affinity for inhibition and binding for each channel subtype can be ascribed to differences in experimental conditions, since it is well known that high cation concentrations and possibly temperature change the binding ability of apamin [11, 23]. In contrast, it is not clear why apamin seems to inhibit two components of the current through hSK1, while ^{125}I-labelled apamin apparently interacts with only one binding site (Table 1). One possibility is that, at low concentrations, apamin partially blocks the hSK1 channels, and is only able to completely block the channel at high concentrations. This may be clarified in single-channel studies of apamin's interaction with hSK1.

The IC_{50} values found in the present study for apamin-induced inhibition of rSK2 and rSK3 are close to the values (rSK2: 62 pM and rSK3: 2 nM) reported recently by Köhler et al. [15] and Ishii et al. [13], but in the same studies it was claimed that hSK1 is apamin-insensitive [13, 15]. This statement was based on experiments using apamin at a concentration of 100 nM, and might therefore reflect the use of apamin at too low a concentration. In an elegant series of experiments, Ishii et al. [13] pinpointed two amino acids in rSK2, Asp-330 and Asn-357, which determine the apamin sensitivity. One of these amino acids is present in rSK3, and none in hSK1. If one of the determinants was introduced in hSK1, it acquired an apamin sensitivity comparable to that of rSK3, and if both were introduced in hSK1, the mutant showed an apamin sensitivity similar to that of rSK2. Taking the present data into account, it must be

concluded that two amino acids are not obligatory for apamin's ability to block, but rather that the absence of both amino acids gives a low apamin sensitivity, the presence of one results in intermediate apamin sensitivity, whereas the presence of both is required for high apamin sensitivity, as found for SK2 channels.

Recently, it was shown that, after expression in mammalian cells, SK1 channels are inhibited by apamin with IC_{50} values of 3.3–8 nM in HEK 293 cells [27, 30] and 12 nM in COS cells [27]). At first glance, there seems to be some inconsistency between the sensitivity of SK1 channels expressed in oocytes (this study) as compared to those expressed in mammalian cells. However, if the IC_{50} for apamin-induced inhibition of SK1 channels is read directly from Fig. 2A, disregarding the apparent two-site interaction, a value of 30 nM is obtained. This is not drastically different from the values obtained in studies of mammalian cells.

The question of the kinetics of inhibition remains. In mammalian cells, it is claimed that apamin interacts with only one binding site [27, 30], whereas in oocytes the data fit a two-site competition model (cf. Fig. 2A). However, if the data obtained from HEK 293 cells in the study of Shay and Haylett [27] are closely inspected, it seems that in this expression system the apamin inhibition curve may also fit a two-site competition model, whereas this seems not to be the case in the study of Stroebaek et al. [30]. Thus, the kinetics of apamin-induced inhibition of SK1 channels remain to be clarified, and in particular whether they depend on the expression system used.

Based on their observations as discussed above, Ishii et al. [13] suggest that the apparent apamin-insensitive SK currents observed in certain parts of the rat brain are due to the expression of SK1 channels. This is apparently supported by in situ hybridization showing the expression of SK1 channels in the CA2 region of the hippocampus [15]. The question arises, however, as to whether the apparent apamin-insensitive currents are in fact insensitive to apamin or just reflect the fact that relatively low concentrations of apamin have been applied. In hippocampal pyramidal slices [29], cultured hippocampal cells [19], vagal motorneurones [25] and adrenal chromaffin cells [21], apamin-insensitive currents are defined as currents that are not inhibited by 200 nM apamin or less. Therefore, these currents could be mediated by incompletely blocked SK1 channels. However, in slices from the lateral septum [4], pituitary gonadotrophs [31] and pancreatic beta-cells [1], SK-like currents are apparently not sensitive to apamin at a concentration of 1 μM, suggesting the presence of another SK-like channel with an as yet unclarified molecular identity.

In native tissues, such as brain, rat synaptosomes, intestinal smooth muscle, rat myotubes, rabbit and guinea-pig liver, ^{125}I-labelled apamin has been shown to bind with K_d values ranging from 2 pM to 30 pM (for reviews, see [7, 32]). When compared with Table 1, these results seem to reflect the fact that mainly SK2 and SK3 subtypes are expressed. Since the in situ hybridization studies mentioned above clarify that SK1 channels are expressed in the brain, it is not clear why the corresponding lower affinity binding site for ^{125}I-labelled apamin was not detected. In contrast, in rat liver ^{125}I-labelled apamin binds with a K_d of 50 nM [17] and in rat intestinal mucosa binding sites with K_d values between 0.5 and 1.1 nM have been detected [23]. This could reflect the expression of SK1 channels.

In conclusion, we have shown that apamin interacts with the three cloned SK subunits with distinct parameters, and apamin may therefore be a useful tool for determining the expression of each subunit in native tissues provided that sufficient concentrations are applied.

Acknowledgements Dr. J. Adelman is thanked for the hSK1, rSK2 and rSK3 clones. Birthe Lynderup, Inge Kjeldsen and Tove Soland are thanked for excellent technical assistance. This work was supported by the Danish Medical Research Council, The Danish Natural Science Research Council, The Novo Nordic Foundation, The Velux Foundation, The Beckett Foundation and Fonden til Laegevideskabens Fremme. B.S.J. is a Poul Bergsoe Research Fellow.

References

1. Ämmälä C, Bokvist K, Larsson O, Berggren PO, Rorsman P (1993) Demonstration of a novel apamin-insensitive calcium-activated K^+ channel in mouse pancreatic B cells. Pflügers Arch 422:443–448
2. Banks BEC, Brown C, Burgess GM, Burnstock G, Claret M, Cocks TM, Jenkinson DH (1979) Apamin blocks certain neurotransmitter-induced increases in potassium permeability. Nature 282:415–417
3. Blatz AL, Magleby KL (1986) Single apamin-blocked Ca-activated K^+ channels of small conductance in cultured rat skeletal muscle. Nature 323:718–720
4. Caretta B (1994) Calcium-activated hyperpolarizations in neurons of the mediolateral part of the lateral septum: intracellular studies from guinea pig brain slices. Exp Brain Res 102: 297–304
5. Grissmer S, Lewis RS, Cahalan MD (1992) Ca^{2+}-activated K^+ channels in human leukemic T cells. J Gen Physiol 99:63–84
6. Grunnet M, Solander C, Knaus, HG, Klaerke DA (1999) Distribution and quantification of Ca^{2+}-activated maxi K^+ channels in rabbit distal colon. Am J Physiol 277:G22–G30
7. Habermann E (1984) Apamin. Pharmacol Ther 25:255–270
8. Haux P, Sawerthal H, Habermann E (1967) Sequence analysis of bee venom neurotoxin (apamin) from its tryptic and chymotryptic cleavage products. Hoppe Seylers Z Physiol Chem 348: 737–738
9. Hirschberg B, Maylie J, Adelman JP, Marrion NV (1998) Gating of recombinant small-conductance Ca^{2+}-activated K^+ channels by calcium. J Gen Physiol 111:565–581
10. Hotson JR, Prince DA (1980) A calcium-activated hyperpolarization follows repetitive firing in hippocampal neurons. J Neurophysiol 43:409–419
11. Hugues M, Duval D, Kitabgi P, Lazdunski M, Vincent JP (1982) Preparation of a monoiodo derivate of the bee venom neurotoxin apamin and its binding properties to rat brain synaptosomes. J Biol Chem 257:2762–2769
12. Ishii TM, Silvia C, Hirschberg B, Bond CT, Adelman JP, Maylie J (1997) A human intermediate conductance calcium-activated potassium channel. Proc Natl Acad Sci USA 94: 11651–11656
13. Ishii TM, Maylie J, Adelman JP (1997) Determinants of apamin *d*-tubocurarine block in SK potassium channels. J Biol Chem 272:23195–23200

14. Jensen BS, Stroebaek D, Christophersen P, Jorgensen TD, Hansen C, Silahtaroglu A, Olesen SP, Ahring PK (1998) Characterization of the cloned human intermediate-conductance Ca^{2+}-activated K^+ channel. Am J Physiol 275:C848–C856
15. Köhler M, Hirschberg B, Bond CT, Kinzie JM, Marrion NV, Maylie J, Adelman JP (1996) Small-conductance, calcium-activated potassium channels from mammalian brain. Science 273:1709–1714
16. Koschak A, Koch RO, Liu J, Kaczorowski GJ, Reinhart PH, Garcia ML, Knaus HG (1997) ^{125}I-Iberiotoxin-D29Y/Y36 F, the first selective, high specific activity radioligand for high-conductance calcium-activated potassium channels. Biochemistry 36:1943–1952
17. Kovalevskaya GI, Miroshnikov A (1981) Specific binding of apamin, a neurotoxin from bee venom, with rat liver plasma membranes. Biorg Chem 7:1838–1841
18. Lancaster B, Adams PR (1986) Calcium-dependent current generating the afterhyperpolarization of hippocampal neurons. J Neurophysiol 55:1268–1282
19. Lancaster B, Nicoll RA, Perkel DJ (1991) Calcium activates two types of potassium channels in rat hippocampal neurons in culture. J Neurosci 11:23–30
20. Lang DG, Ritchie AK (1990) Tetraethylammonium blockade of apamin-sensitive and insensitive Ca2(+)-activated K^+ channels in a pituitary cell line. J Physiol (Lond) 425:17–132
21. Neely A, Lingle CJ (1992) Two components of calcium-activated potassium current in rat adrenal chromaffin cells. J Physiol (Lond) 453:97–131
22. Ogden DC, Capiod T, Walker JW, Trentham RD (1990) Kinetics of the conductance evoked by noradrenaline, inositol trisphosphate or Ca^{2+} in guinea-pig isolated hepatocytes. J Physiol (Lond) 422:585–602
23. Pácha J, Vorlicek J, Teisinger J (1992) Identification of apamin binding sites in rat intestinal mucosa. Life Sci 51:423–429
24. Pennefather P, Lancaster B, Adams PR, Nicoll RA (1985) Two distinct Ca-dependent K currents in bullfrog sympathetic ganglion cells. Proc Natl Acad Sci USA 82:3040–3044
25. Sah P (1995) Properties of channels mediating the apamin-insensitive afterhyperpolarization in vagal motoneurons. J Neurosci 74:1772–1776
26. Selyanko AA, Sim J, Brown DA (1998) Small (SK_{Ca}) Ca^{2+}-activated K^+ channels in cultured rat hippocampal pyramidal neurones. Pflügers Arch 437:161–163
27. Shah M, Haylett DG (2000) The pharmacology of hSK1 Ca^{2+}-activated K^+ channels expressed in mammalian cell lines. Br J Pharmacol 129:627–630
28. Stocker M, Krause M, Pedarzani P (1999) An apamin-sensitive Ca^{2+}-activated K^+ current in hippocampal pyramidal neurone. Proc Natl Acad Sci USA 96:4662–4667
29. Storm JF (1989) An after-hyperpolarization of medium duration in rat hippocampal pyramidal cells. J Physiol (Lond) 409: 171–190
30. Stroebaek D, Jorgensen TD, Christophersen P, Ahring PK, Olsens SP (2000) Pharmacological characterization of small-conductance Ca^{2+}-activated K^+ channels expressed in HEK 293 cells. Br J Pharmacol 129:991–999
31. Vergara L, Rojas E, Stojilkovic SS (1997) A novel calcium-activated apamin-insensitive potassium current in pituitary gonadotrophs. Endocrinology 138:2658–2664
32. Wadsworth JDF, Doorty KB, Strong PN (1994) Comparable 30-kDa apamin binding polypeptides may fulfill equivalent roles within putative subtypes of small conductance Ca^{2+}-activated K^+ channels. J Biol Chem 269:18053–18061
33. Wiener H, Klaerke DA, Jørgensen PL (1990) Rabbit distal colon epithelium: III. Ca^{2+}-activated K^+ channels in basolateral plasma membrane vesicles of surface and crypt cells. J Membr Biol 117:275–283
34. Zhang L, McBain CJ (1995) Potassium conductances underlying repolarization and after-hyperpolarization in rat CA1 hippocampal interneurones. J Physiol (Lond) 488:661–672